Quark Matter in Compact Stars & Heavy-Ion Coll.

David Blaschke (University of Wroclaw, Poland & JINR Dubna, Russia)

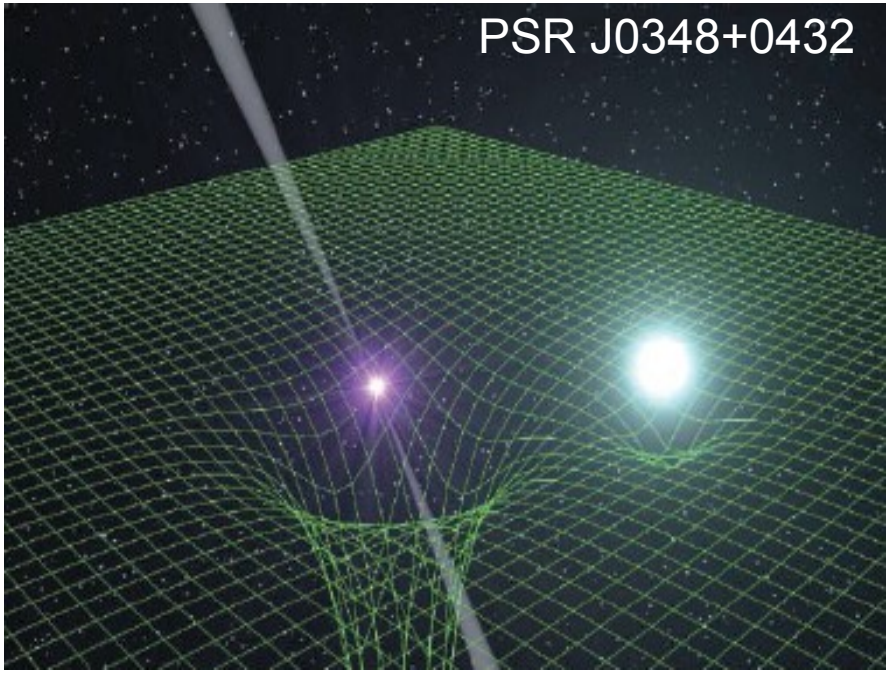

Antoniadis et al., Science 340 (2013) 448
Demorest et al., Nature 467 (2010) 1081

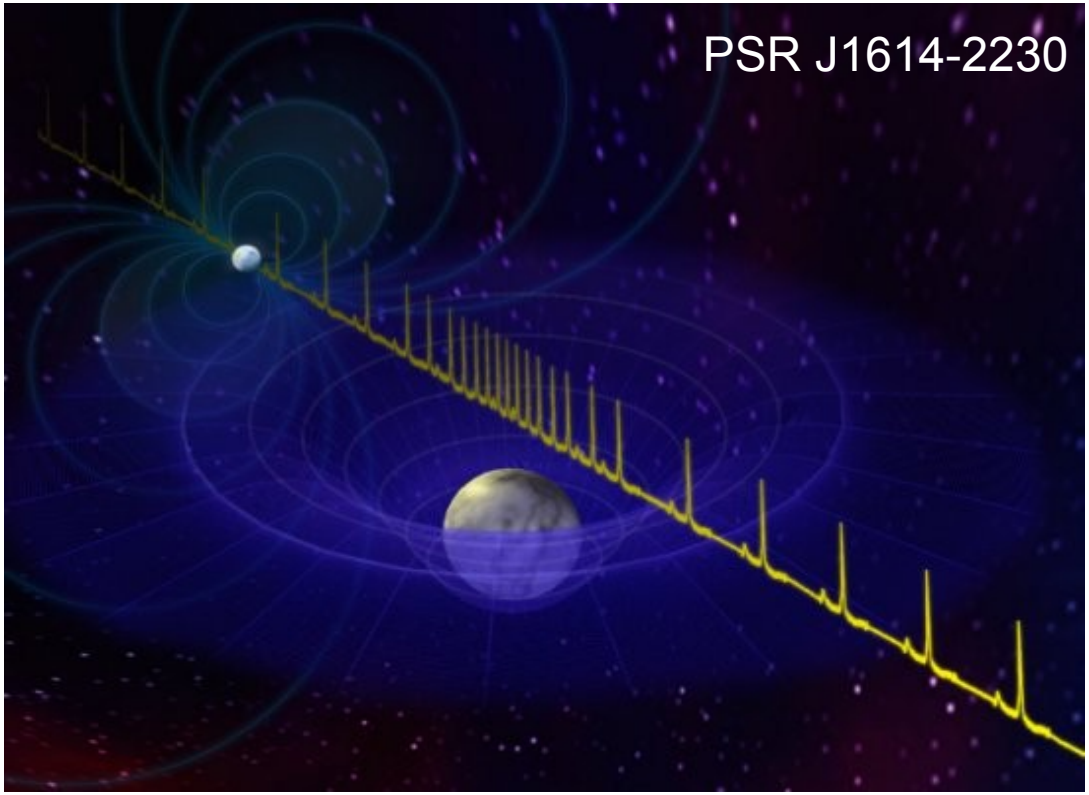

Int. Conf. on New Frontiers in Physics, Kolymbari, 29.08.2015

DUBNA

Quark Matter in Compact Stars & Heavy-Ion Coll.

David Blaschke (University of Wroclaw, Poland & JINR Dubna, Russia)

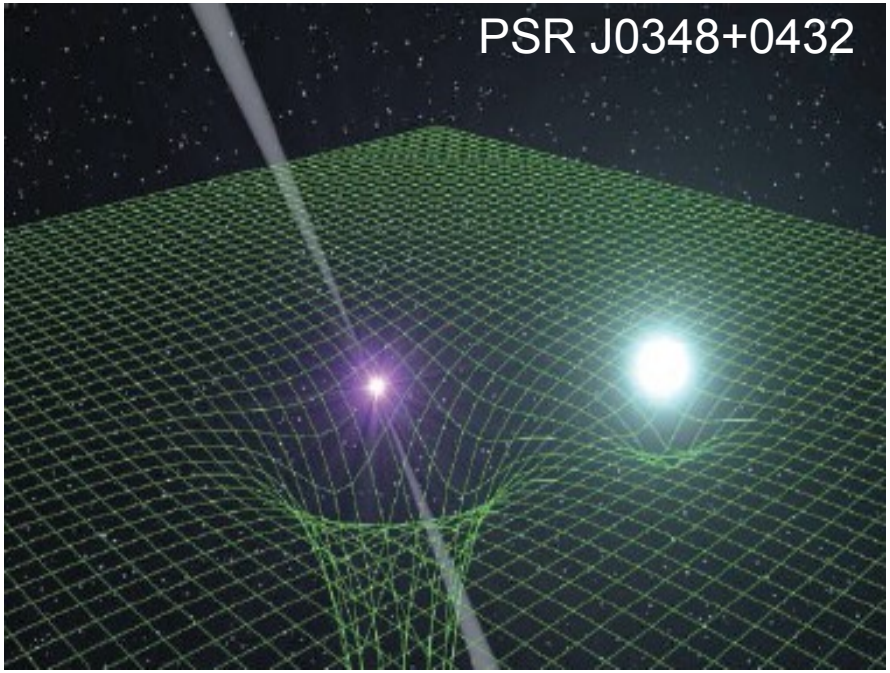

Antoniadis et al., Science 340 (2013) 448

http://theor0.jinr.ru/twiki~cgi/view/NICA/WebHome

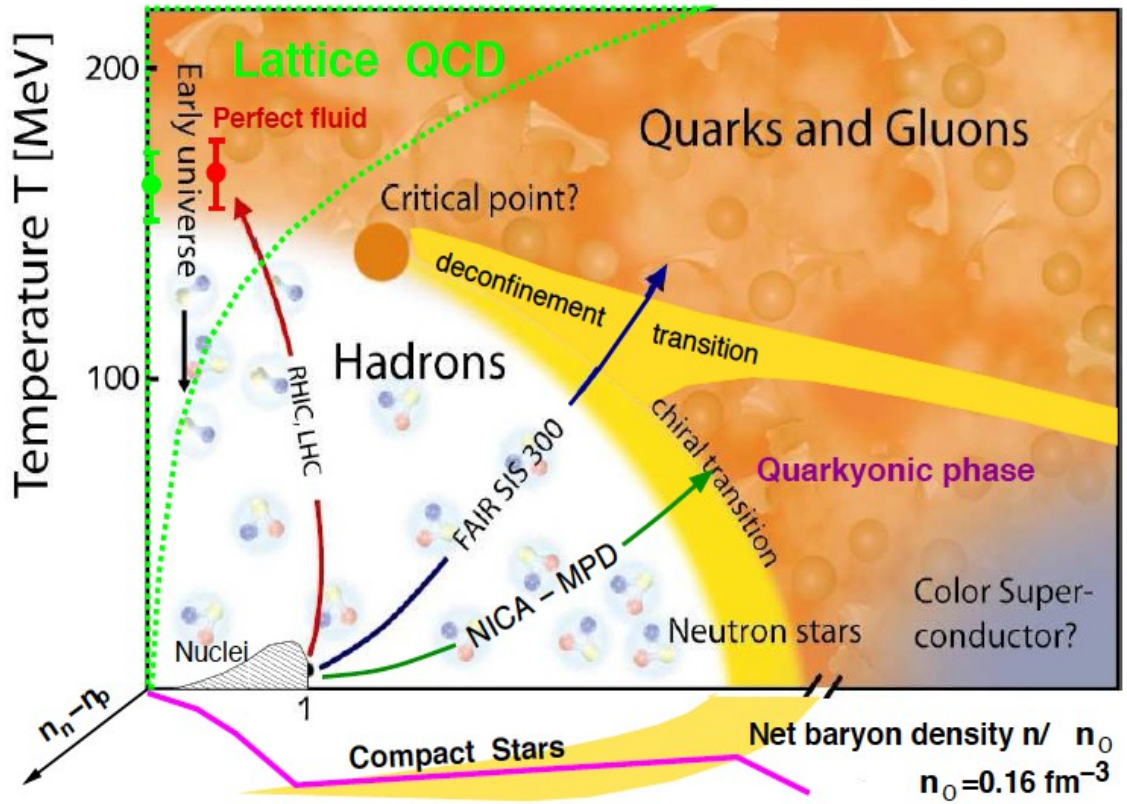

Int. Conf. on New Frontiers in Physics, Kolymbari, 29.08.2015

DUBNA

NAVI

NARODOWE CENTRUM NAUKI

Uniwersytet Wrocławski

Quark Matter in Compact Stars & Heavy-Ion Coll.

David Blaschke (University of Wroclaw, Poland & JINR Dubna, Russia)

0. Support for the QCD Critical EndPoint from Astrophysics?!

1. "Measuring" the cold Equation of States with Compact Stars

2. Microphysics of strong 1st order Phase Transitions

3. New Bayesian Analysis Scheme

4. Hybrid Star Matter @ NICA & FAIR

The New is often the well-forgotten Old

cost
EUROPEAN COOPERATION
IN SCIENCE AND TECHNOLOGY

Int. Conf. on New Frontiers in Physics, Kolymbari, 29.08.2015

JOINT INSTITUTE FOR NUCLEAR RESEARCH
JINR
DUBNA

NAVI

NARODOWE CENTRUM NAUKI

Uniwersytet Wrocławski

Support a CEP in QCD phase diagram with Astrophysics?

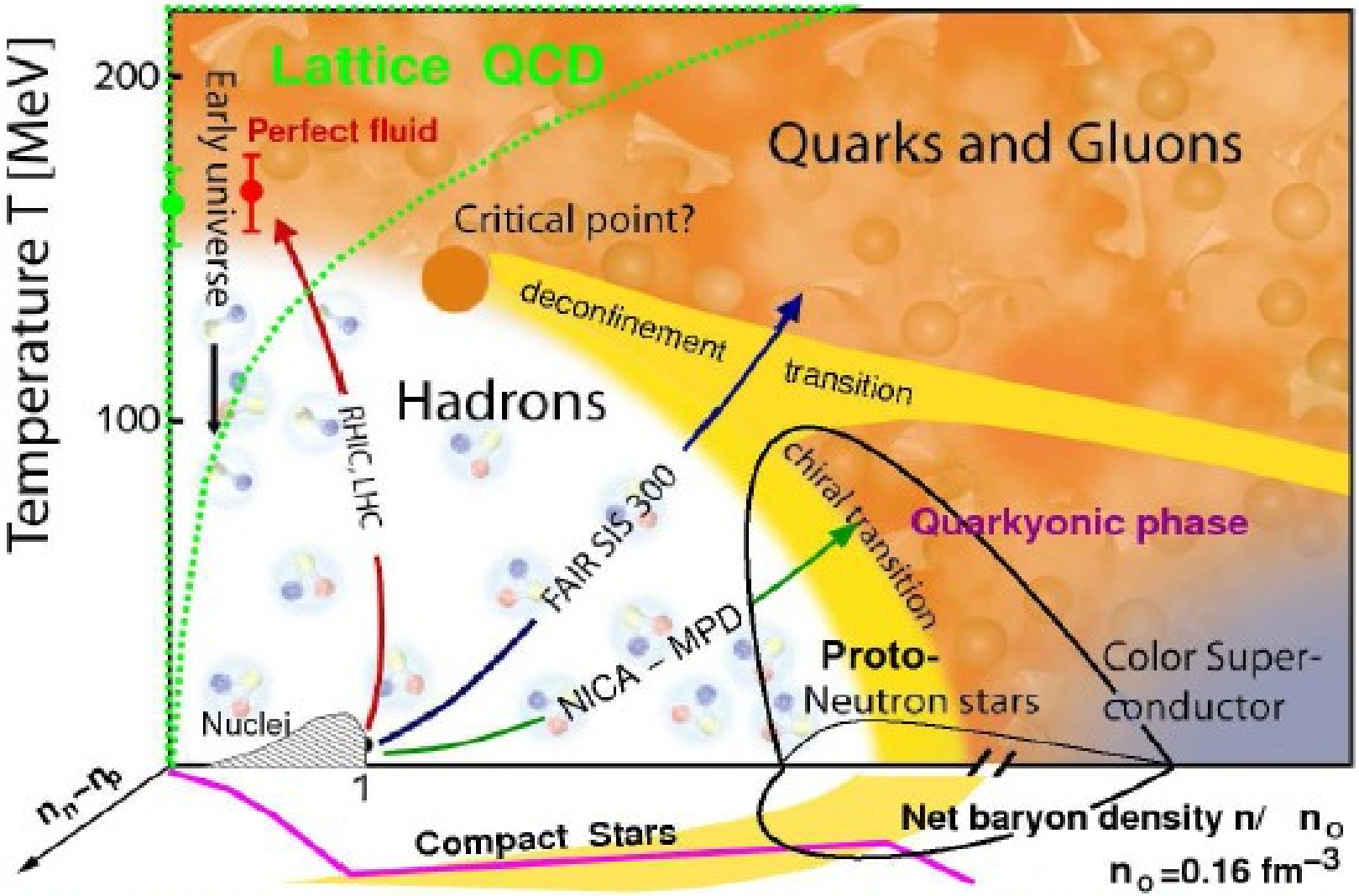

NICA White Paper, http://theor.jinr.ru/twiki-cgi/view/NICA/WebHome

Crossover at finite T (Lattice QCD) + First order at zero T (Astrophysics) = Critical endpoint exists!

Goal: Measure the cold EoS !

Direct approach:

EoS is given as P(ρ)
→ solve the TOV Equation
to find M(R)

Idea: Invert the approach

Given M(R) → find the EoS

Bayesian analysis

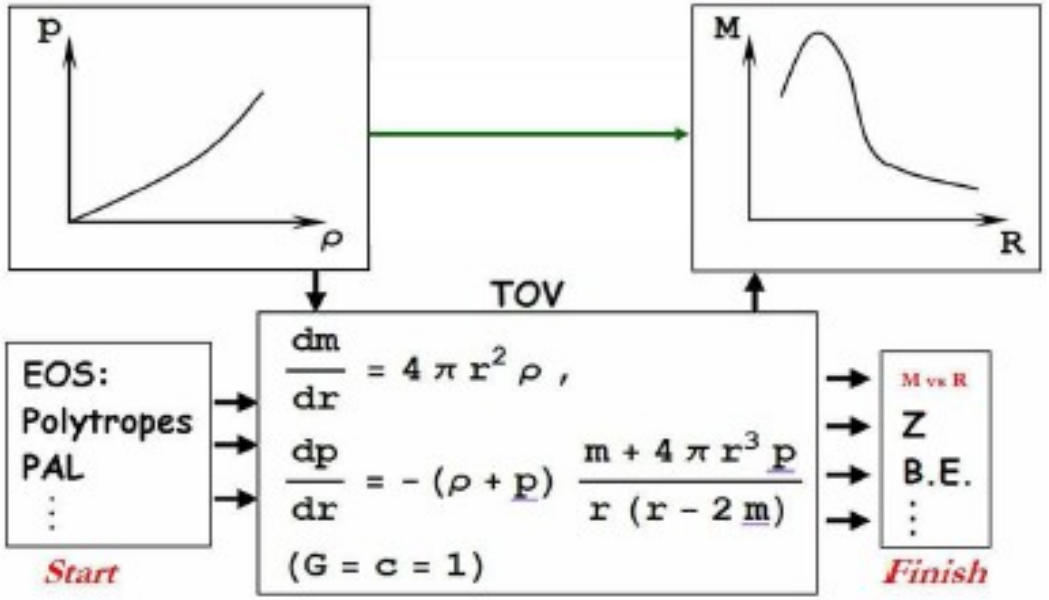

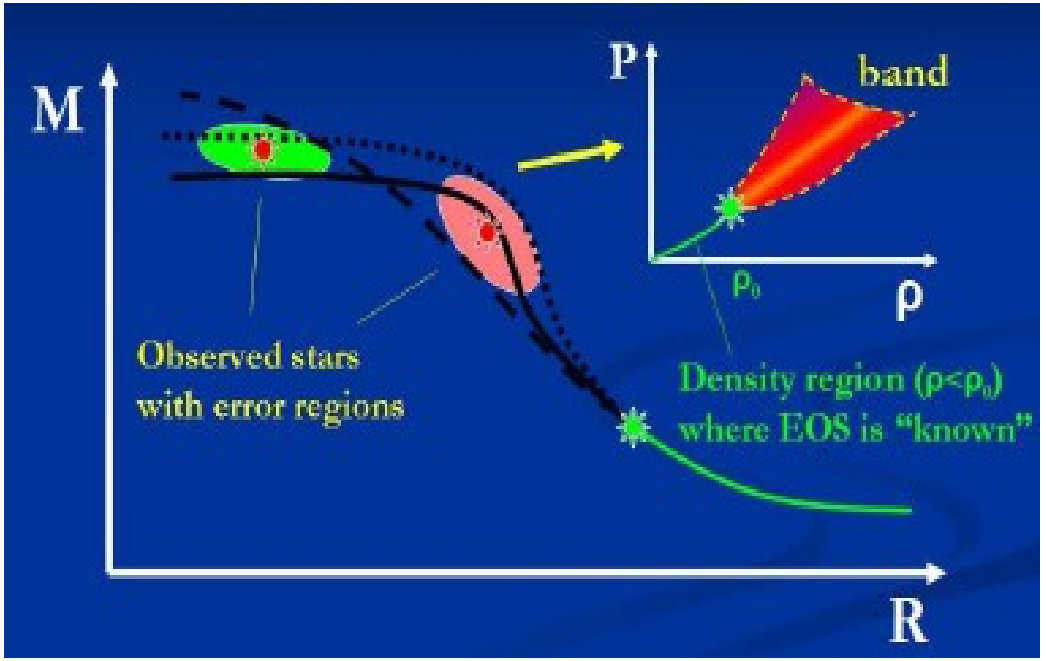

Plots: M. Prakash, Talk Hirschegg 2009

Measure masses and radii of CS!

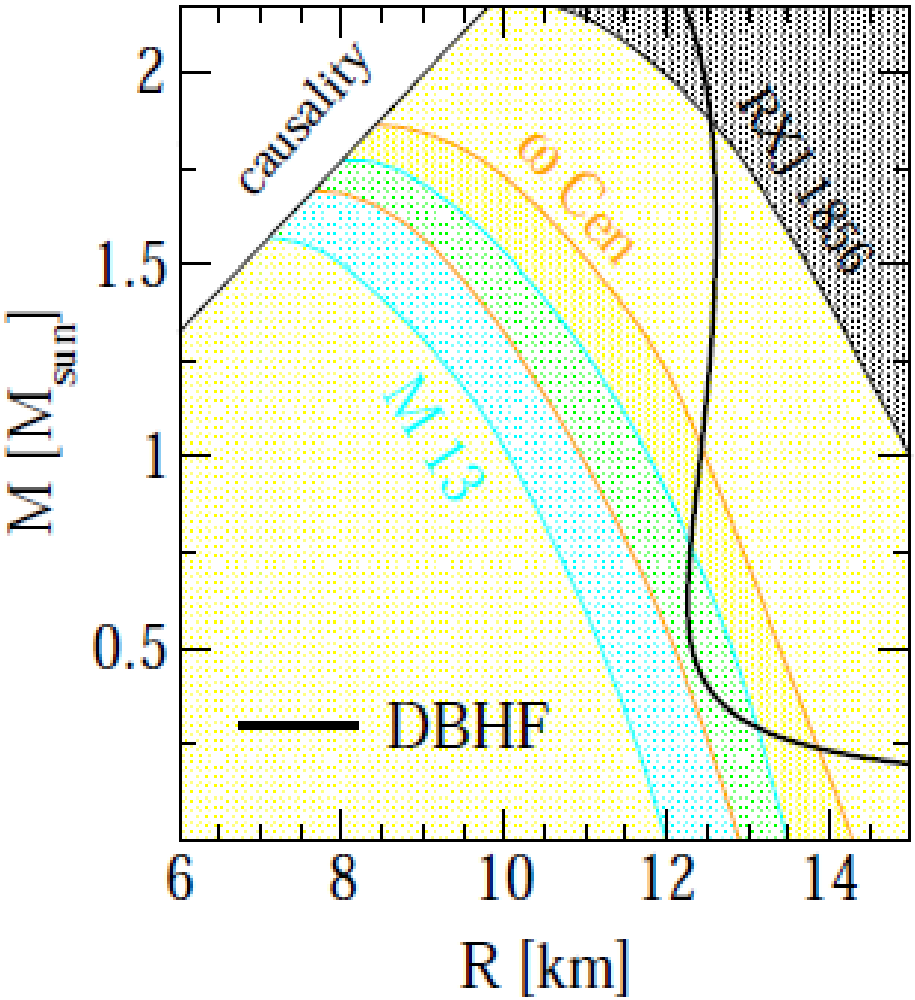

- Distance measured
- Spectrum measured (ROSAT, XMM, Chandra)
- Luminosity measured

→ effective temperature T_∞

→ photospheric radius

$$R_\infty = \frac{R}{\sqrt{1 - R_s/R}}, \qquad R_s = 2GM$$

Object	R_∞ [km]	Reference
RXJ 1856	16.8	Trümper et al. (2004)
ωCen	13.6 $\pm$0.3	Gendre et al. (2003)
M13	12.8 $\pm$0.4	Gendre et al. (2004)

Lower limit from RXJ 1856 incompatible with ω Cen and M13 ?

Measure masses and radii of CS!

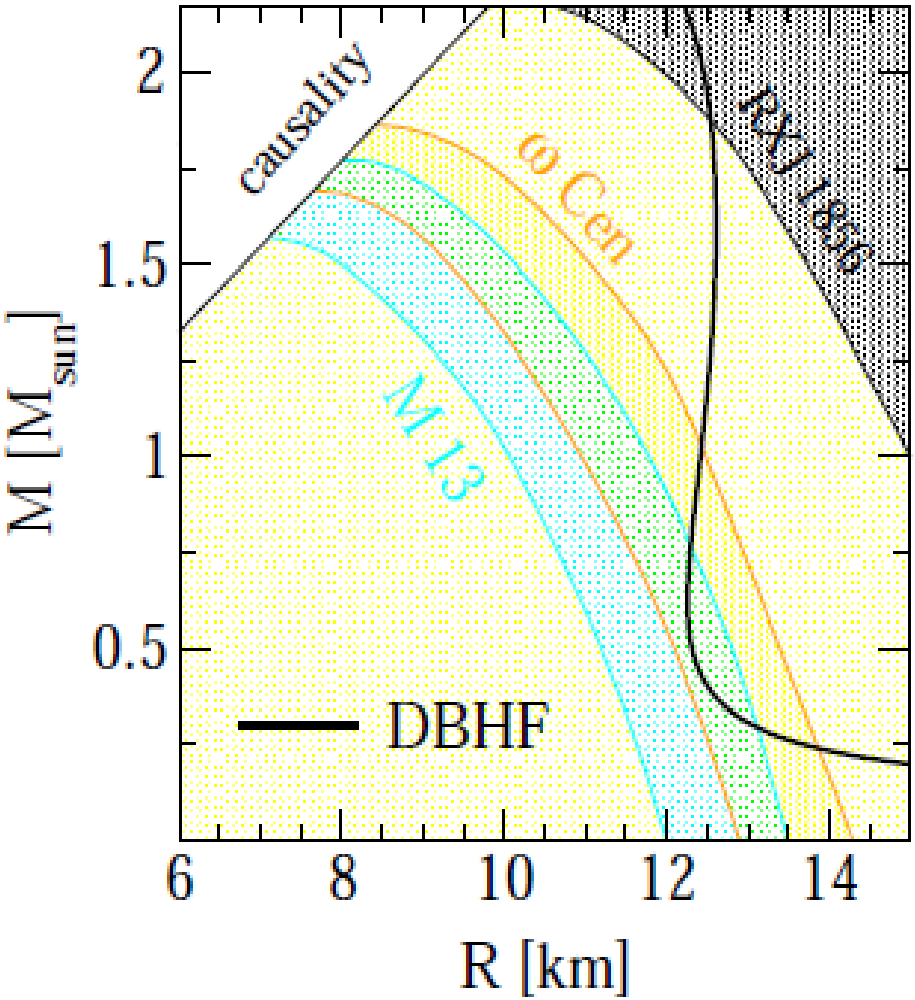

- Distance measured
- Spectrum measured (ROSAT, XMM, Chandra)
- Luminosity measured

→ effective temperature T_∞

→ photospheric radius

$$R_\infty = \frac{R}{\sqrt{1 - R_s/R}}, \qquad R_s = 2GM$$

Object	R_∞ [km]	Reference
RXJ 1856	16.8	Trümper et al. (2004)
ωCen	13.6 $\pm$0.3	Gendre et al. (2003)
M13	12.8 $\pm$0.4	Gendre et al. (2004)

Lower limit from RXJ 1856 incompatible with ω Cen and M13 ?

... unless the latter sources emit X-rays from “hot spots” → lower limit on R

The lesson learned from RX J1856

blackbody fits to the optical and X-ray spectra of RX J1856.5-3754 (Trümper,2004)

radius determination ⇒ EoS ⇒ state of matter at high densities

two-component model

model with continuous T-distribution

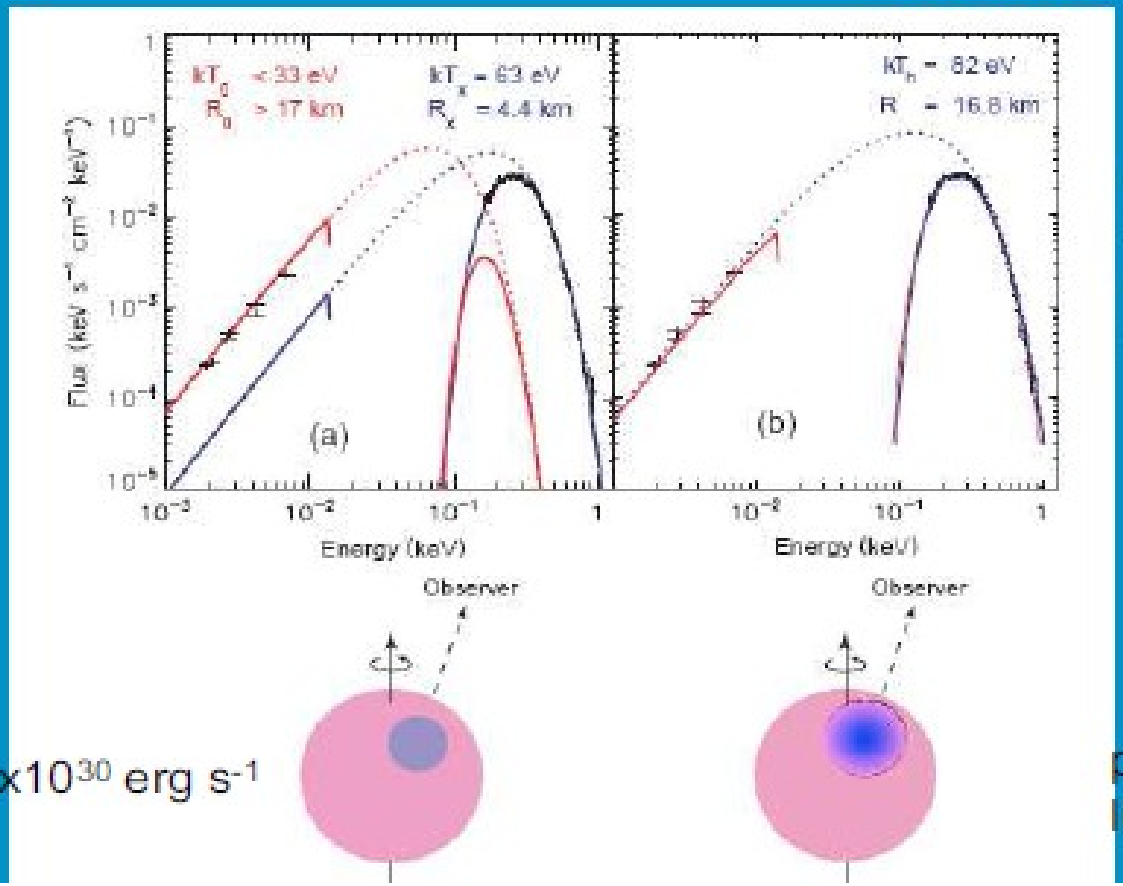

completely featureless X-ray spectrum: condensed surface? ⇒ strong B?

$L_x = 5.4 \times 10^{30}$ erg s^{-1}

pulsed fraction < 1% ⇒ line of sight || rotation axis?

X-ray emitting region is a “hot spot”, J. Trumper et al., Nucl. Phys. Proc. Suppl. 132 (2004) 560

Which constraints can be trusted ?

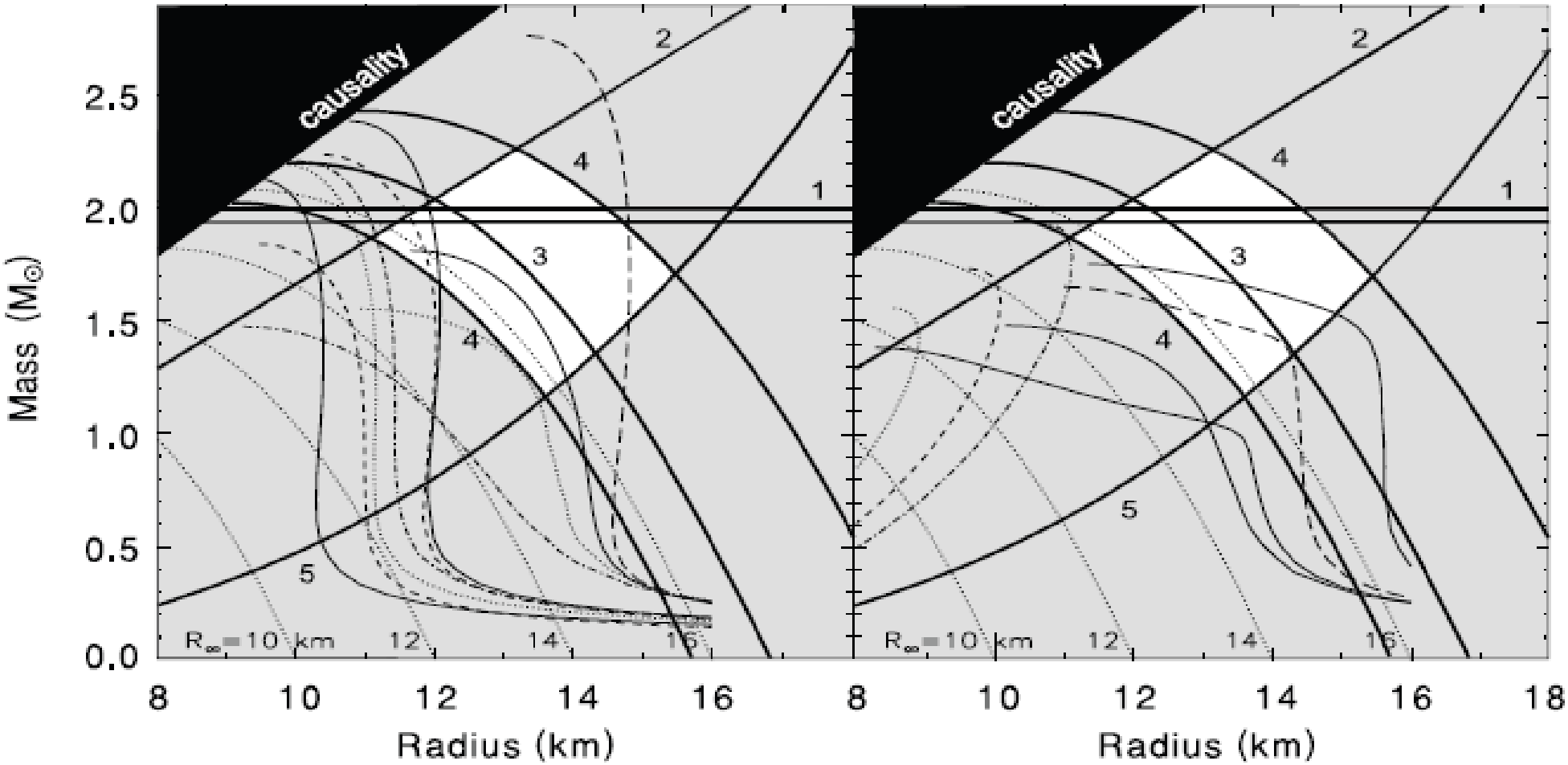

1 – Largest mass J1614 – 2230 (Demorest et al. 2010)
2 – Maximum gravity XTE 1814 – 338 (Bhattacharyya et al. (2005)
3 – Minimum radius RXJ 1856 – 3754 (Trumper et al. 2004)
4 – Radius, 90% confidence limits LMXB X7 in 47 Tuc (Heinke et al. 2006)
5 – Largest spin frequency J1748 – 2446 (Hessels et al. 2006)

Which constraints can be trusted ?

Nearest millisecond pulsar PSR J0437 – 4715 revisited by XMM Newton
Distance: d = 156.3 +/- 1.3 pc
Period: P= 5.76 ms, dot P = 10^-20 s/s, field strength B = 3x10^8 G

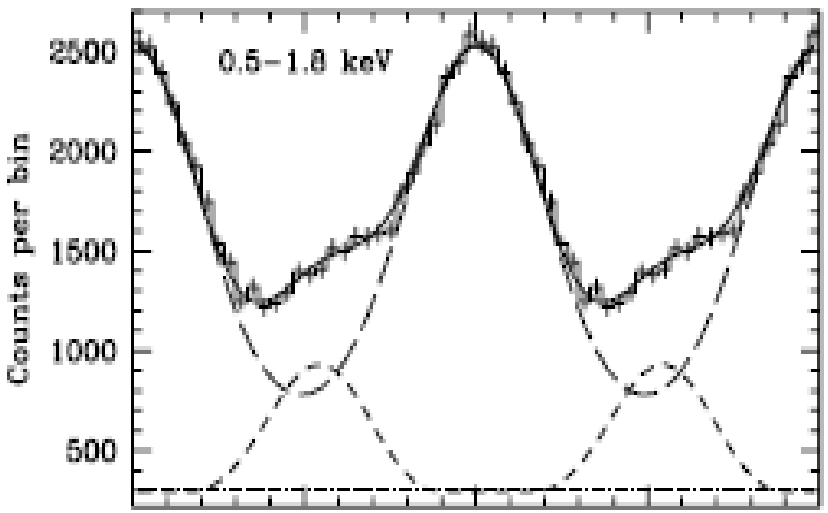

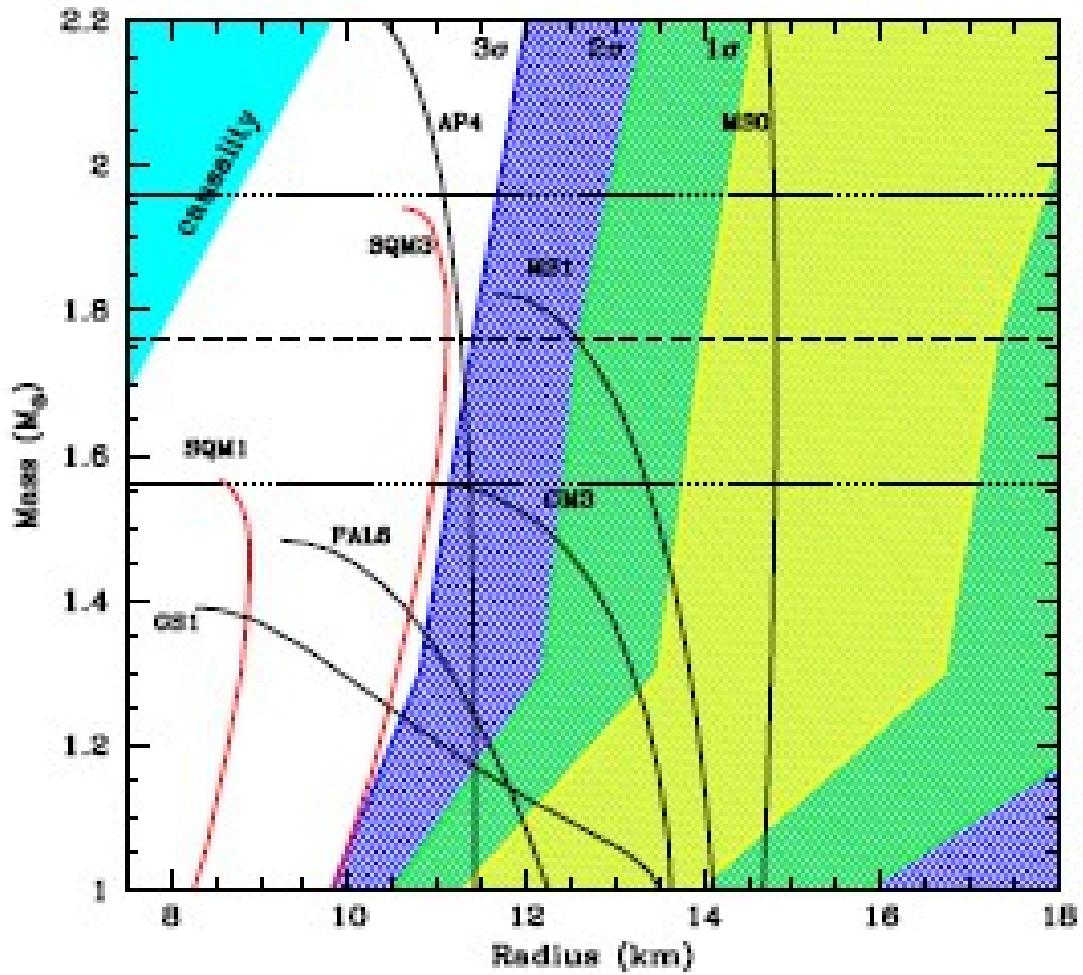

Three thermal component fit
R > 11.1 km (at 3 sigma level)
M = 1.76 M_sun

S. Bogdanov, arxiv:1211.6113 (2012)

Measure the cold EoS by Bayesian TOV!

Bayesian TOV analysis:
Steiner, Lattimer, Brown, ApJ 722 (2010) 33

Most Probable Values for Masses and Radii for Neutron Stars Constrained to Lie on One Mass Versus Radius Curve

Object	$M\ (M_\odot)$	R (km)	$M\ (M_\odot)$	R (km)
	$r_{ph} = R$		$r_{ph} \gg R$	
4U 1608–522	$1.52^{+0.22}_{-0.18}$	$11.04^{+0.53}_{-1.50}$	$1.64^{+0.34}_{-0.41}$	$11.82^{+0.42}_{-0.89}$
EXO 1745–248	$1.55^{+0.12}_{-0.36}$	$10.91^{+0.86}_{-0.65}$	$1.34^{+0.450}_{-0.28}$	$11.82^{+0.47}_{-0.72}$
4U 1820–30	$1.57^{+0.13}_{-0.15}$	$10.91^{+0.39}_{-0.92}$	$1.57^{+0.37}_{-0.31}$	$11.82^{+0.42}_{-0.82}$
M13	$1.48^{+0.21}_{-0.64}$	$11.04^{+1.00}_{-1.28}$	$0.901^{+0.28}_{-0.12}$	$12.21^{+0.18}_{-0.62}$
ω Cen	$1.43^{+0.26}_{-0.61}$	$11.18^{+1.14}_{-1.27}$	$0.994^{+0.51}_{-0.21}$	$12.09^{+0.27}_{-0.66}$
X7	$0.832^{+1.19}_{-0.051}$	$13.25^{+1.37}_{-3.50}$	$1.98^{+0.10}_{-0.36}$	$11.3^{+0.95}_{-1.03}$

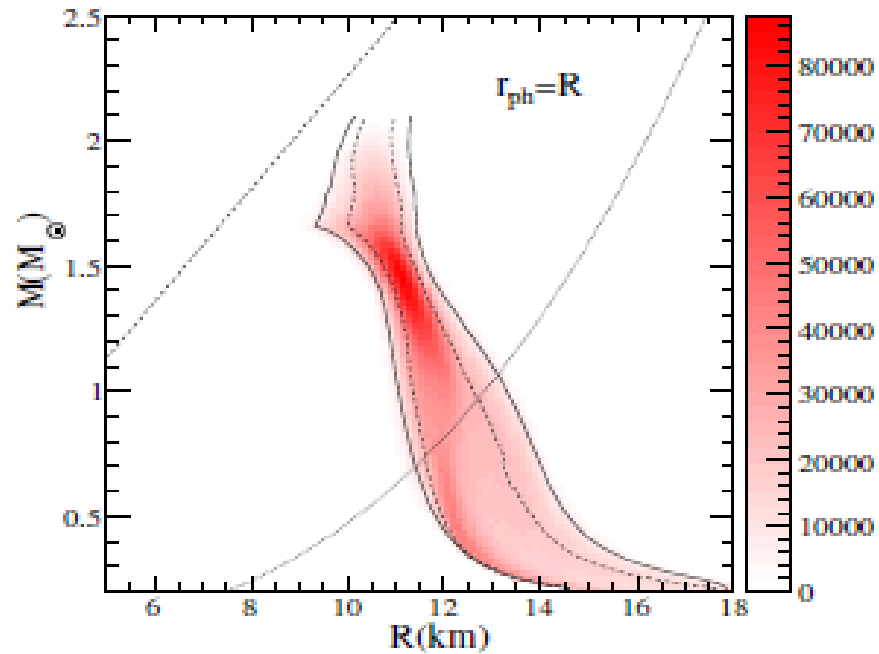

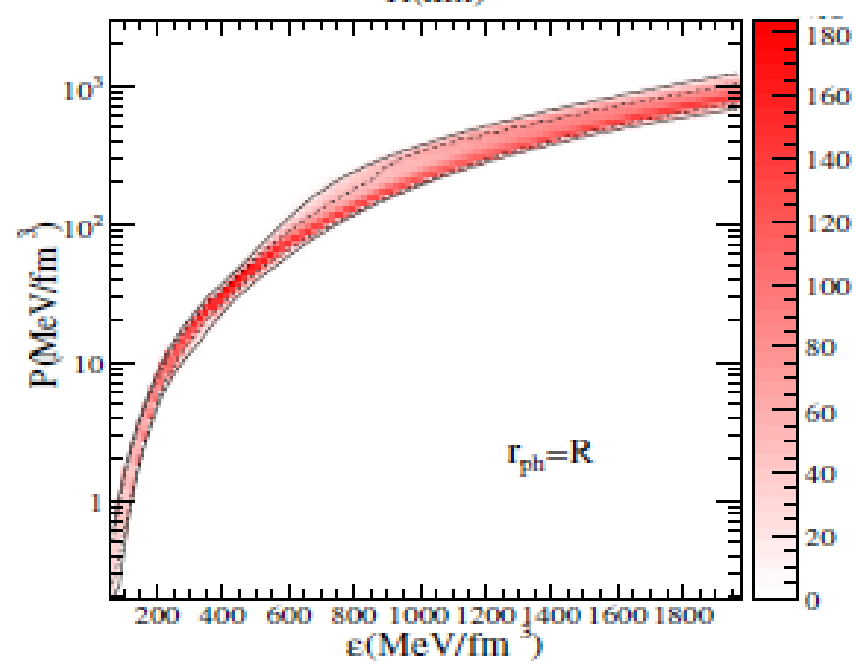

Caution:
If optical spectra are not measured, the observed X-ray spectrum may not come from the entire surface But from a hot spot at the magnetic pole!
J. Trumper, Prog. Part. Nucl. Phys. 66 (2011) 674

Such systematic errors are not accounted for in Steiner et al. → M(R) is a lower limit → softer EoS

Which constraints require caution ?

A. Steiner, J. Lattimer, E. Brown, ApJ Lett. 765 (2013) L5

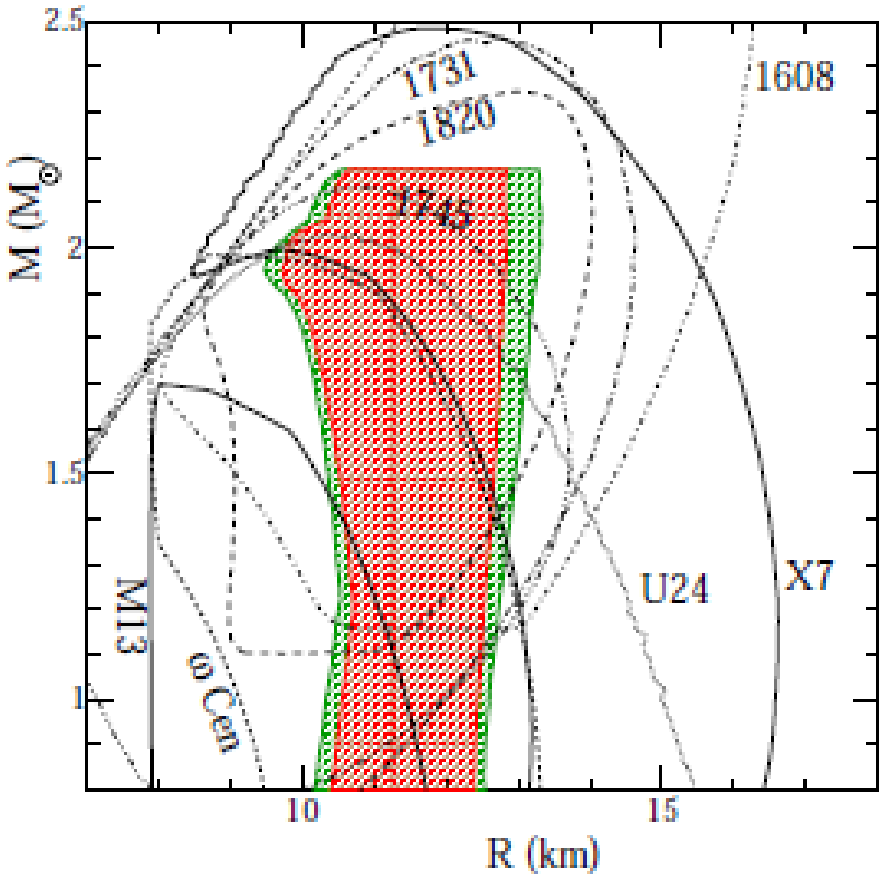

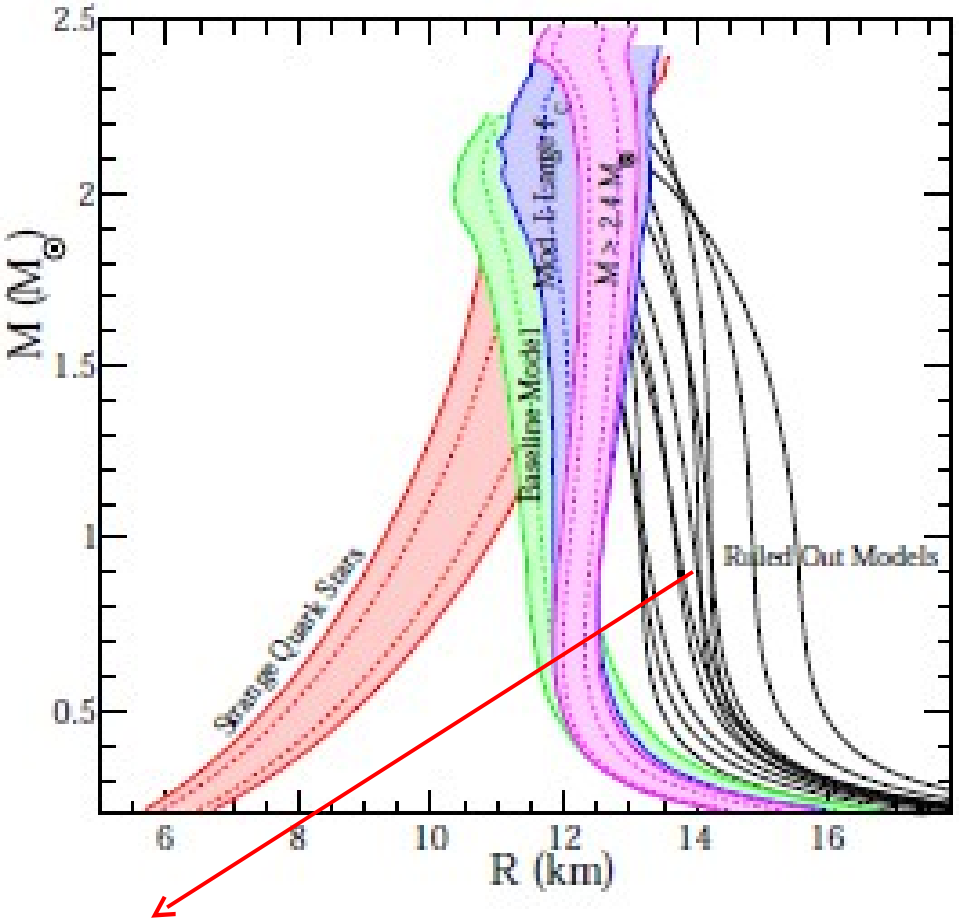

"Ruled out models" - too strong a conclusion!
M(R) constraint is a lower limit, which is itself included in that from RX J1856, which is one of the best known sources.

Key fact: Mass "twins" ↔ 1st order PT

Alford, Han, Prakash, arxiv:1302.4732

First order PT can lead to a stable branch of hybrid stars with quark matter cores which, depending on the size of the "latent heat" (jump in energy density), can even be disconnected from the hadronic one by an unstable branch → **"third family of CS"**.

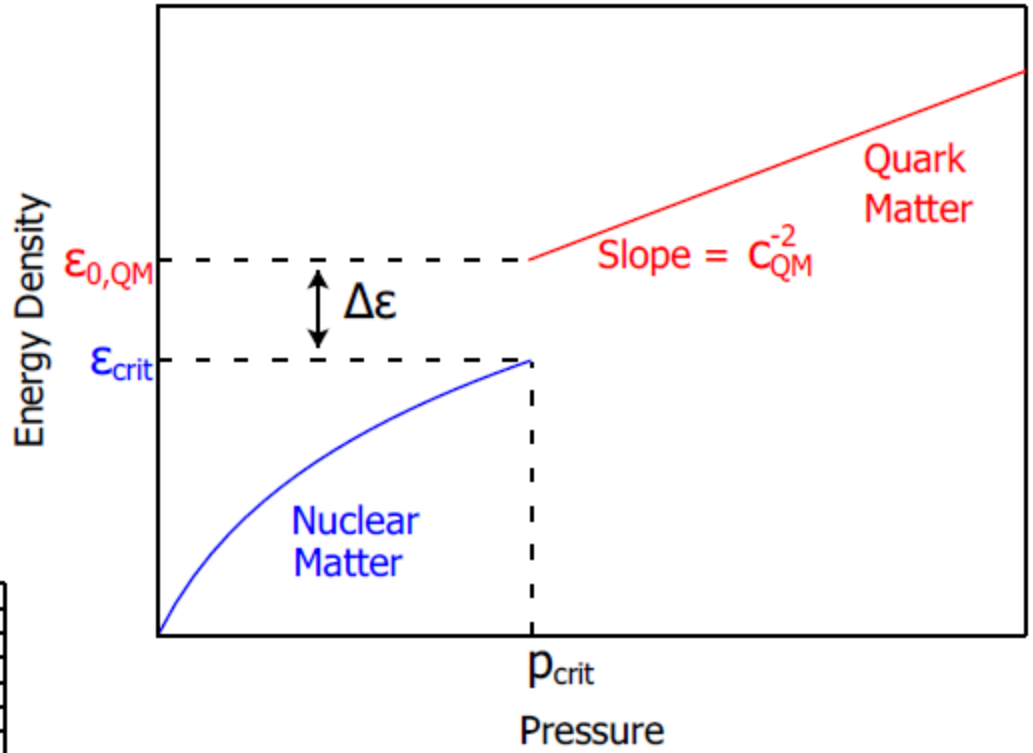

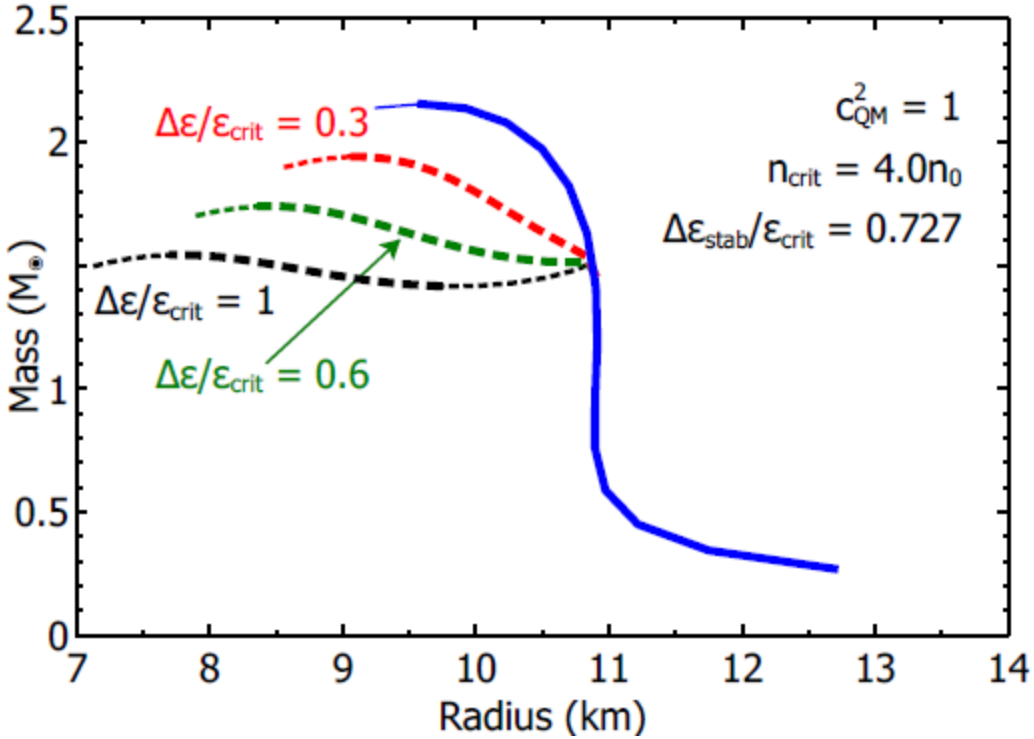

Measuring two **disconnected populations** of compact stars in the M-R diagram would be the **detection of a first order phase transition** in compact star matter and thus the indirect proof for the existence of a **critical endpoint (CEP) in the QCD phase diagram**!

Key fact: Mass "twins" ↔ 1st order PT

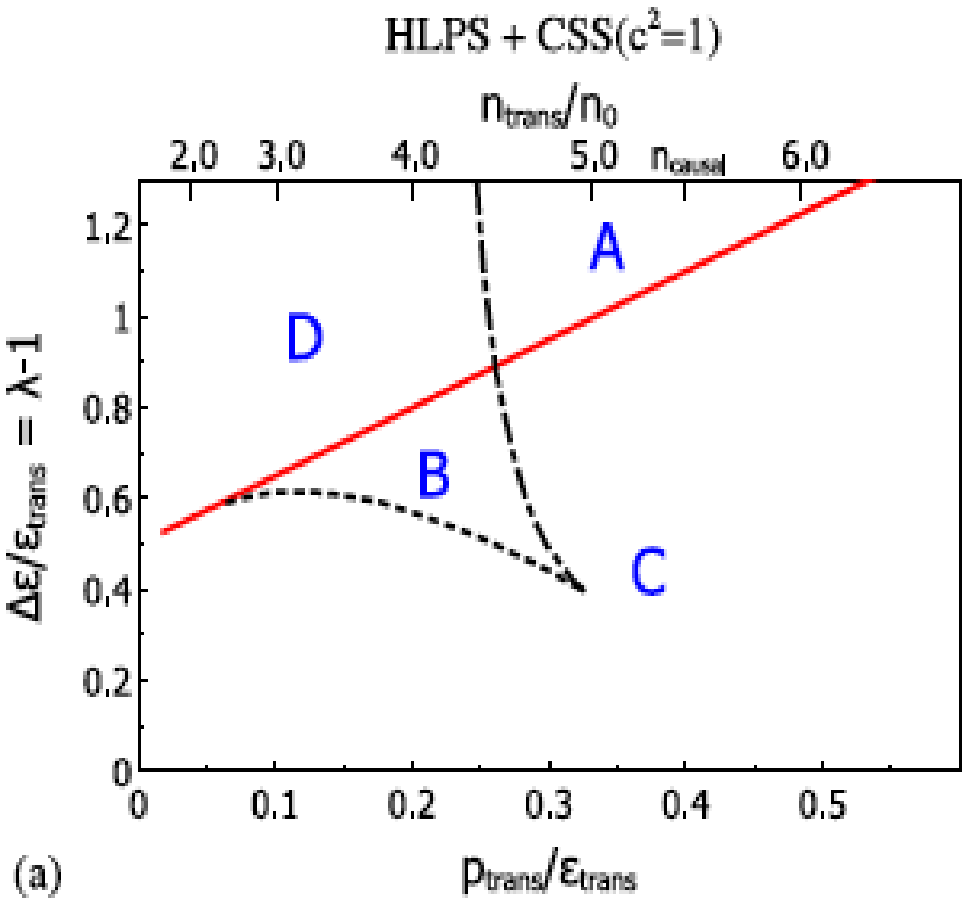

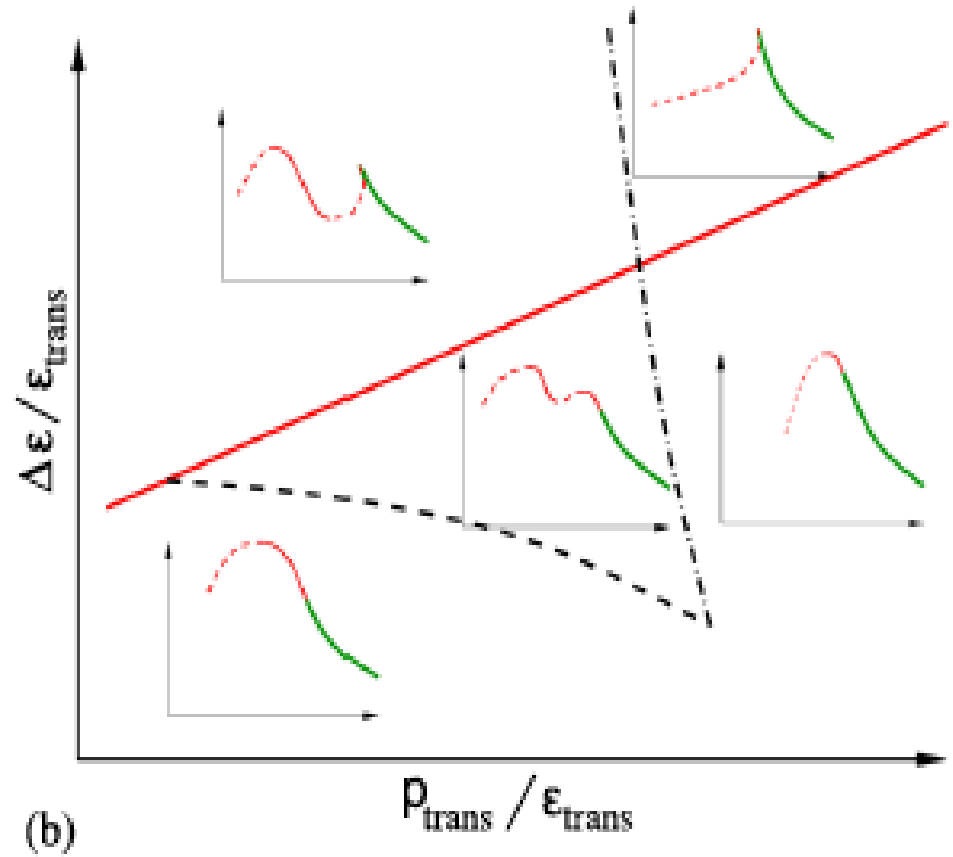

Systematic Classification [Alford, Han, Prakash: PRD88, 083013 (2013)]

EoS P(ε) <--> Compact star phenomenology M(R)

Most interesting and clear-cut cases: (D)isconnected and (B)oth – high-mass twins!

“Holy Grail” - High-Mass Twin Stars

Twins prove exitence of **disconnected populations** (third family) in the M-R diagram
Consequence of a **first order phase transition**
Question: Do twins prove the 1st order phase trans.?

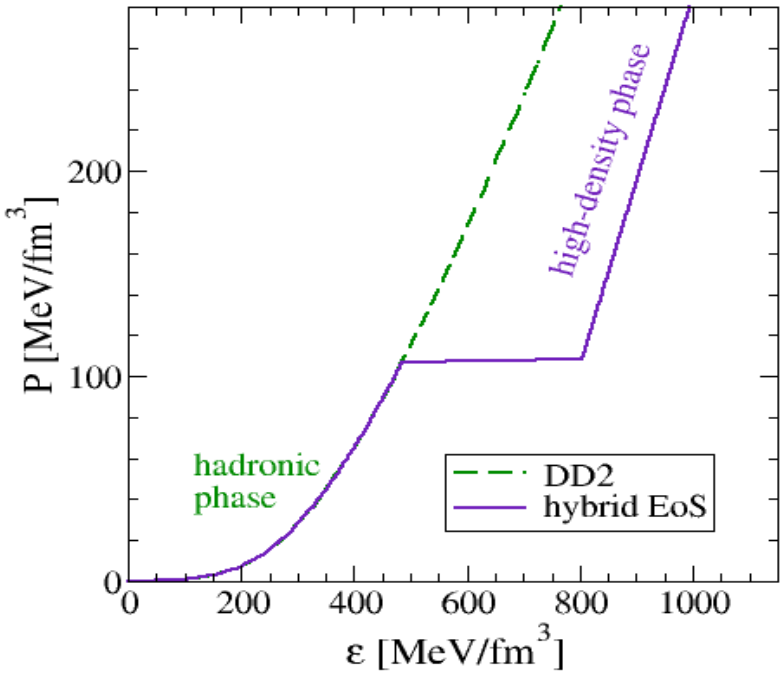

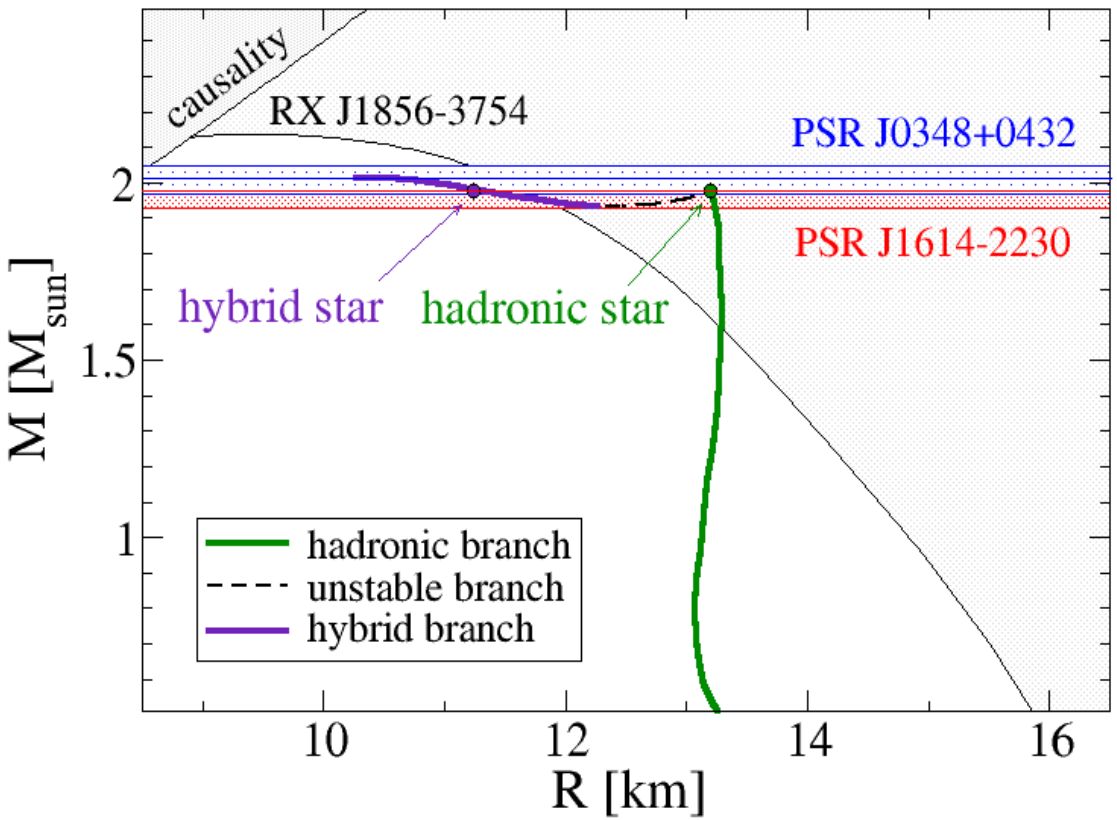

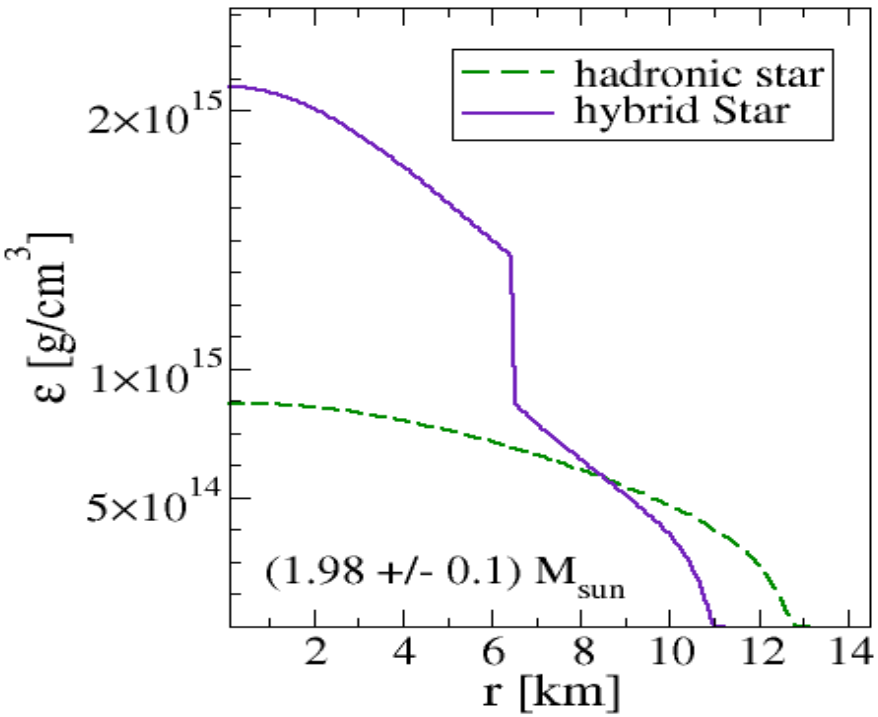

Alvarez & Blaschke, arxiv:1304.7758

Hyperon puzzle & quark matter

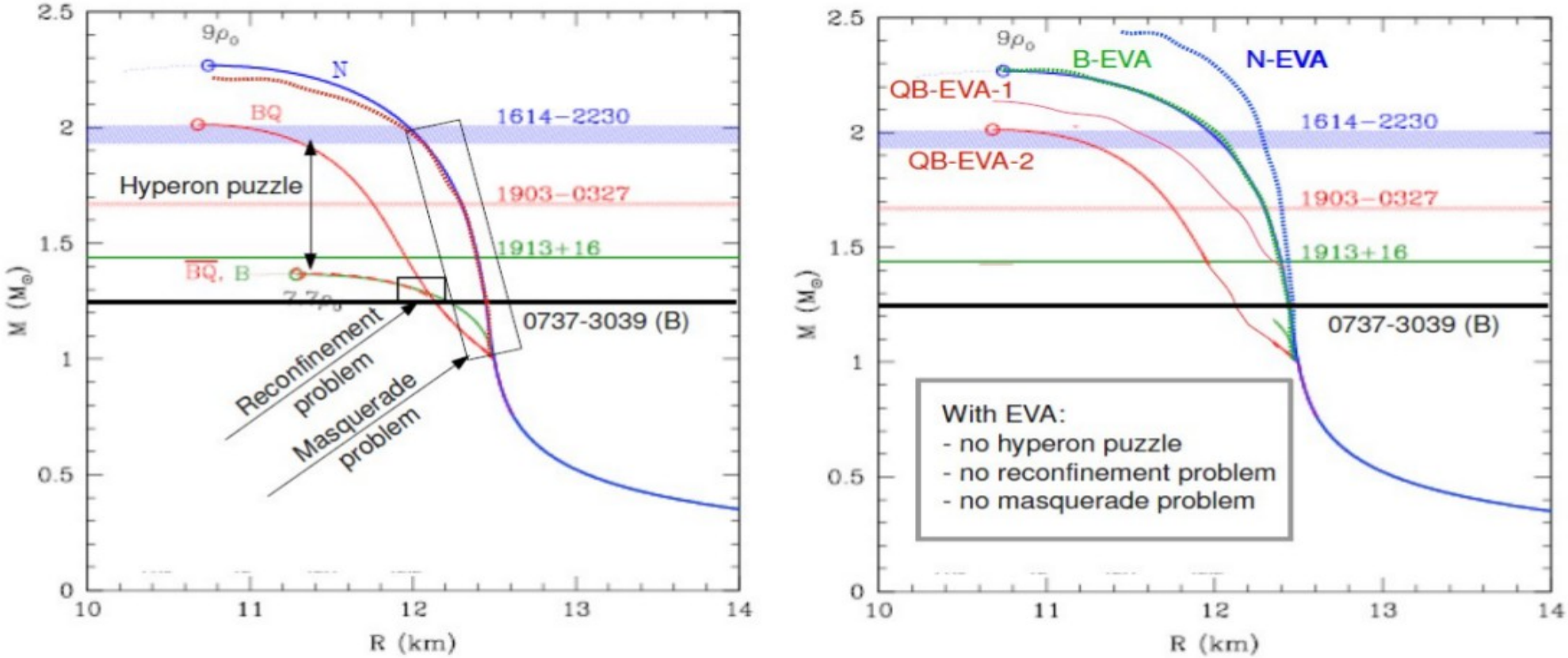

Mass-radius sequences for different model equations of state (EoS) illustrate how the **three major problems** in the theory of exotic matter in compact stars (left panel) can be solved (right panel) by taking into account the baryon size effect within a excluded volume approximation (EVA). Due to the EVA both, the nucleonic (N-EVA) and hyperonic (B-EVA) EoS get sufficiently stiffened to describe high-mass pulsars so that the hyperon puzzle gets solved which implies a removal of the reconfinement problem. Since the EVA does not apply to the quark matter EoS it shall be always sufficiently different from the hadronic one so that the masquerade problem is solved.

2. Microphysical approach to strong 1st order PT

2.1. Pauli blocking among baryons

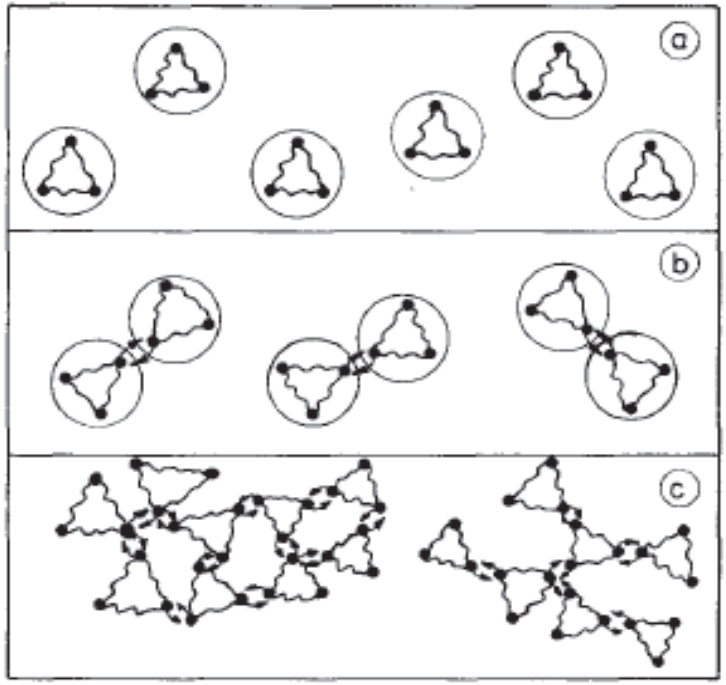

a) Low density: Fermi gas of nucleons (baryons)

b) ~ saturation: Quark exchange interaction and Pauli blocking among nucleons (baryons)

c) high density: Quark cluster matter (string-flip model ...)

Roepke & Schulz, Z. Phys. C 35, 379 (1987); Roepke, DB, Schulz, PRD 34, 3499 (1986)

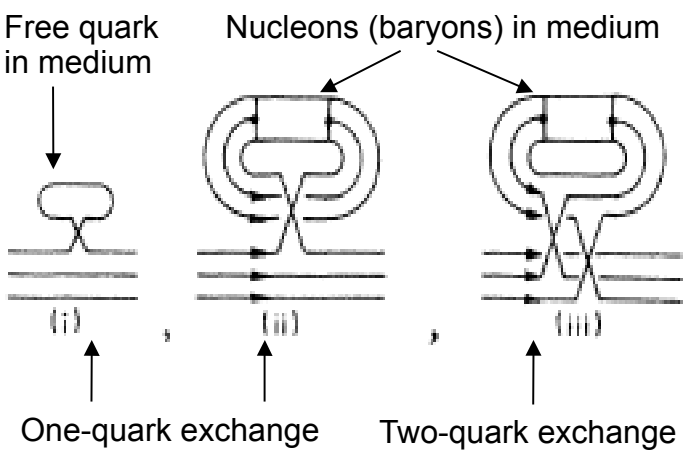

Nucleon (baryon) self-energy --> Energy shift

$$\Delta E_{\nu P}^{\text{Pauli}} = \sum_{123} |\psi_{\nu P}(123)|^2 [E(1)+E(2)+E(3)-E_{\nu P}^0][f_{\alpha_1}(1)+f_{\alpha_2}(2)+f_{\alpha_3}(3)]$$

$$+\sum_{123}\sum_{456}\sum_{\nu' P'} \psi_{\nu P}^*(123)\psi_{\nu' P'}(456) f_3(E_{\nu' P'}^0)\{\delta_{36}\psi_{\nu P}(123)\psi_{\nu' P'}^*(456)-\psi_{\nu P}(453)\psi_{\nu' P'}^*(126)\}$$

$$\times[E(1)+E(2)+E(3)+E(4)+E(5)+E(6)-E_{\nu P}^0-E_{\nu' P'}^0]$$

$$=\Delta E_{\nu P}^{\text{Pauli, free}}+\Delta E_{\nu P}^{\text{Pauli, bound}} .$$

2.1. Pauli blocking among baryons - details

$$\Sigma_\nu(p, p_{Fn}, p_{Fp}) = \sum_{\nu'=\{n,p\}} \sum_{\alpha=1,2} C^{(\alpha)}_{\nu\nu'} W_\alpha(p_{F\nu'}, p)$$

$$W_\alpha(p_{F\nu'}, p) = \frac{\Omega}{2\pi^2} \int_0^{p_{F\nu'}} p'^2 \bar{V}^{(\alpha)}(p, p') dp';$$

$$\bar{V}^{(\alpha)}(p, p') = \frac{1}{2} \int_{-1}^{1} V^{(\alpha)}(\vec{p}, \vec{p}') dz;$$

$$V^{(\alpha)}(\vec{p}, \vec{p}') = \frac{V_0 b}{\Omega m} \left(\frac{15}{2} - \lambda_\alpha^2 (\vec{p} - \vec{p}')^2 \right) \exp(-\lambda_\alpha^2 (\vec{p} - \vec{p}')^2).$$

	$C^{(1)}_{n\,\nu}$	$C^{(2)}_{n\,\nu}$
neutron	$-\frac{96}{243}$	$\frac{10}{27}$
proton	$-\frac{28}{81}$	$\frac{8}{27}$

$$b^{-2} = \sqrt{3} m \omega$$

$$\omega = 178.425 \text{ MeV}$$

$$m = 350 \text{ MeV} \qquad b = 0.6 \text{ fm}$$

$$V_0 = \frac{9\sqrt{3}\pi^{3/2}}{2} \text{ and } \lambda_\alpha = \frac{b}{\sqrt{3}\alpha}.$$

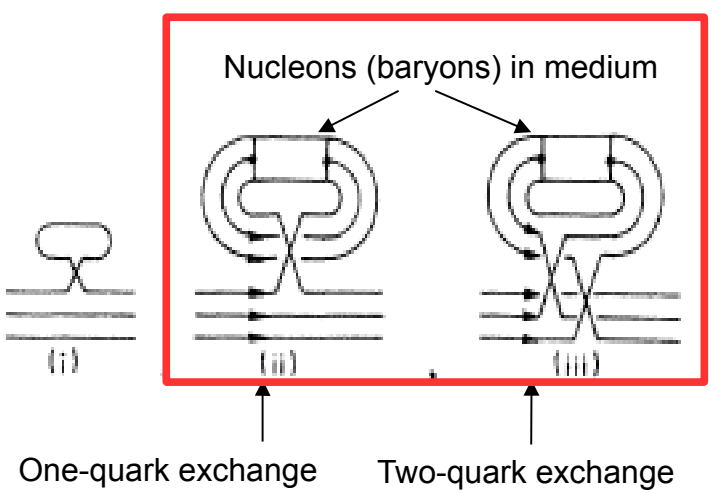

$$W_\alpha(p_{F\nu'}, p) = \frac{V_0 b}{32\pi^2 \lambda_\alpha^4 m} \{12\lambda_\alpha \sqrt{\pi} [\text{erf}(\lambda_\alpha(p_{F\nu'} - p)) + \text{erf}(\lambda_\alpha(p_{F\nu'} + p))]$$
$$+ \frac{1}{p} [(11 - 2\lambda_\alpha^2 p_{F\nu'}(p_{F\nu'} + p)) e^{-\lambda_\alpha^2 (p_{F\nu'} + p)^2}$$
$$+ (11 - 2\lambda_\alpha^2 p_{F\nu'}(p_{F\nu'} - p)) e^{-\lambda_\alpha^2 (p_{F\nu'} - p)^2}]\}$$

$$\Delta^{Pauli}_{\nu_A, P} = \frac{1}{24\sqrt{3\pi}} \frac{b}{m} \sum_{\nu'} [15 a_{\nu,\nu'} P_F(\nu')^3 + \frac{17}{12} b_{\nu,\nu'} b^2 (P^2 + P_F(\nu')^2) P_F(\nu')^3]$$

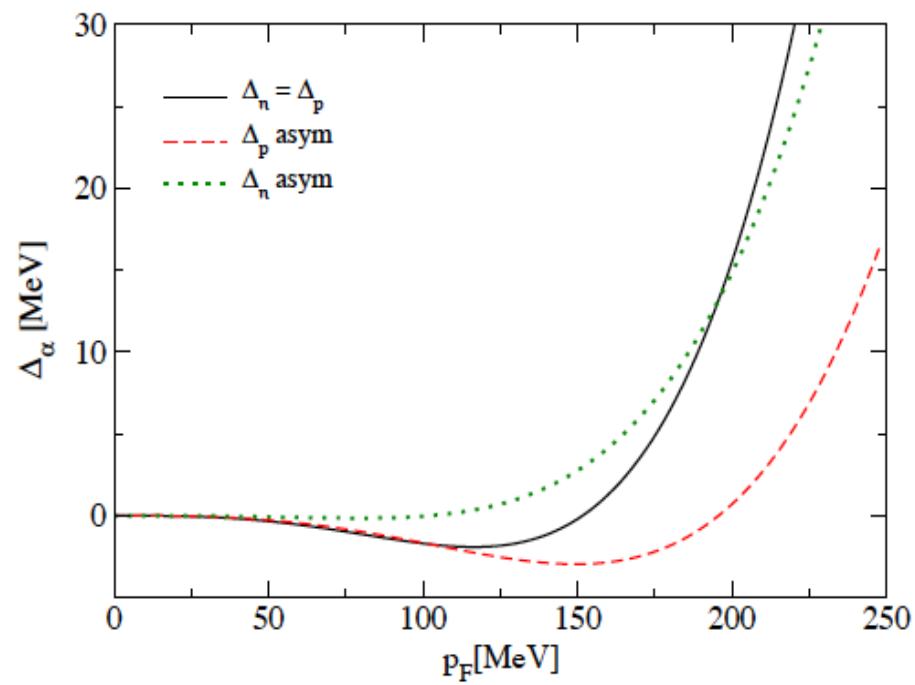

2.1. Pauli blocking among baryons – details

New aspect: chiral restoration --> dropping quark mass

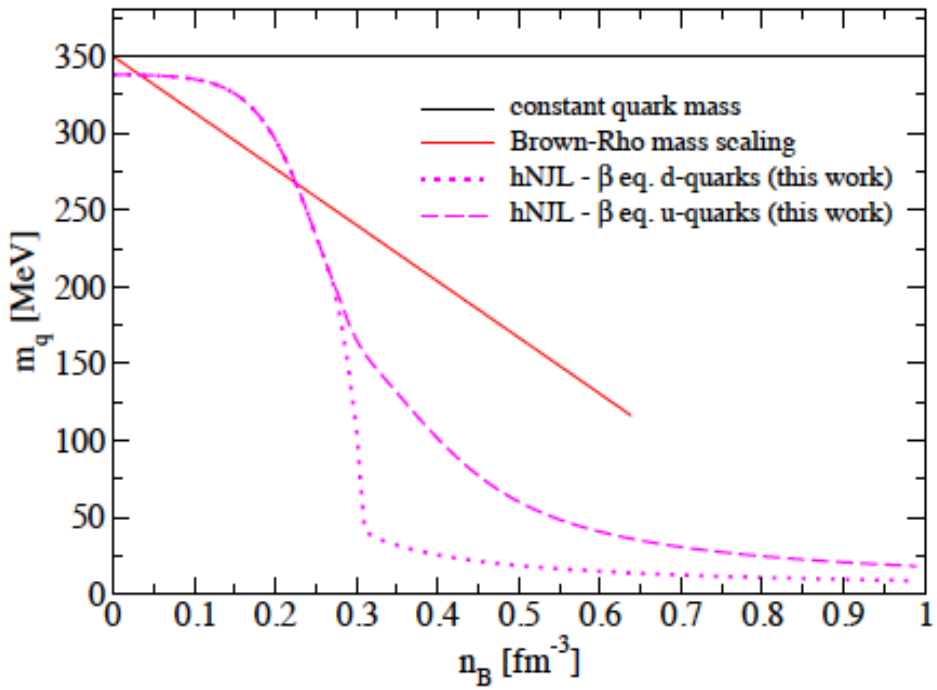

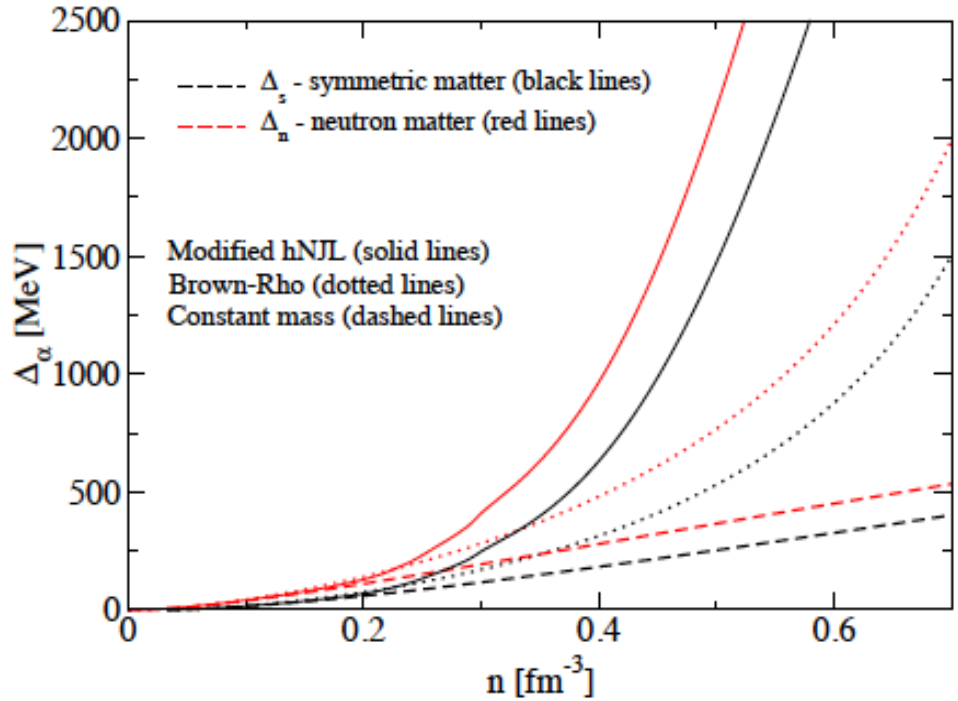

Increased baryon swelling at supersaturation densities:
--> dramatic enhancement of the Pauli repulsion !!

D.B., H. Grigorian, G. Roepke: “Quark exchange effects in dense nuclear matter”, STSM 2014

2.2. Pauli blocking among baryons – results

New EoS: Joining RMF (Linear Walecka) for pointlike baryons with chiral Pauli blocking

$$p = \frac{1}{4\pi^2}\sum_\nu \left[-E_\nu^* m_\nu^{*2} p_{F\nu} + \frac{2}{3}E_\nu^* p_{F\nu}^3 + m_\nu^{*4}\log\left(\frac{E_\nu^* + p_{F\nu}}{m_\nu^*}\right)\right]$$
$$+ \frac{1}{2}\left(\frac{g_\omega}{m_\omega}\right)^2 n^2 - \frac{1}{2}\left(\frac{g_\sigma}{m_\sigma}\right)^2 n_s^2 + p_{ex};$$
$$\epsilon = \frac{1}{4\pi^2}\sum_\nu \left[2\,E_\nu^{*3} p_{F\nu} - E_\nu^* m_\nu^{*2} p_{F\nu} - m_\nu^{*4}\log\left(\frac{E_I^* + p_{F\nu}}{m_\nu^*}\right)\right]$$
$$+ \frac{1}{2}\left(\frac{g_\omega}{m_\omega}\right)^2 n^2 + \frac{1}{2}\left(\frac{g_\sigma}{m_\sigma}\right)^2 n_s^2 + \epsilon_{ex},$$

$$\mu_{ex,\nu} = \Delta_\nu(n,x) = \Sigma_\nu(p_{F,\nu}; p_{Fn,}, p_{Fp}),$$
$$\epsilon_{ex} = \sum_\nu \int_0^n dn'\{x\Delta_p(n',x) + (1-x)\Delta_n(n',x)\},$$
$$p_{ex} = \sum_\nu \mu_{ex,\nu}\, n_\nu - \epsilon_{ex},$$

$$n_{s,\nu} = \frac{m_\nu^*}{\pi^2}\left[E_\nu^* p_{F\nu} - m_\nu^{*2}\log\left(\frac{E_\nu^* + p_{F\nu}}{m_\nu^*}\right)\right],$$
$$E_\nu^* = \sqrt{m_\nu^{*2} + p_{F\nu}^2}$$
$$n_\nu = \frac{p_{F\nu}^3}{3\pi^2},$$
$$m_\nu^* = m_\nu - \left(\frac{g_\sigma}{m_\sigma}\right)^2 n_{s,\nu},$$
$$\mu_\nu = E_\nu^* + \left(\frac{g_\omega}{m_\omega}\right)^2 n_\nu + \mu_{ex,\nu}.$$

2.2. Pauli blocking among baryons – results

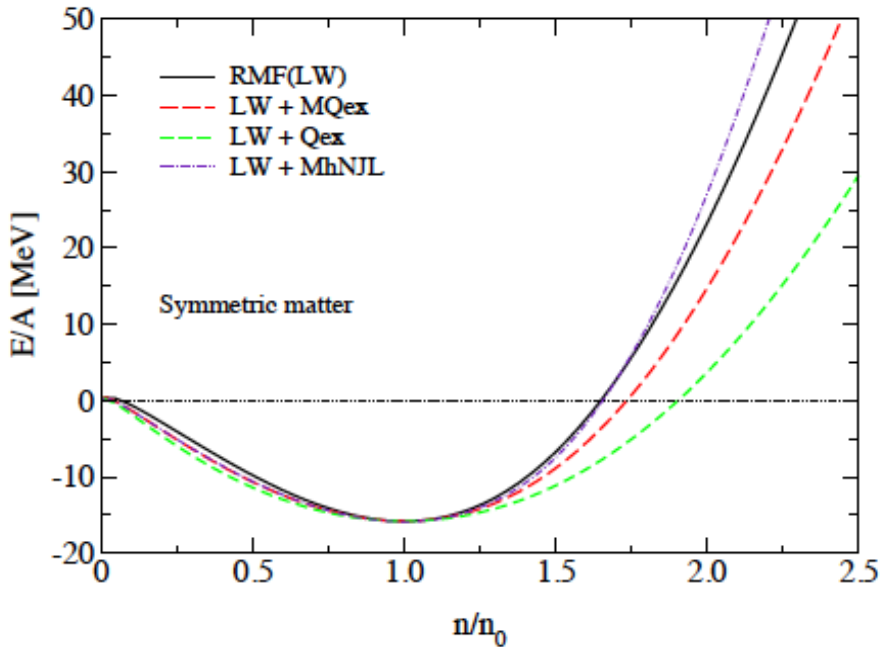

Parametrization: from saturation properties

	$(g_\omega/m_\omega)^2$[fm^2]	$(g_\sigma/m_\sigma)^2$ [fm^2]
RMF (LW)	11.6582	15.2883
LW+Qex	6.11035	9.91197
LW+MQex	6.59170	13.29118
LW+MhNJL	9.25683	13.9474

Prediction: symmetry energy

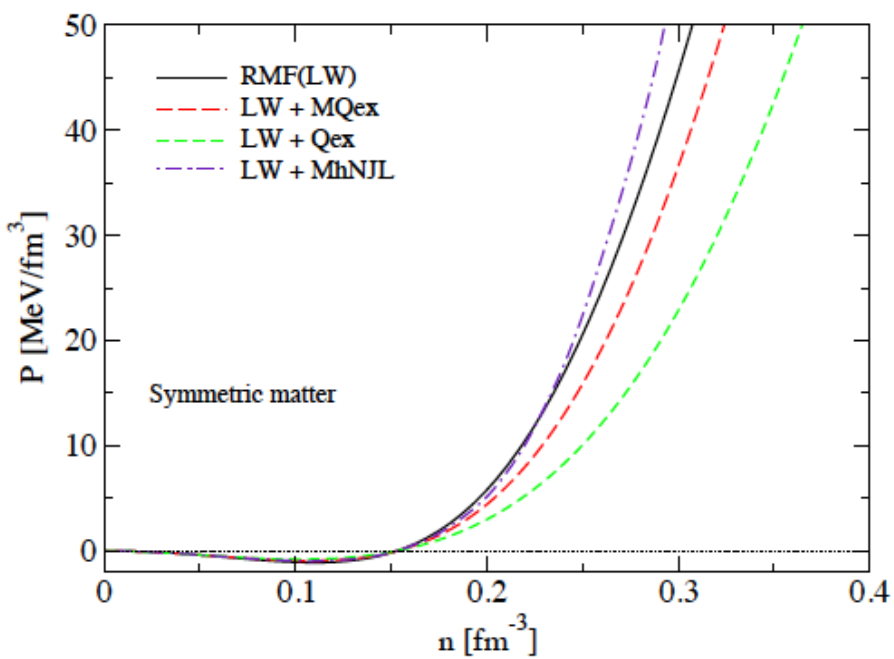

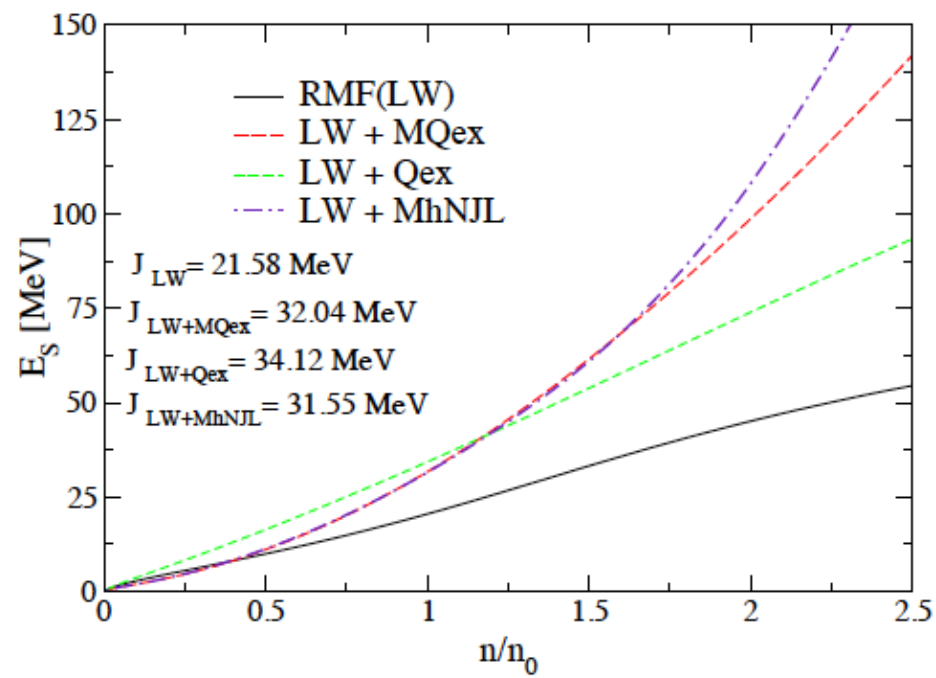

2.2. Pauli blocking among baryons – results

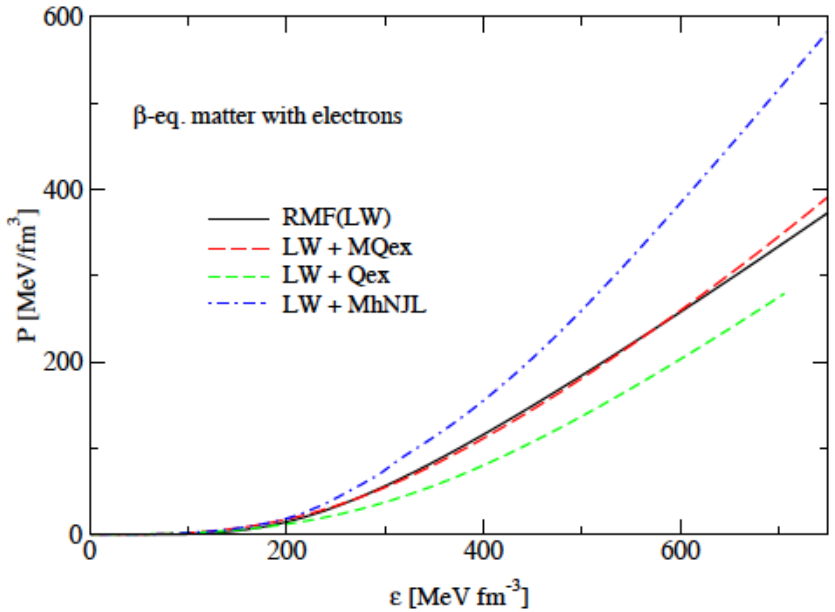

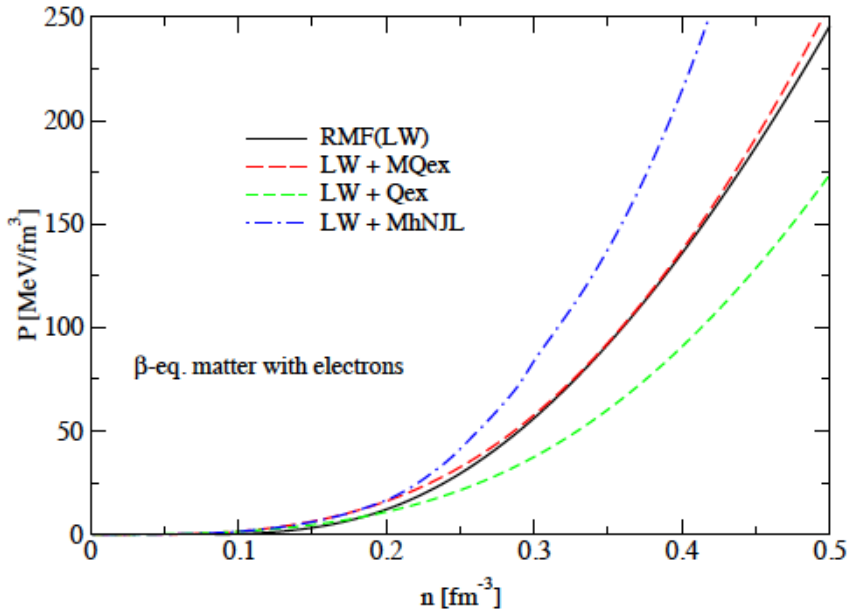

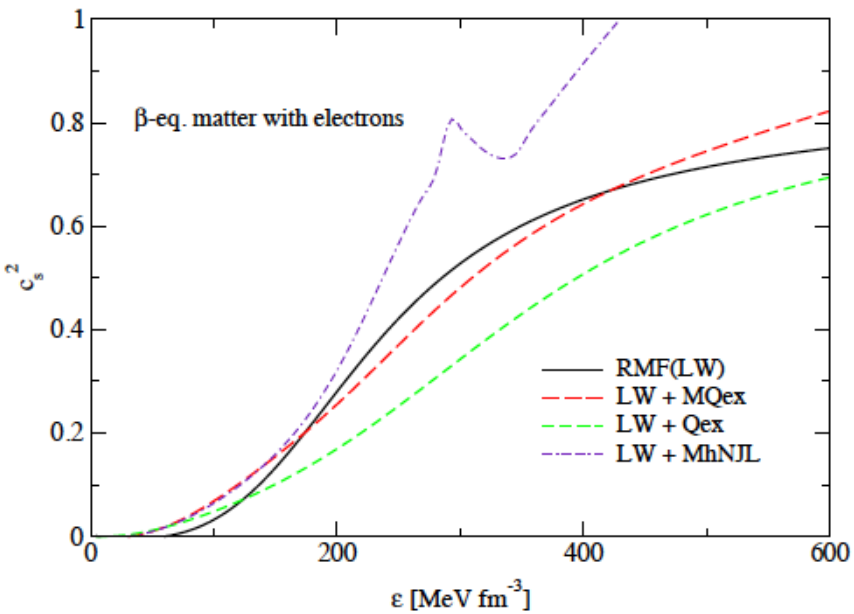

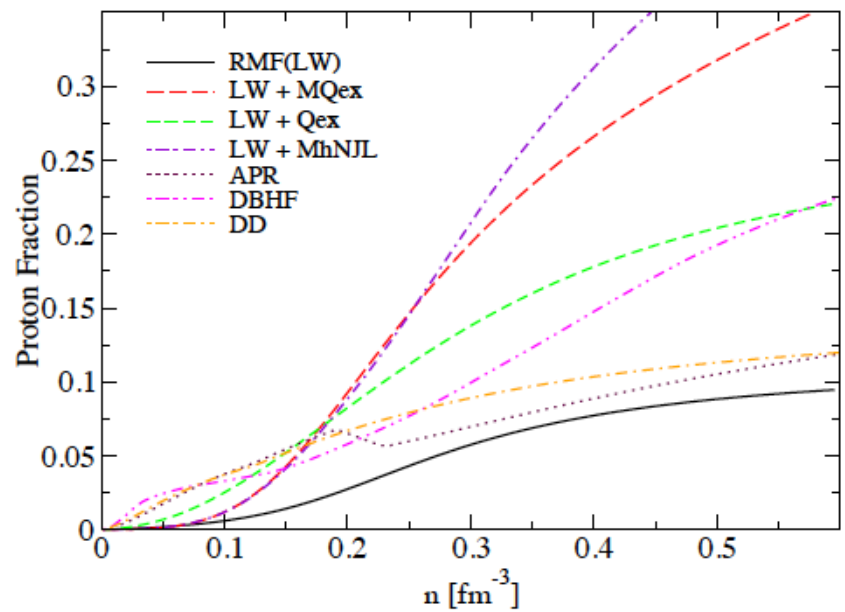

2.2. Pauli blocking among baryons – results

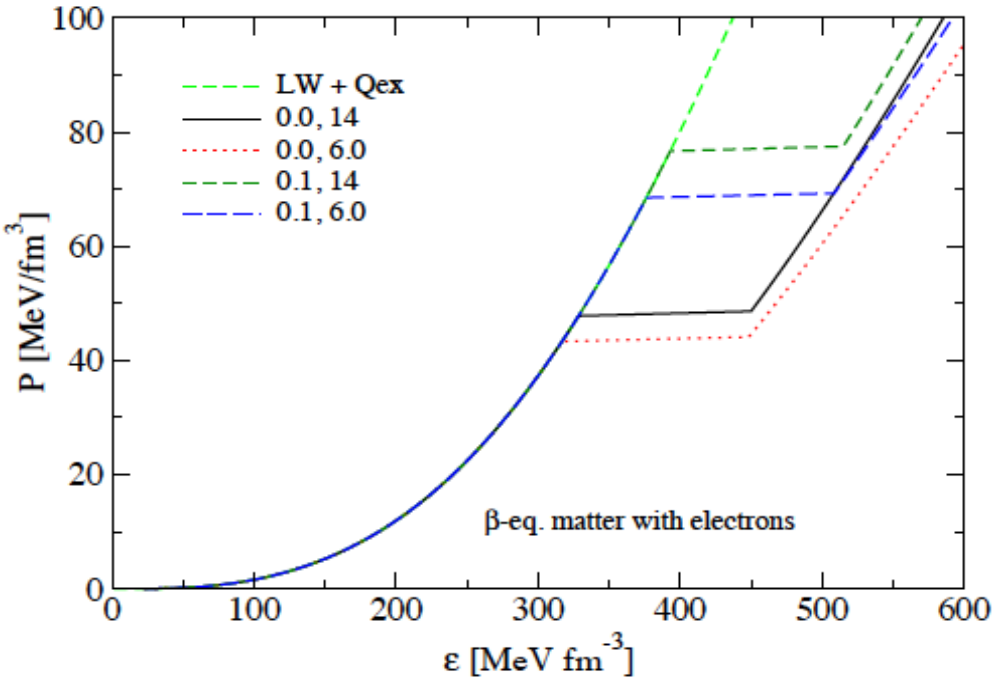

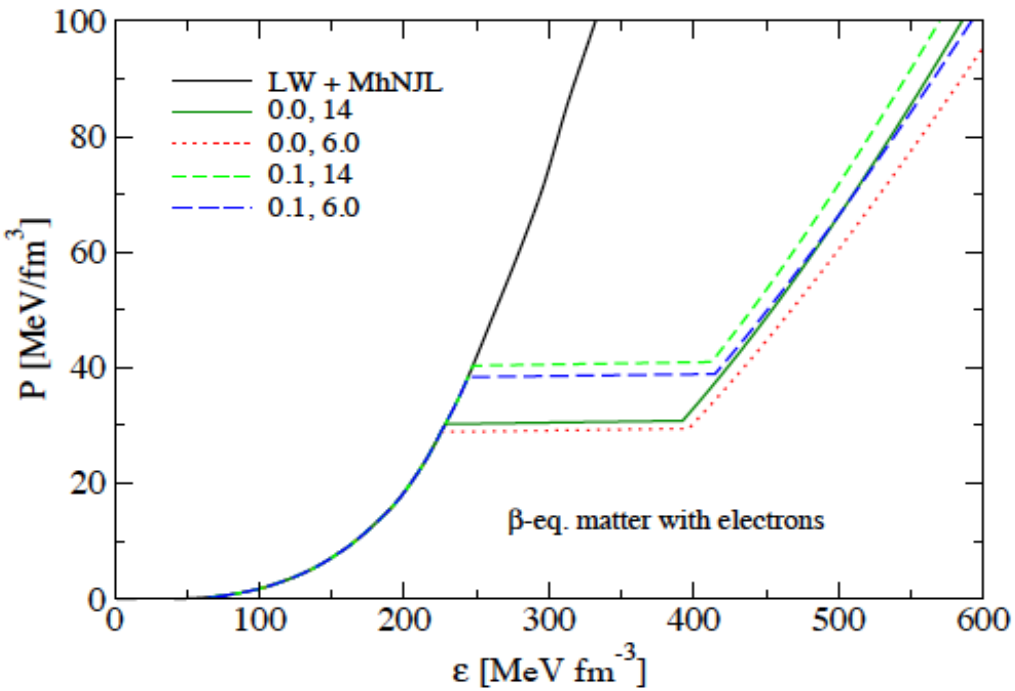

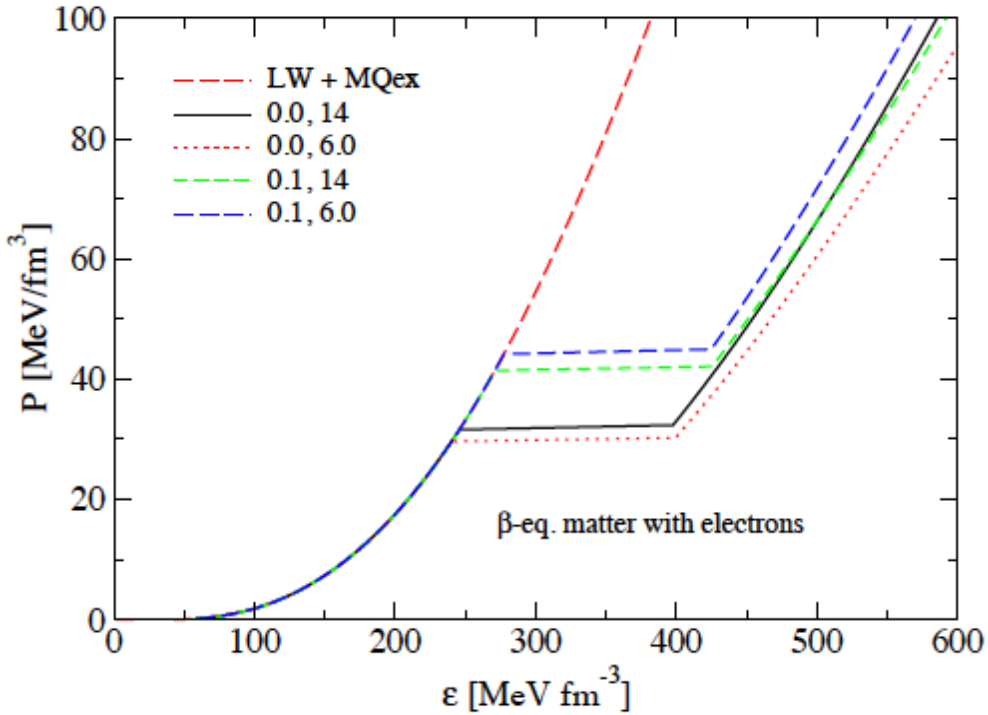

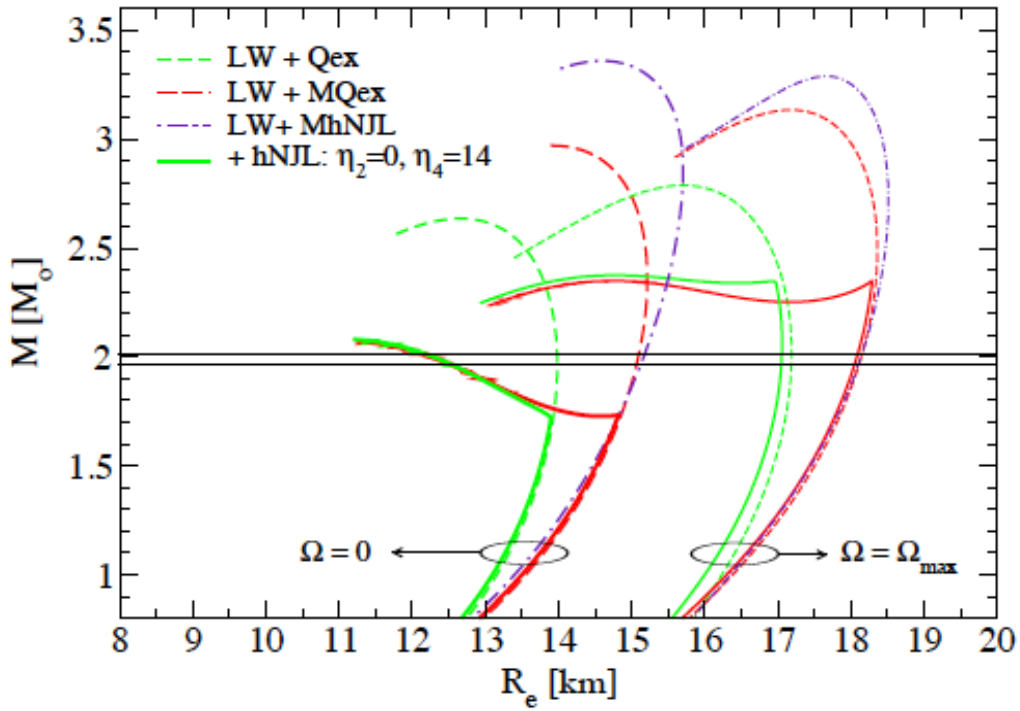

2.3. Pauli blocking among baryons – Summary

Pauli blocking selfenergy (cluster meanfield) calculable in potential models for baryon structure

Partial replacement of other short-range repulsion mechanisms (vector meson exchange)

Modern aspects:
- onset of chiral symmetry restoration enhances nucleon swelling and Pauli blocking at high n
- quark exchange among baryons -> six-quark wavefunction -> “bag melting” -> deconfinement

Chiral stiffening of nuclear matter --> reduces onset density for deconfinement

Hybrid EoS:
Convenient generalization of RMF models,
Take care: eventually aspects of quark exchange already in density dependent vertices!

Other baryons:
- hyperons
- deltas

Again calculable, partially done in nonrelativistic quark exchange models, chiral effects not yet!

Relativistic generalization:
Box diagrams of quark-diquark model ...

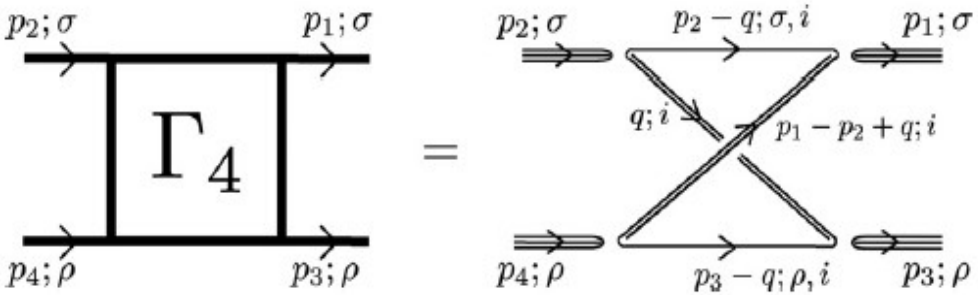

K. Maeda, Ann. Phys. 326 (2011) 1032

2.4. Pauli blocking effect → Excluded volume

Well known from modeling dissociation of clusters in the supernova EoS:

- excluded volume: Lattimer-Swesty (1991), Shen-Toki-Oyematsu-Sumiyoshi (1996), ...
- Pauli blocking: Roepke-Grigo-Sumiyoshi-Shen (2003), Typel et al. PRC 81 (2010)
- excl. Vol. vs. Pauli blocking: Hempel, Schaffner-Bielich, Typel, Roepke PRC 84 (2011)

Here: nucleons as quark clusters with finite size --> excluded volume effect !

Available volume fraction: $\Phi = V_{\rm av}/V = 1 - v \sum_{i=n,p} n_i, \quad v = \frac{1}{2}\frac{4\pi}{3}(2r_{\rm nuc})^3 = 4V_{\rm nuc}$

Equations of state for T=0 nuclear matter:

$$p_{\rm tot}(\mu_{\rm n},\mu_{\rm p}) = \frac{1}{\Phi}\sum_{i=n,p} p_i + p_{\rm mes},$$

$$\varepsilon_{\rm tot}(\mu_{\rm n},\mu_{\rm p}) = -p_{\rm tot} + \sum_{i=n,p} \mu_i n_i,$$

$$p_i = \frac{1}{4}\left(E_i n_i - m_i^* n_i^{(s)}\right),$$

$$n_i = \frac{\Phi}{3\pi^3} k_i^3,$$

$$n_i^{(s)} = \frac{\Phi m_i^*}{2\pi^2}\left[E_i k_i - (m_i^*)^2 \ln\frac{k_i + E_i}{m_i^*}\right],$$

$$E_i = \sqrt{k_i^2 + (m_i^*)^2} = \mu_i - V_i - \frac{v}{\Phi}\sum_{j=p,n} p_j,$$

Effective mass: $m_i^* = m_i - S_i.$

Scalar meanfield: $S_i \sim n_i^{(s)}$

Vector meanfield: $V_i \sim n_i$

2.5. Stiff quark matter at high densities

S. Benic, Eur. Phys. J. A 50, 111 (2014)

$$\mathcal{L} = \bar{q}(i\partial\!\!\!/ - m)q + \mu_q \bar{q}\gamma^0 q + \mathcal{L}_4 + \mathcal{L}_8 \,, \quad \mathcal{L}_4 = \frac{g_{20}}{\Lambda^2}[(\bar{q}q)^2 + (\bar{q}i\gamma_5\tau q)^2] - \frac{g_{02}}{\Lambda^2}(\bar{q}\gamma_\mu q)^2 \,,$$

$$\mathcal{L}_8 = \frac{g_{40}}{\Lambda^8}[(\bar{q}q)^2 + (\bar{q}i\gamma_5\tau q)^2]^2 - \frac{g_{04}}{\Lambda^8}(\bar{q}\gamma_\mu q)^4 - \frac{g_{22}}{\Lambda^8}(\bar{q}\gamma_\mu q)^2[(\bar{q}q)^2 + (\bar{q}i\gamma_5\tau q)^2]$$

Meanfield approximation: $\mathcal{L}_{\rm MF} = \bar{q}(i\partial\!\!\!/ - M)q + \tilde{\mu}_q \bar{q}\gamma^0 q - U \,,$

$$M = m + 2\frac{g_{20}}{\Lambda^2}\langle\bar{q}q\rangle + 4\frac{g_{40}}{\Lambda^8}\langle\bar{q}q\rangle^3 - 2\frac{g_{22}}{\Lambda^8}\langle\bar{q}q\rangle\langle q^\dagger q\rangle^2 \,,$$

$$\tilde{\mu}_q = \mu_q - 2\frac{g_{02}}{\Lambda^2}\langle q^\dagger q\rangle - 4\frac{g_{04}}{\Lambda^8}\langle q^\dagger q\rangle^3 - 2\frac{g_{22}}{\Lambda^8}\langle\bar{q}q\rangle^2\langle q^\dagger q\rangle \,,$$

$$U = \frac{g_{20}}{\Lambda^2}\langle\bar{q}q\rangle^2 + 3\frac{g_{40}}{\Lambda^8}\langle\bar{q}q\rangle^4 - 3\frac{g_{22}}{\Lambda^8}\langle\bar{q}q\rangle^2\langle q^\dagger q\rangle^2 - \frac{g_{02}}{\Lambda^2}\langle q^\dagger q\rangle^2 - 3\frac{g_{04}}{\Lambda^8}\langle q^\dagger q\rangle^4 \,.$$

Thermodynamic Potential:

$$\Omega = U - 2N_f N_c \int \frac{d^3p}{(2\pi)^3}\left\{E + T\log[1 + e^{-\beta(E-\tilde{\mu}_q)}] + T\log[1 + e^{-\beta(E+\tilde{\mu}_q)}]\right\} + \Omega_0$$

Result: high-mass twins ↔ 1st order PT

S. Benic, D. Blaschke, D. Alvarez-Castillo, T. Fischer, S. Typel, arxiv:1411.2856

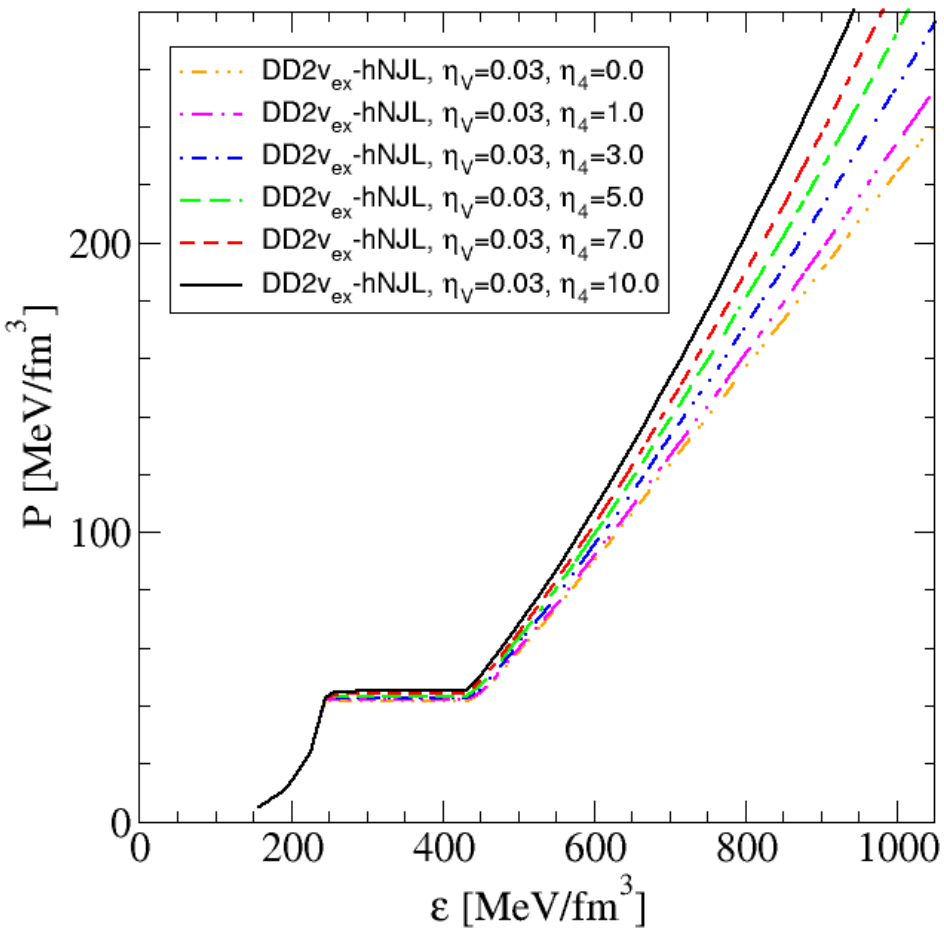

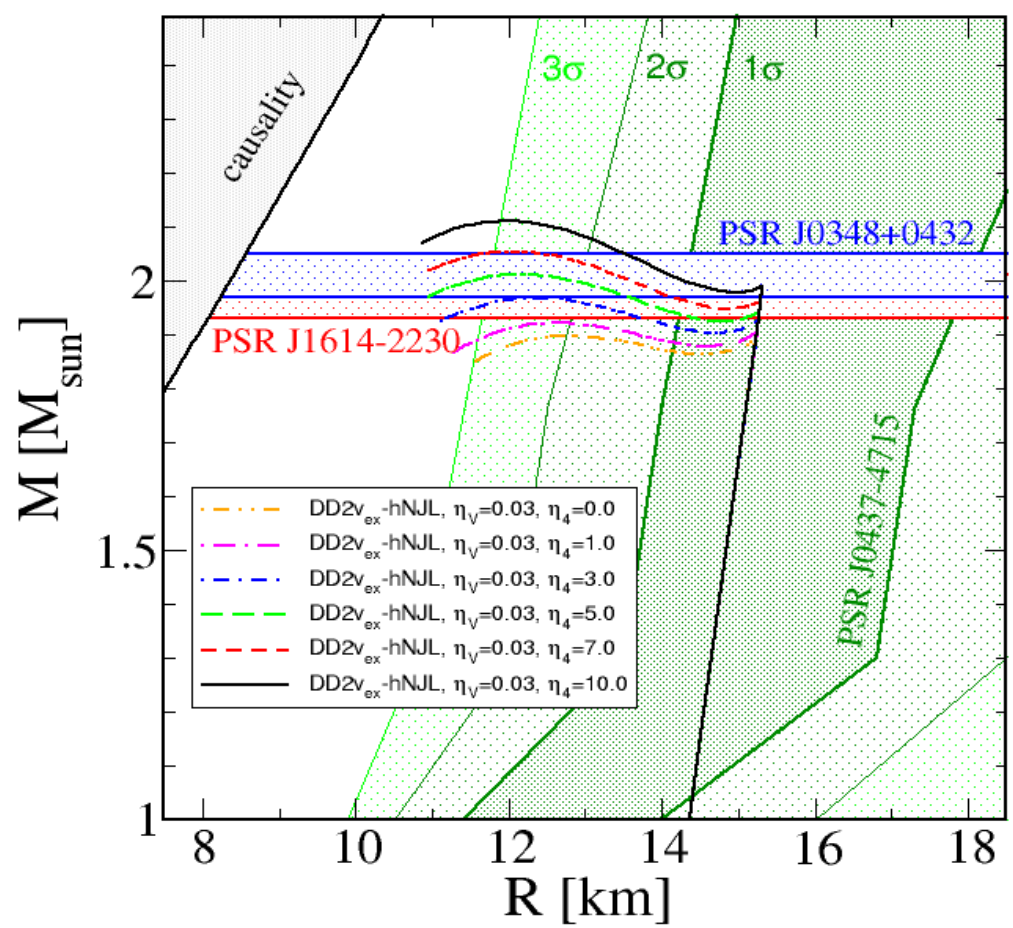

Hybrid EoS supports M-R sequences with high-mass twin compact stars

2.5. Stiff quark matter at high densities

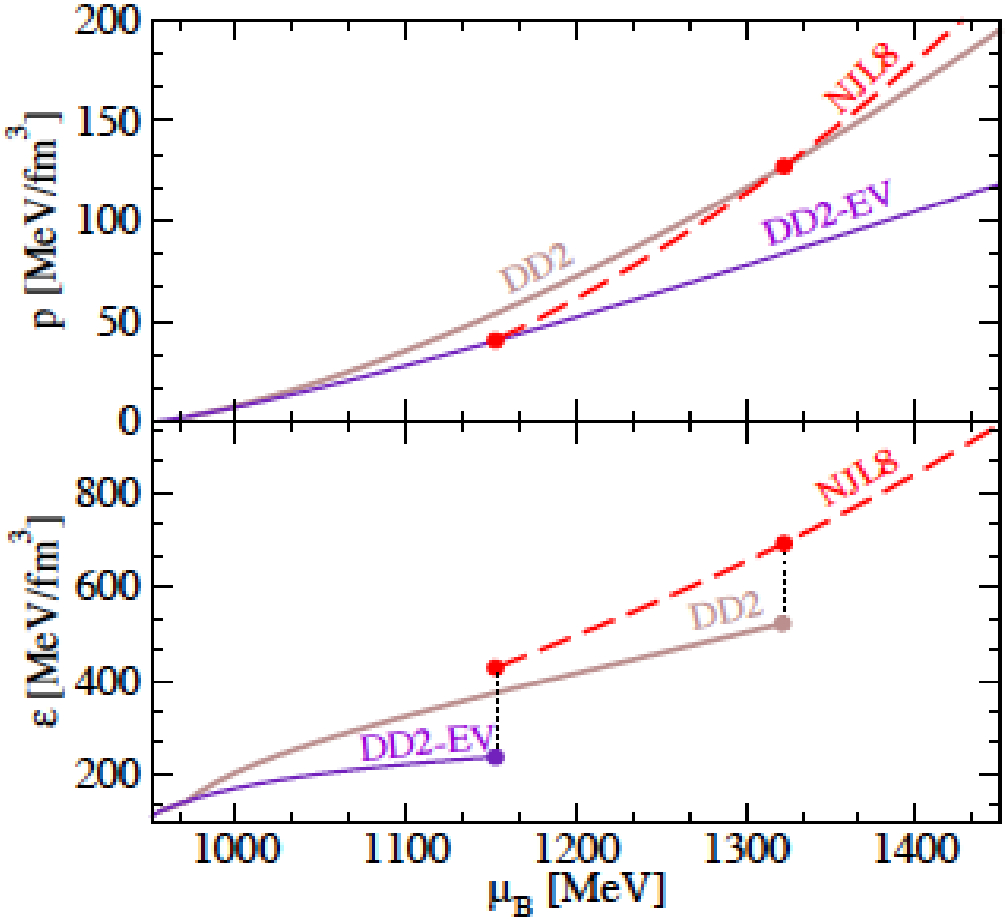

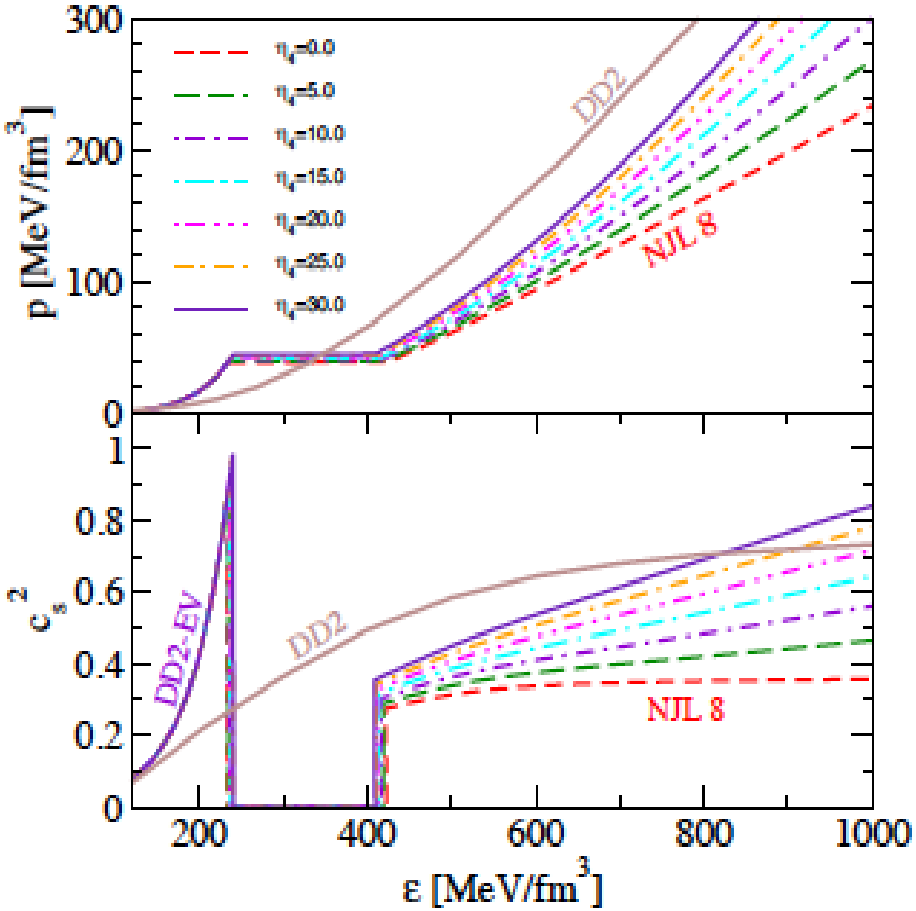

Here: Stiffening of dense hadronic matter by excluded volume in density-dependent RMF

S. Benic, D.B., D. Alvarez-Castillo, T. Fischer, S. Typel, A&A 577, A40 (2015) - STSM 2014

2.5. Stiff quark matter at high densities

Estimate effects of structures in the phase transition region ("pasta")

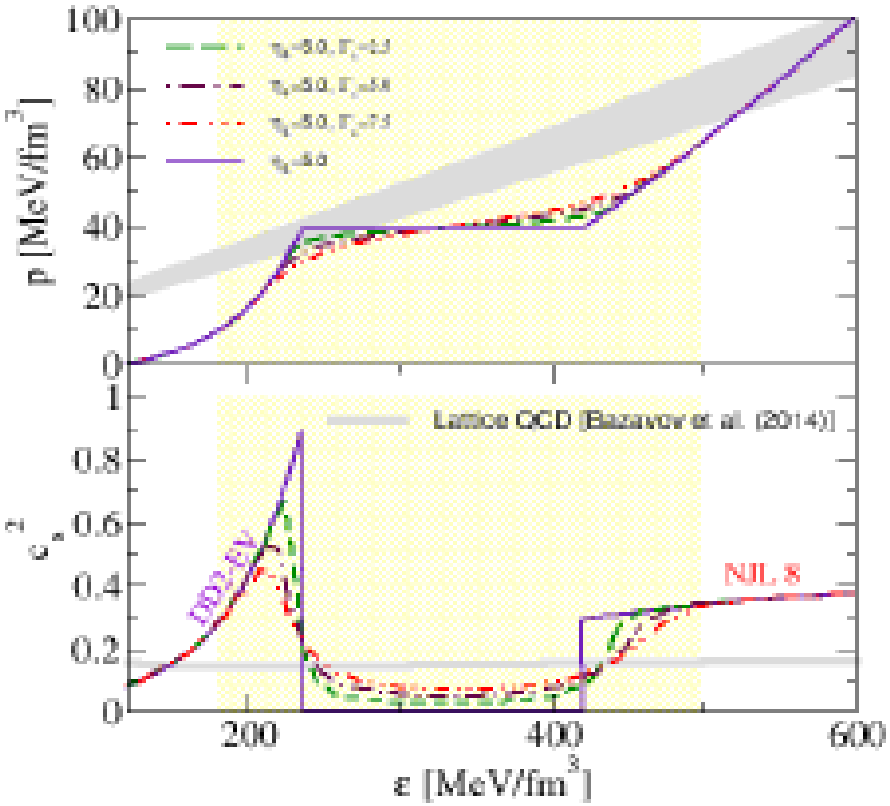

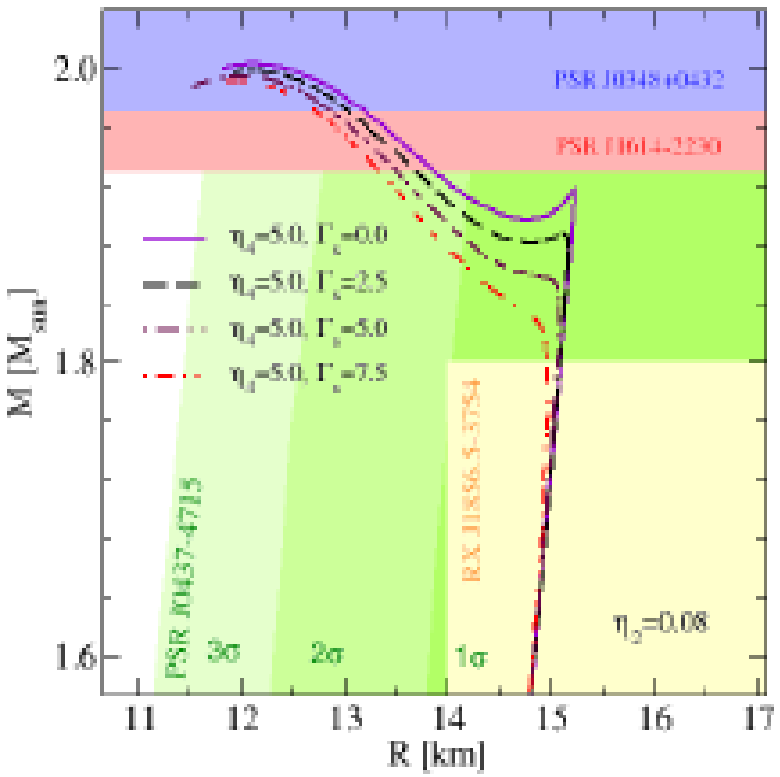

High-mass Twins relatively robust against "smoothing" the Maxwell transition construction

D. Alvarez-Castillo, D.B., arxiv:1412.8463; Phys. Part. Nucl. 46 (2015) 846

2.6. Rotation

- existence of 2 M_sun pulsars and possibility of high-mass twins raises question for their inner structure: (Q)uark or (N)ucleon core ??
  --> degenerate solutions
  --> transition from N to Q branch

- PSR J1614-2230 is millisecond pulsar, period P = 3.41 ms, consider rotation !

- transitions N --> Q must be considered for rotating configurations:
  --> how fast can they be?

(angular momentum J and baryon mass should be conserved simultaneously)

- similar scenario as fast radio bursts (Falcke-Rezzolla, 2013) or braking index (Glendenning-Pei-Weber, 1997)

M. Bejger, D.B., work in preparation (2015)

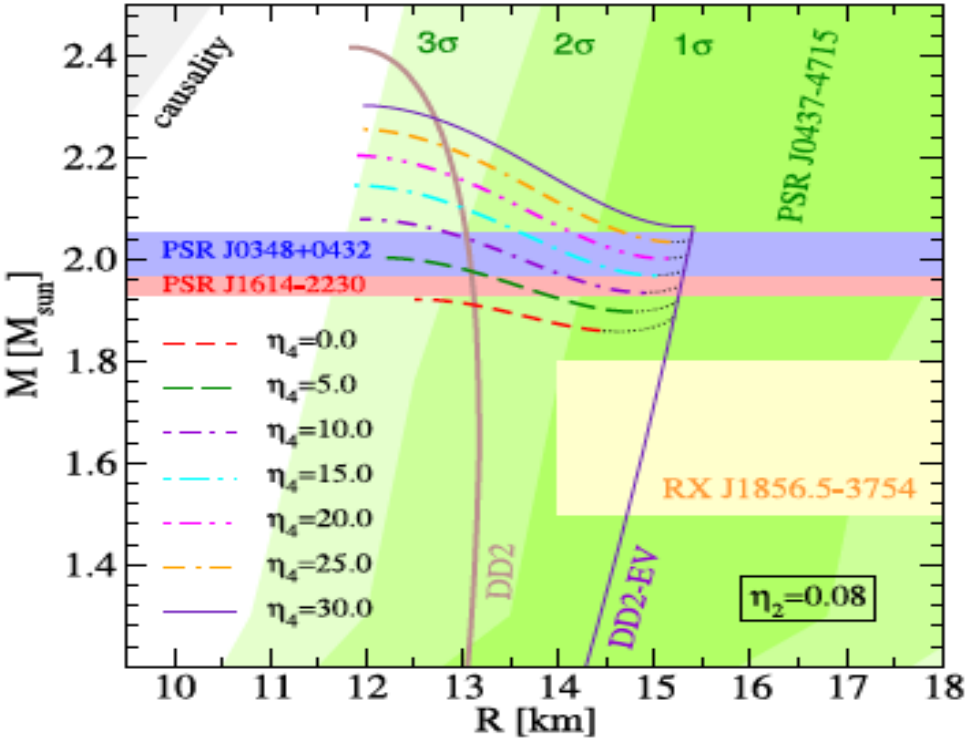

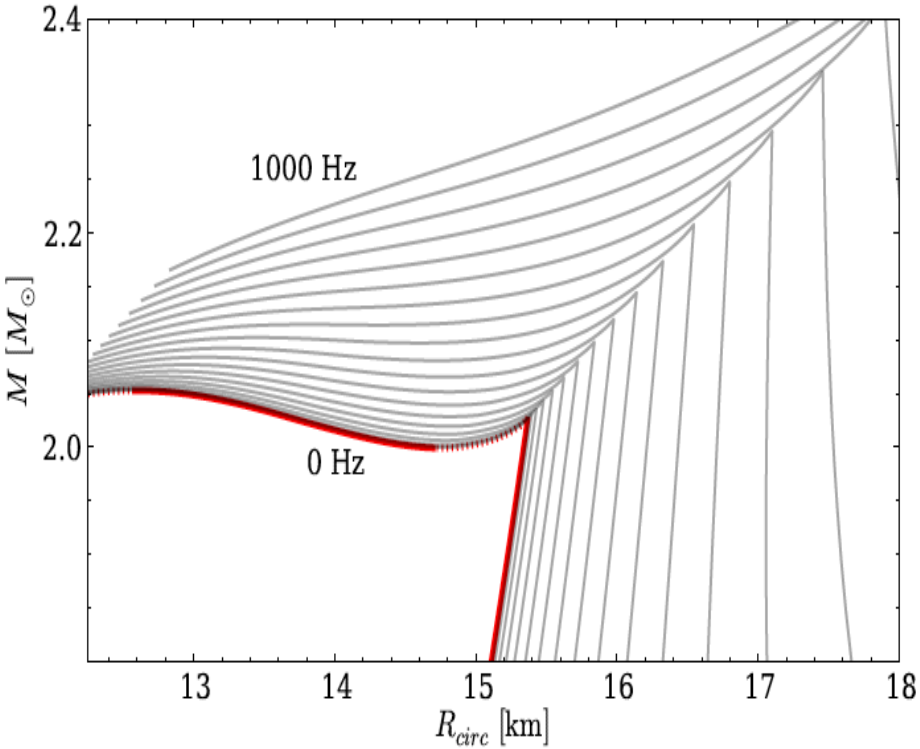

2.6. Rotation and stability

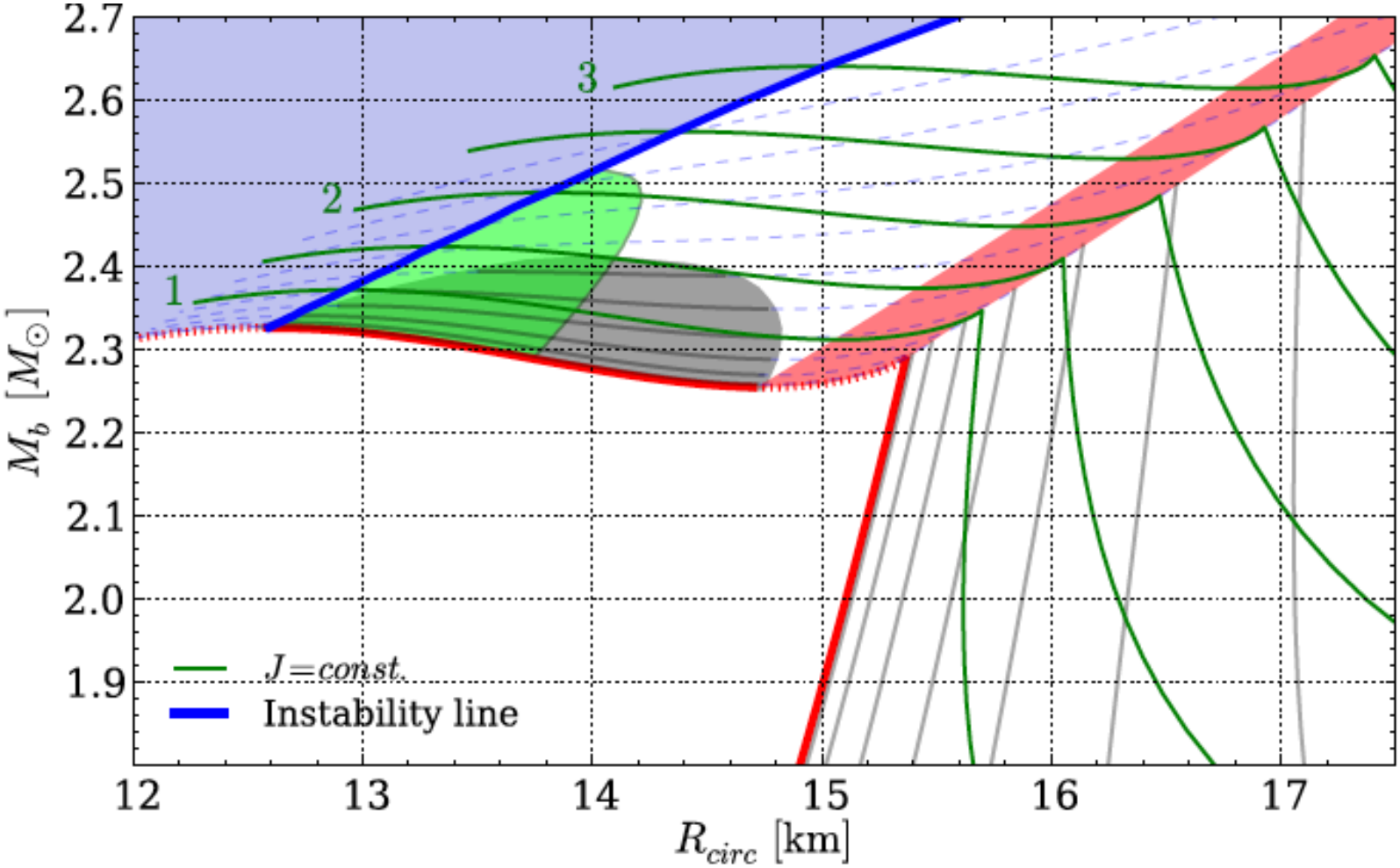

Red region - strong phase-transition instability,
Blue region - unstable w.r.t axisymmetric oscillations,
Grey region - no back-bending,
Green region - stable twin branch reached after the mini-collapse from the tip of $J = const.$ curve, along $M_b = const.$

2.6. Rotation - summary

This type of instability EOS provides a "natural" explanation for:

- ⋆ Lack of back-bending in radiopulsar timing,
- ⋆ Spin frequency cut-off at some moderate (but >716 Hz) frequency,
- ⋆ Falcke & Rezzolla Fast Radio Burst (FRB) engine
  - ⋆ catastrophic mini-collapse to the second branch (or to a black hole),
  - ⋆ massive rearrangement of the magnetic field → energy emission.

Astrophysical predictions:

- ⋆ Way to constraint on M_b, J, I, core EOS etc.,
- ⋆ Specific shape of NS-BH mass function (no mass gap?)
- → population of massive, low B-field NSs (radio-dead?),
- → population of massive, high B-field NSs (collapse enhances the field?),
- ⋆ Characteristic burst-like signature in GW emission during the mini-collapse.

3. New Bayesian Analysis scheme

Disjunct M-R constraints for Bayesian analysis !

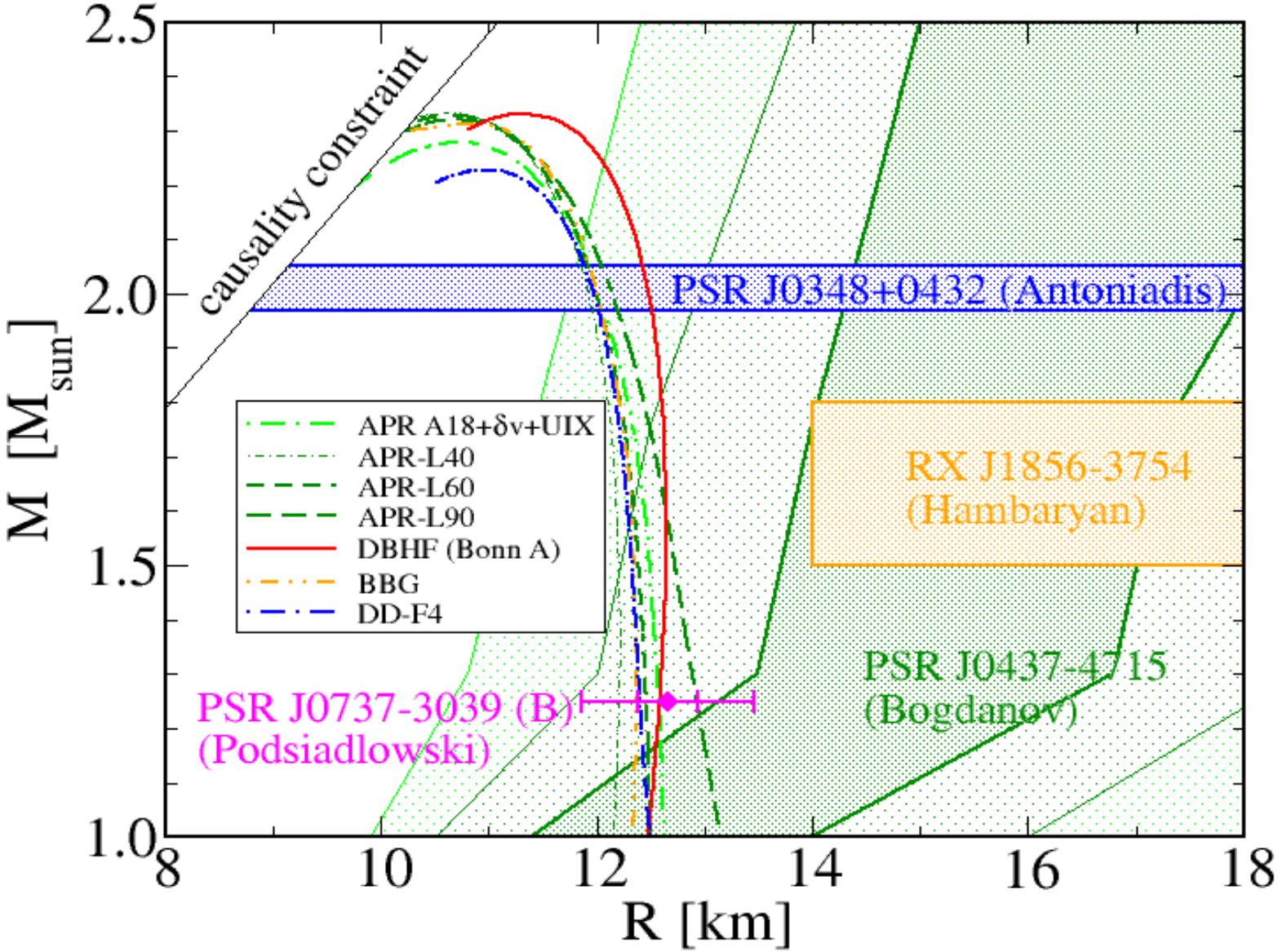

Alvarez, Ayriyan, Blaschke, Grigorian, J. Phys. Conf. Ser. (2014)

Disjunct M-R constraints for Bayesian analysis !

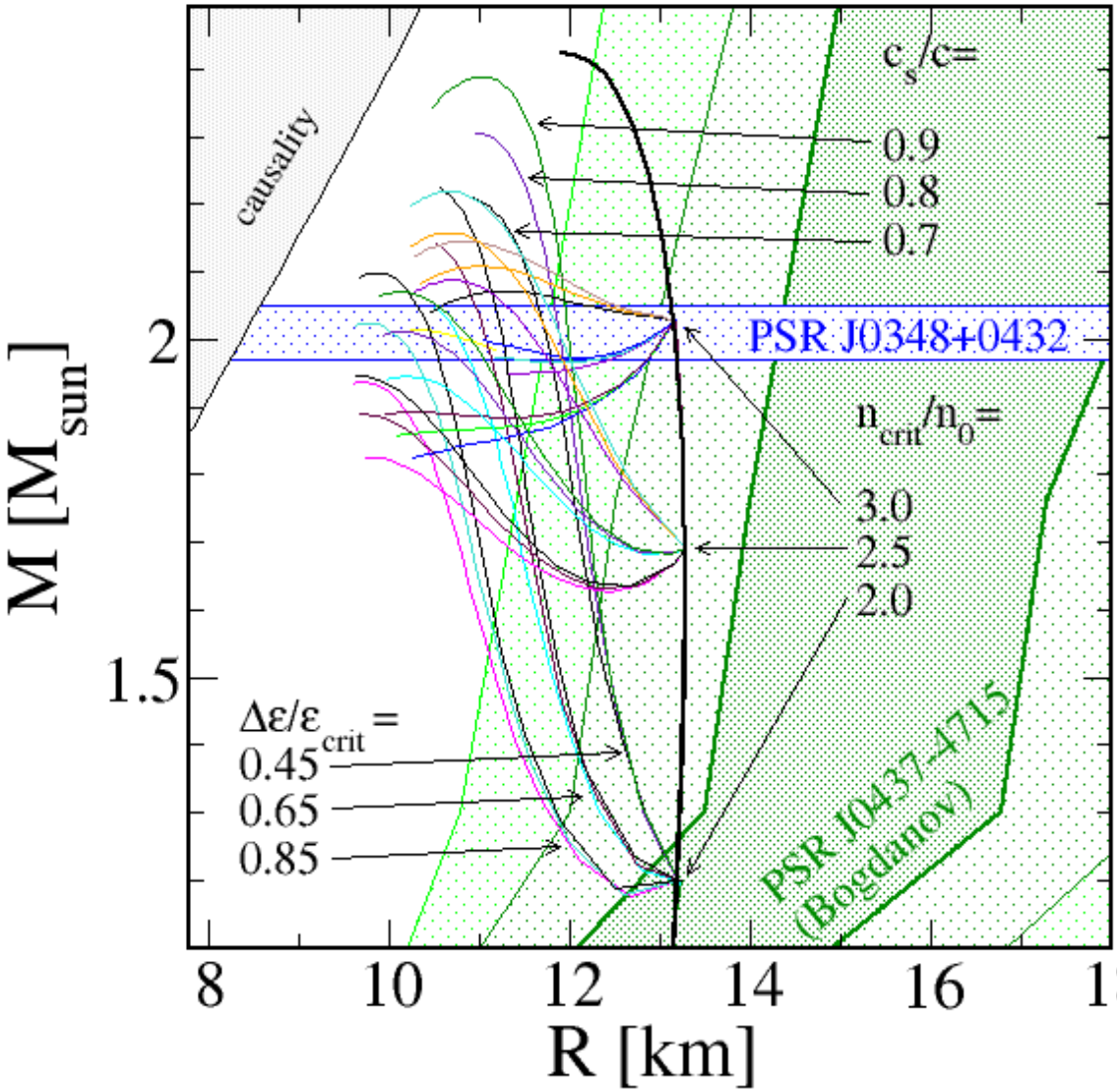

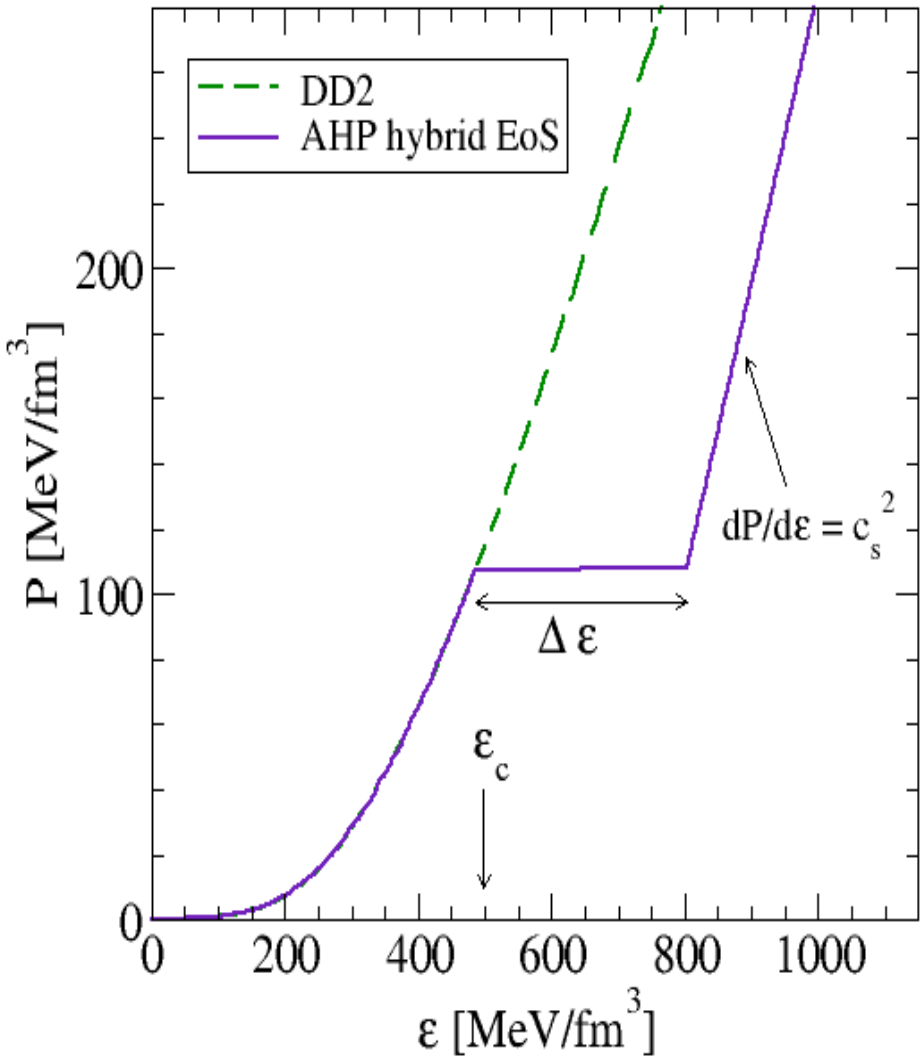

Blaschke, Grigorian, Alvarez, Ayriyan, J. Phys. Conf. Ser. 496 (2014) 012002

Disjunct M-R constraints for Bayesian analysis !

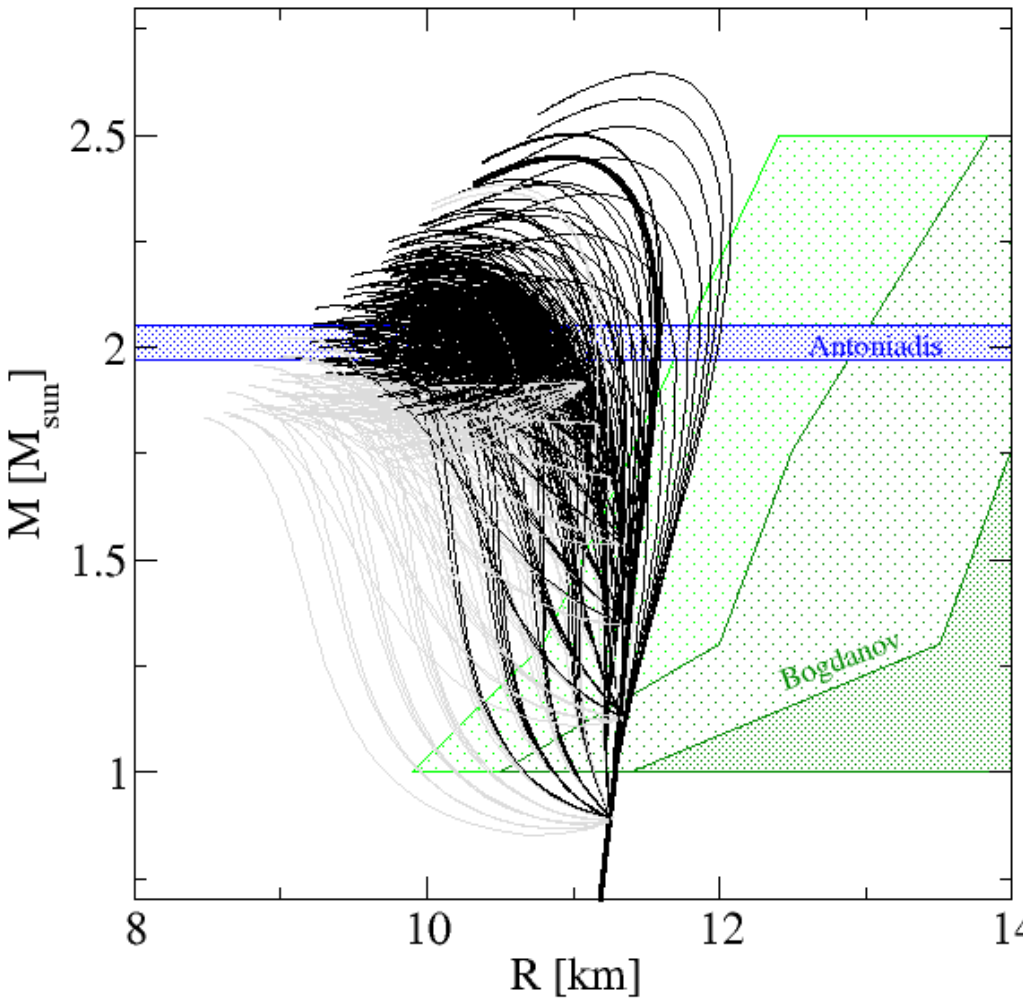

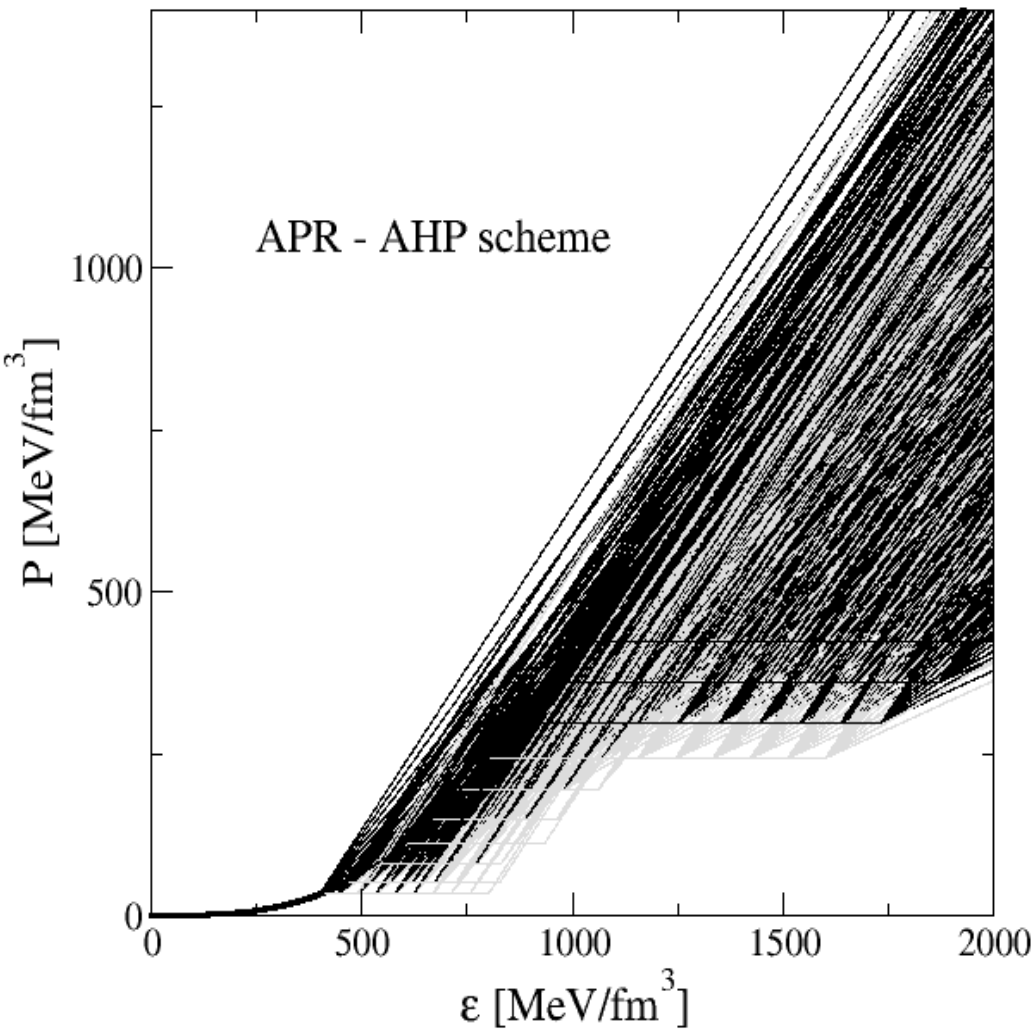

Blaschke, Grigorian, Alvarez, Ayriyan, J. Phys. Conf. Ser. 496 (2014) 012002

Phase transition? Measure different radii at 2Mo !

"Now let us travel into future. It is year **2017**, some new, reliable NS radius measurement methods are discovered and were used to find the size of two most massive pulsars, which still are PSR J0348+0432 and PSR J1614-2230. **The community was shocked** when received the results of observations: one radius is 13 ± 0.5 km, while the other is 11 ± 0.5 km!"

– *Michał Sokołowski*, Master Thesis, 2014

Alvarez, Ayriyan, Blaschke, Grigorian, Sokolowski (in progress, 2014)

Phase transition? Measure different radii at 2Mo !

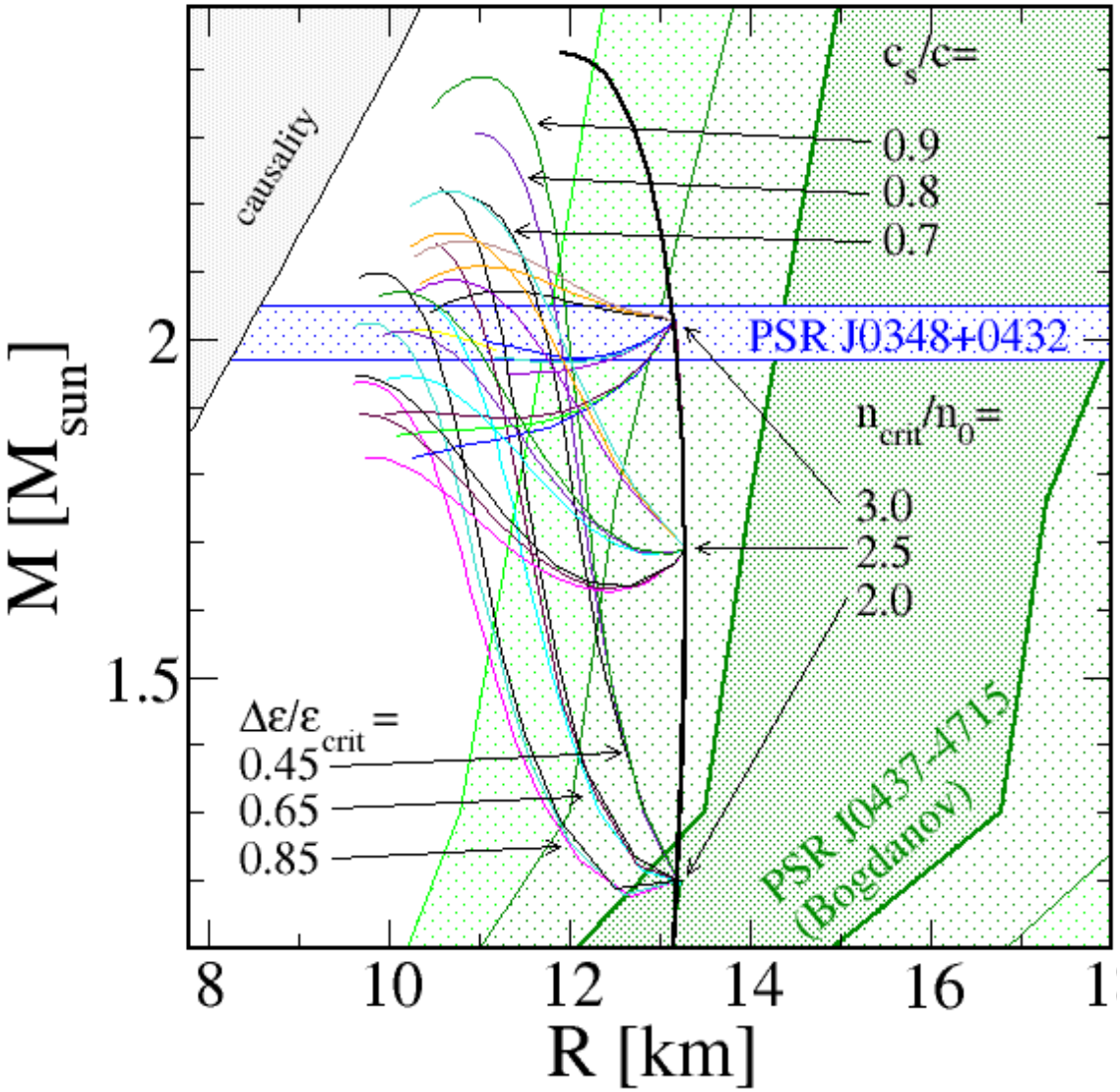

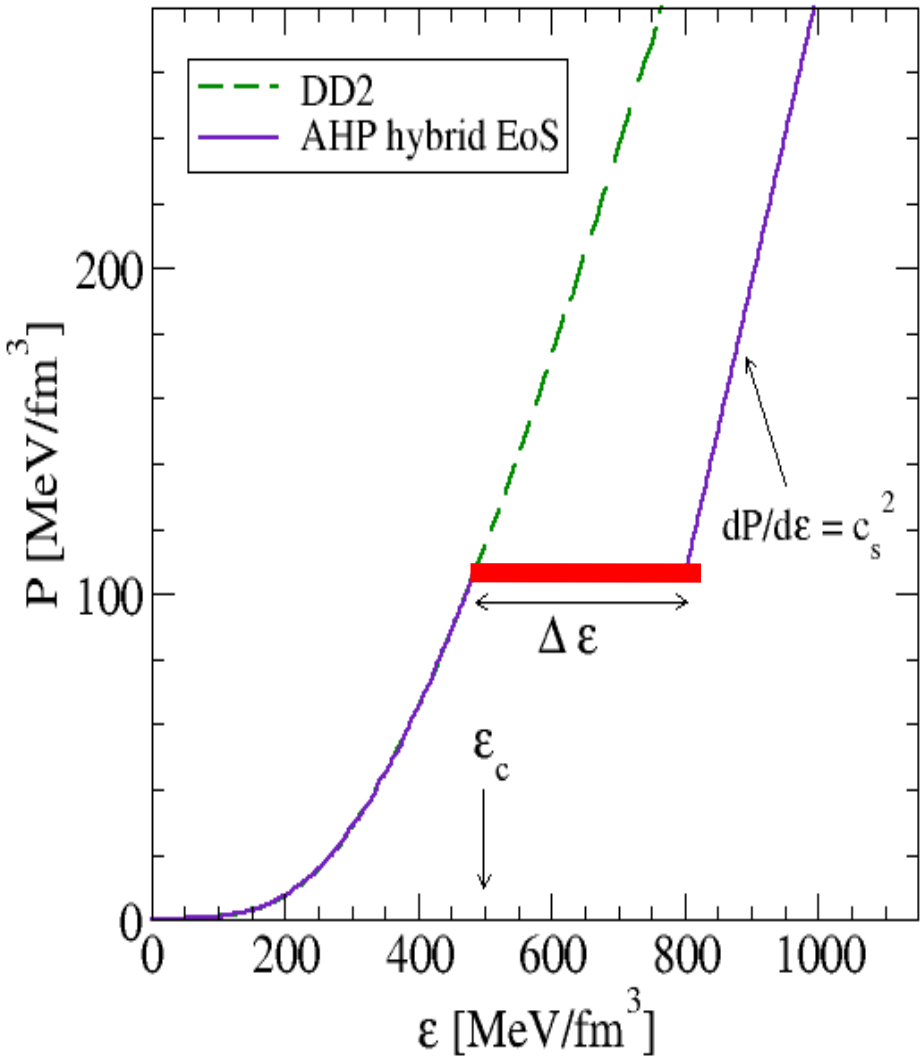

Alvarez, Ayriyan, Blaschke, Grigorian, Sokolowski, arxiv:1412.8226 (2014)

Phase transition? Measure different radii at 2Mo !

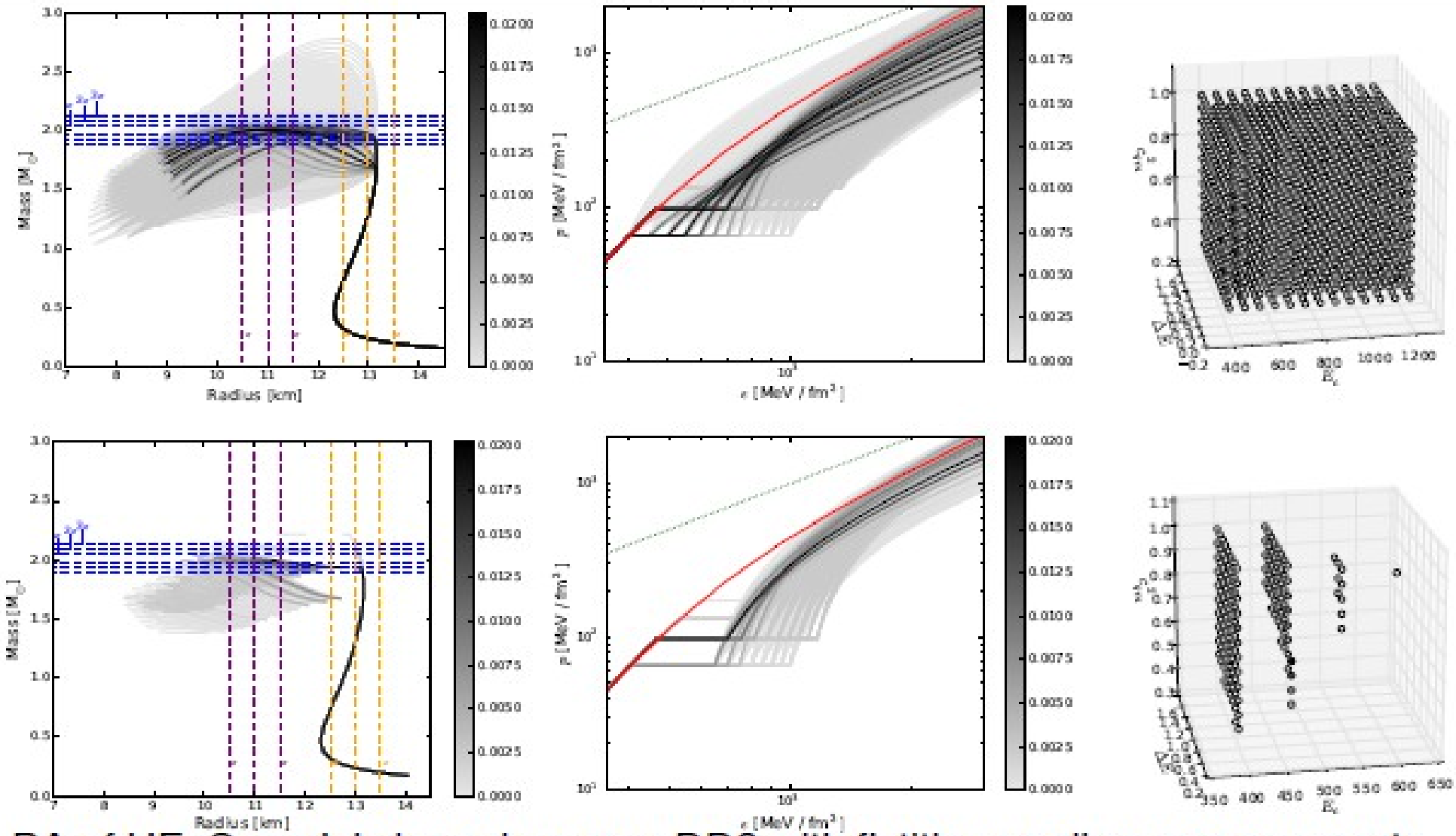

BA of HEoS models based on pure DD2 with fictitious radius measurements.

Alvarez, Ayriyan, Blaschke, Grigorian, Sokolowski, arxiv:1412.8226 (2014)

Summary: New Class of Hybrid EoS

Modern topics (selected):

- QCD phase diagram: critical point (D. Alvarez, DB, S. Benic et al.)
- Hyperon puzzle (M. Baldo et al.; P. Haensel at al..; ...)
- Direct Urca problem (T. Klaehn et al.)
- Supernova explosion mechanism (T. Fischer et al.)

Solutions can be provided by

- Stiffening of hadronic matter by quark substructure effects
  (Pauli blocking: DB, H.Grigorian, G.Roepke → excluded vol: S.Typel)
- Stiffening of quark matter at high densities
  (e.g., by multiquark interactions: S. Benic et al.)
- Resulting early onset of quark matter and large latent heat

Cross-talk with Heavy-Ion Collision Experiments

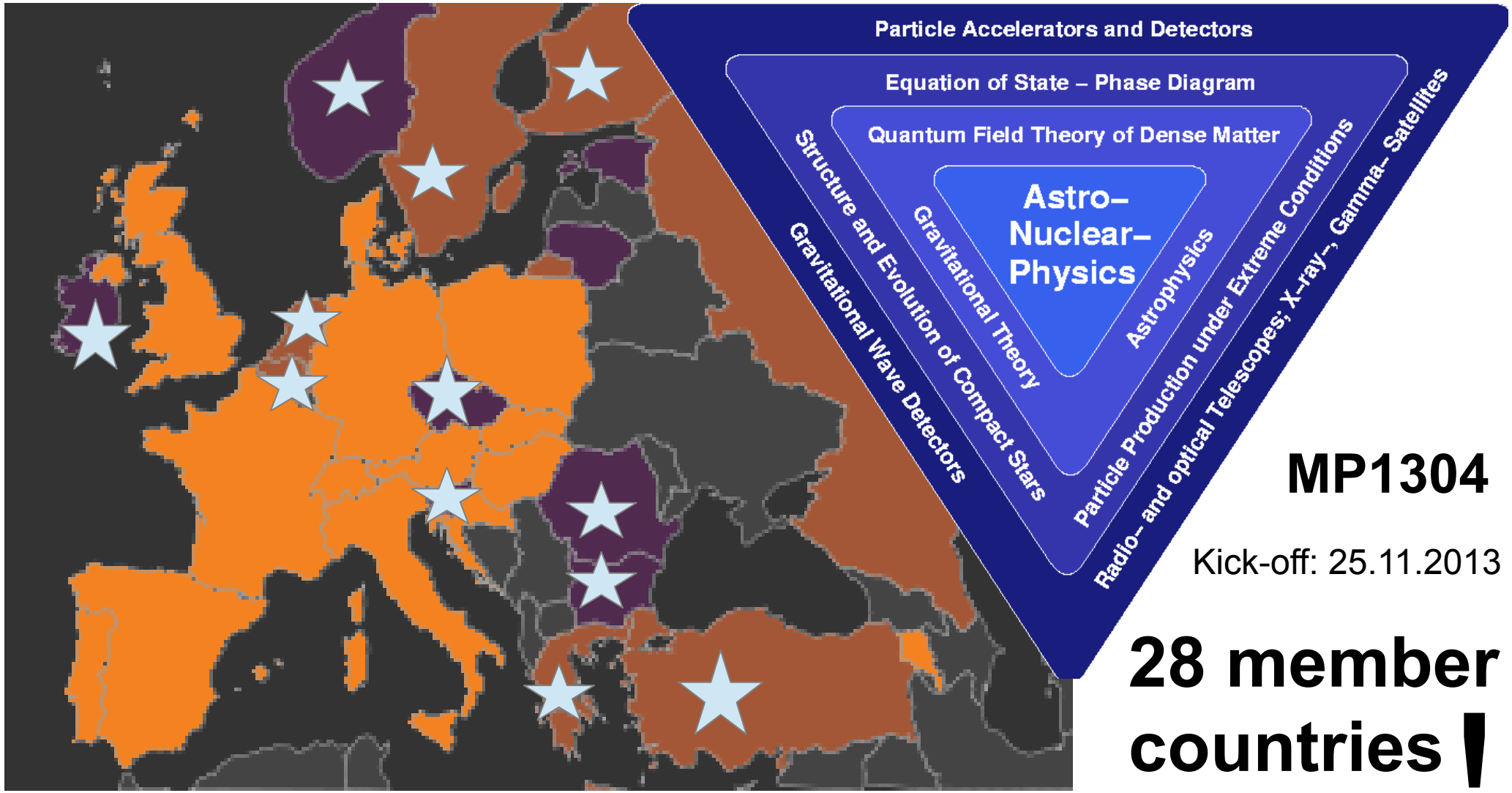

MP1304

Kick-off: 25.11.2013

28 member countries!

New comp star **!**

cost
EUROPEAN COOPERATION
IN SCIENCE AND TECHNOLOGY

http://compstar.uni-frankfurt.de

4. Hybrid star matter at NICA and FAIR

Exploring hybrid star matter at NICA

T.Klähn (1), D.Blaschke (1,2), F.Weber (3)
(1) Institute for Theoretical Physics, University of Wroclaw, Poland
(2) Joint Institute for Nuclear Research, Dubna
(3) Department of Physics, San Diego State University, USA

Heavy-Ion Collisions

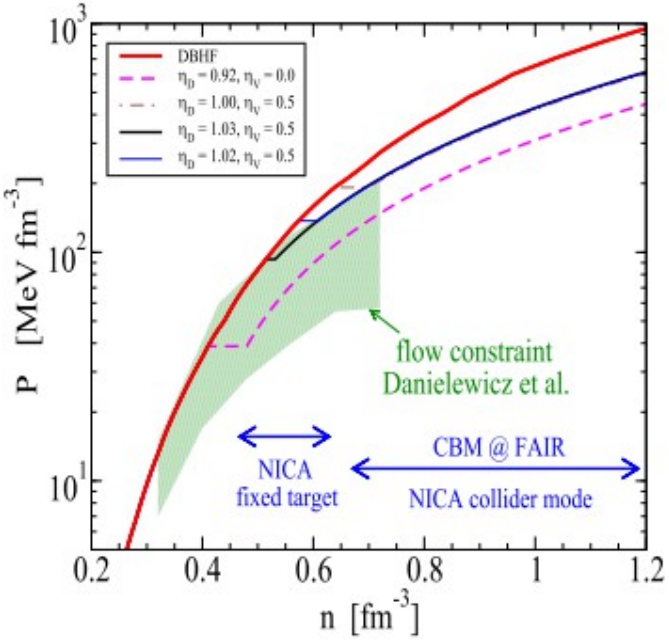

- stiff EoS (at flow limit)
- low ncrit (at NICA fixT)
- soft EoS (dashed line)

- high Mmax (J1614-2230)
- low Monset (all NS hybrid)
- excluded (J1614-2230)

Compact Stars

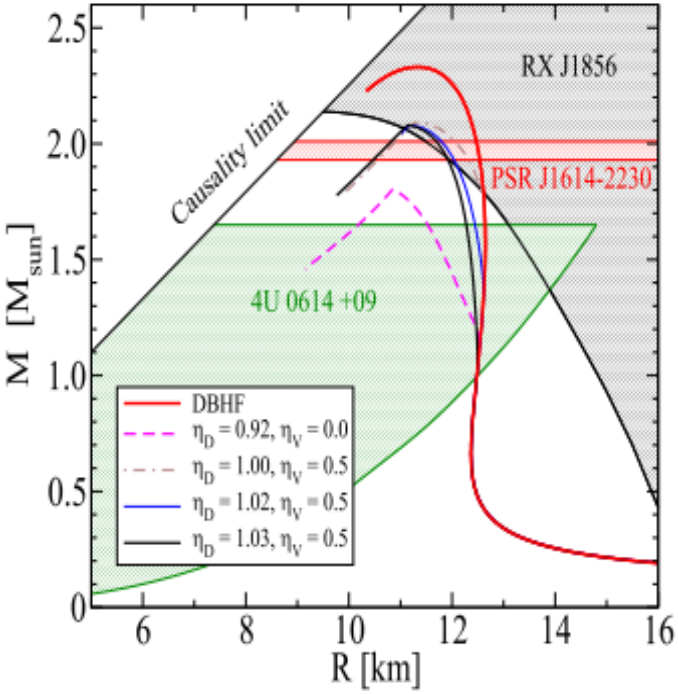

Proposal:

1. Measure transverse and elliptic flow for a wide range of energies (densities) at NICA and perform Danielewicz's flow data analysis --> constrain stiffness of high density EoS
2. Provide lower bound for onset of mixed phase ---> constrain QM onset in hybrid stars

„The CBM Physics Book“, Springer LNP 841 (2011), pp.158-181
NICA White Paper, http://theor.jinr.ru → BLTP TWikipages

Hydrodynamic modelling for NICA / FAIR

More complicated for lower energies:
→ baryon stopping effects,
→ finite baryon chemical potential,
→ EoS unknown from first principles
We want to simulate the effects of, and ultimately discriminate different EoS/PT types
The model has to be coupled to a detector response code to simulate detector events

Initial state → hydrodynamic evolution → particlization → hadronic corona → detector response

3-fluid hydro,
(Yu. Ivanov)

adapt the procedure
from existing hybrid model
(Iu. Karpenko)

(optionally) cascade:
PHSD, UrQMD, etc
(E. Bratkovskaya,
H. Petersen)

GEANT
MPD, BM @N
(O. Rogachevsky,
V. Voronyuk, et al.)

3-Fluid Dynamics

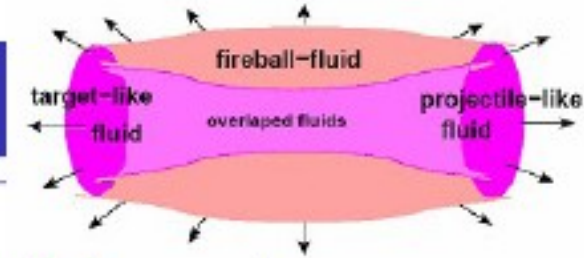

Produced particles populate mid-rapidity
$\Rightarrow$ fireball fluid

Target-like fluid: $\partial_\mu J_t^\mu = 0$ $\qquad$ $\partial_\mu T_t^{\mu\nu} = -F_{tp}^\nu + F_{ft}^\nu$

Leading particles carry bar. charge $\qquad$ exchange/emission

Projectile-like fluid: $\partial_\mu J_p^\mu = 0,$ $\qquad$ $\partial_\mu T_p^{\mu\nu} = -F_{pt}^\nu + F_{fp}^\nu$

Fireball fluid: $J_f^\mu = 0,$ $\qquad$ $\partial_\mu T_f^{\mu\nu} = F_{pt}^\nu + F_{tp}^\nu - F_{fp}^\nu - F_{ft}^\nu$

Baryon-free fluid $\qquad$ Source term $\qquad$ Exchange

The source term is delayed due to a formation time $\tau \sim 1$ fm/c

Total energy-momentum conservation:

$$\partial_\mu (T_p^{\mu\nu} + T_t^{\mu\nu} + T_f^{\mu\nu}) = 0$$

http://theory.gsi.de/~ivanov/mfd/

Yu.B. Ivanov, V.N. Russkikh and V.D. Toneev, Phys. Rev. C73, 044904 (2006)

Net proton rapidity distribution – test case for a 1st order PT signal

Theory: Yu.B. Ivanov, Phys. Rev. C 87, 064904 (2013)

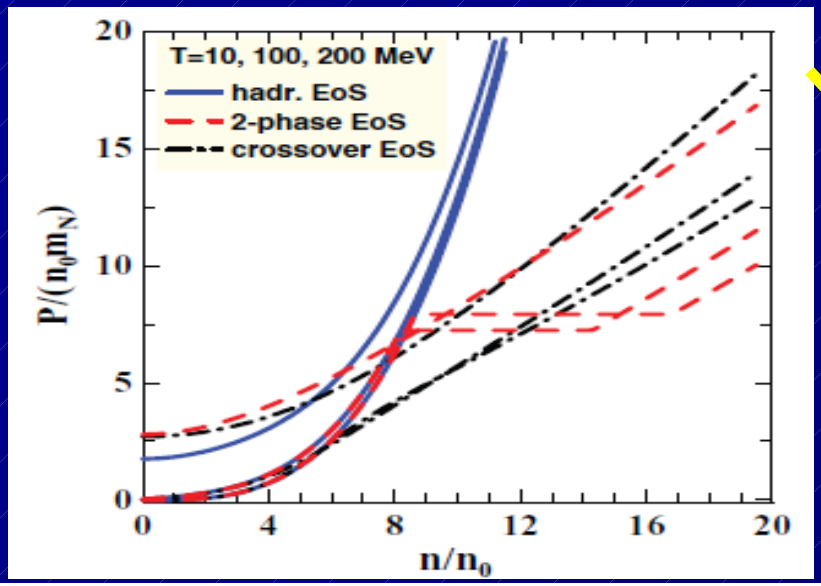

EoS

3-fluid hydro Evolution ...

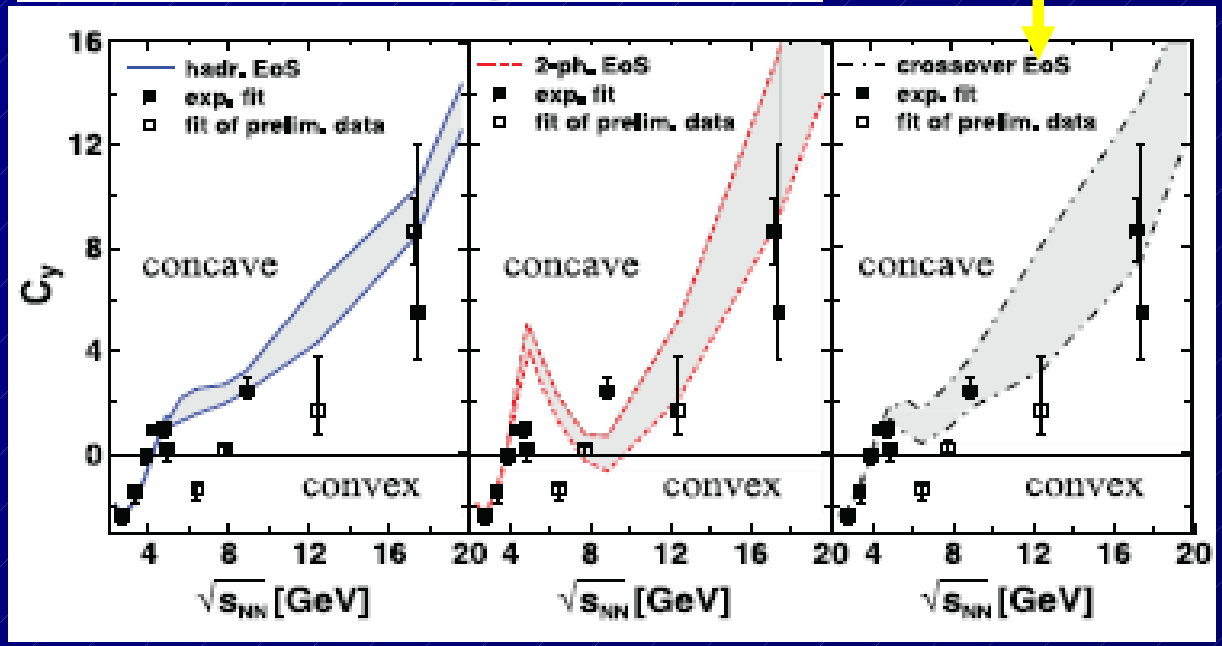

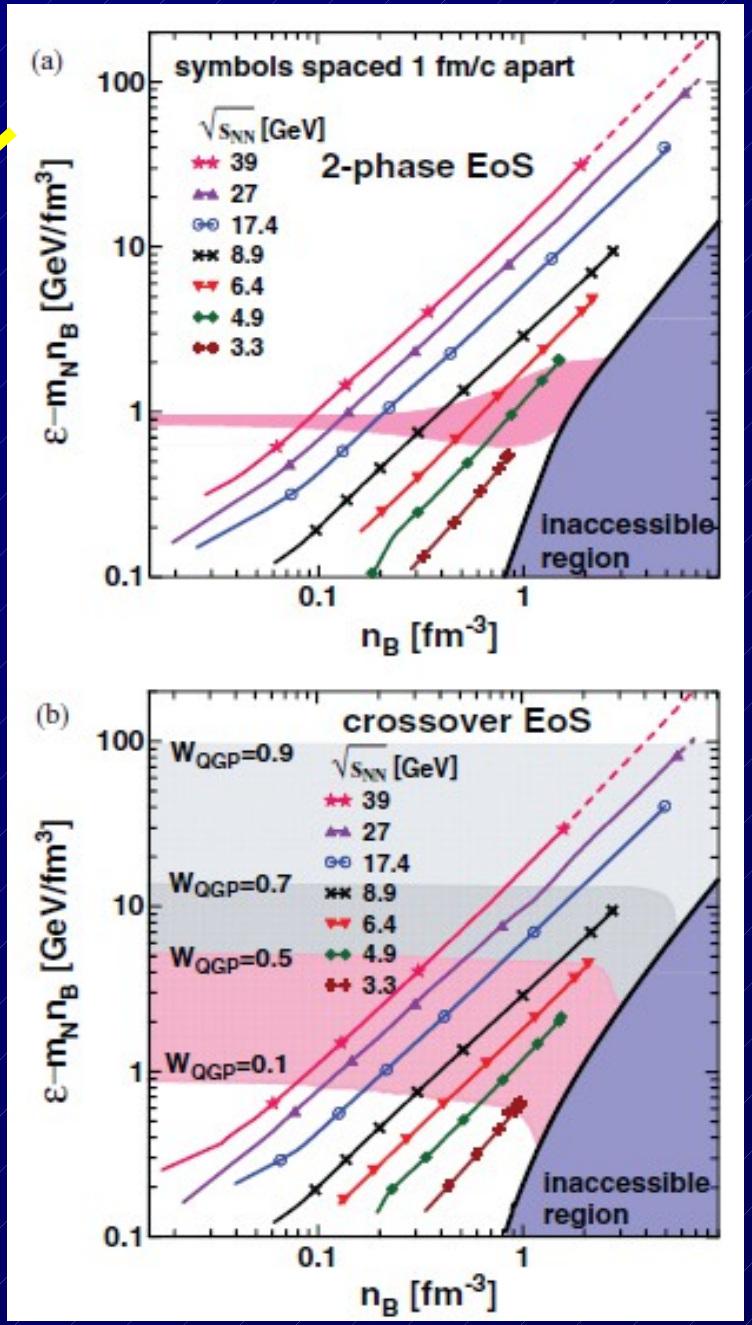

Net proton rapidity distribution – test case for a 1st order PT signal

Theory: Yu.B. Ivanov, Phys. Rev. C 87, 064904 (2013)

$$C_y = \left(y_{\mathrm{c.m.}}^3 \frac{d^3N}{dy^3} \right)_{y=y_{\mathrm{c.m.}}} \Big/ \left(y_{\mathrm{c.m.}} \frac{dN}{dy} \right)_{y=y_{\mathrm{c.m.}}}$$
$$= (y_{\mathrm{c.m.}}/w_s)^2 (\sinh^2 y_s - w_s \cosh y_s).$$

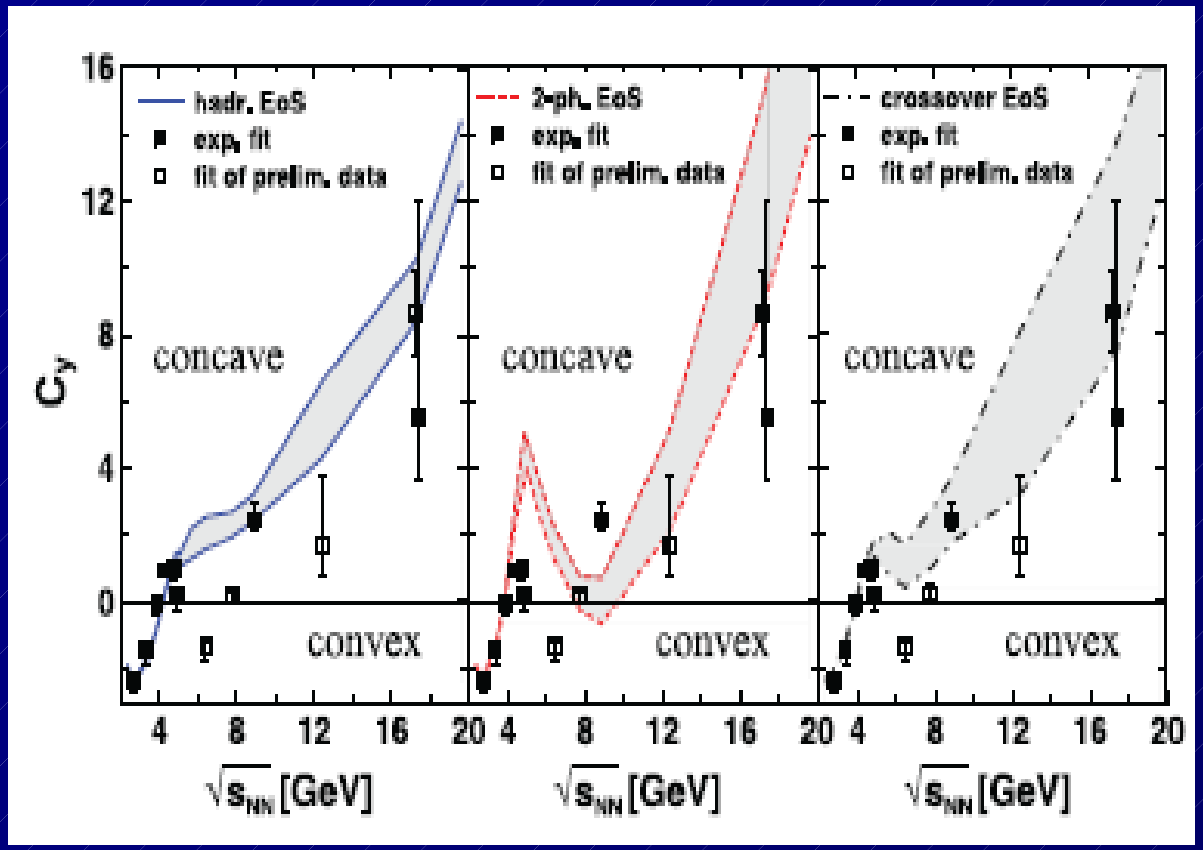

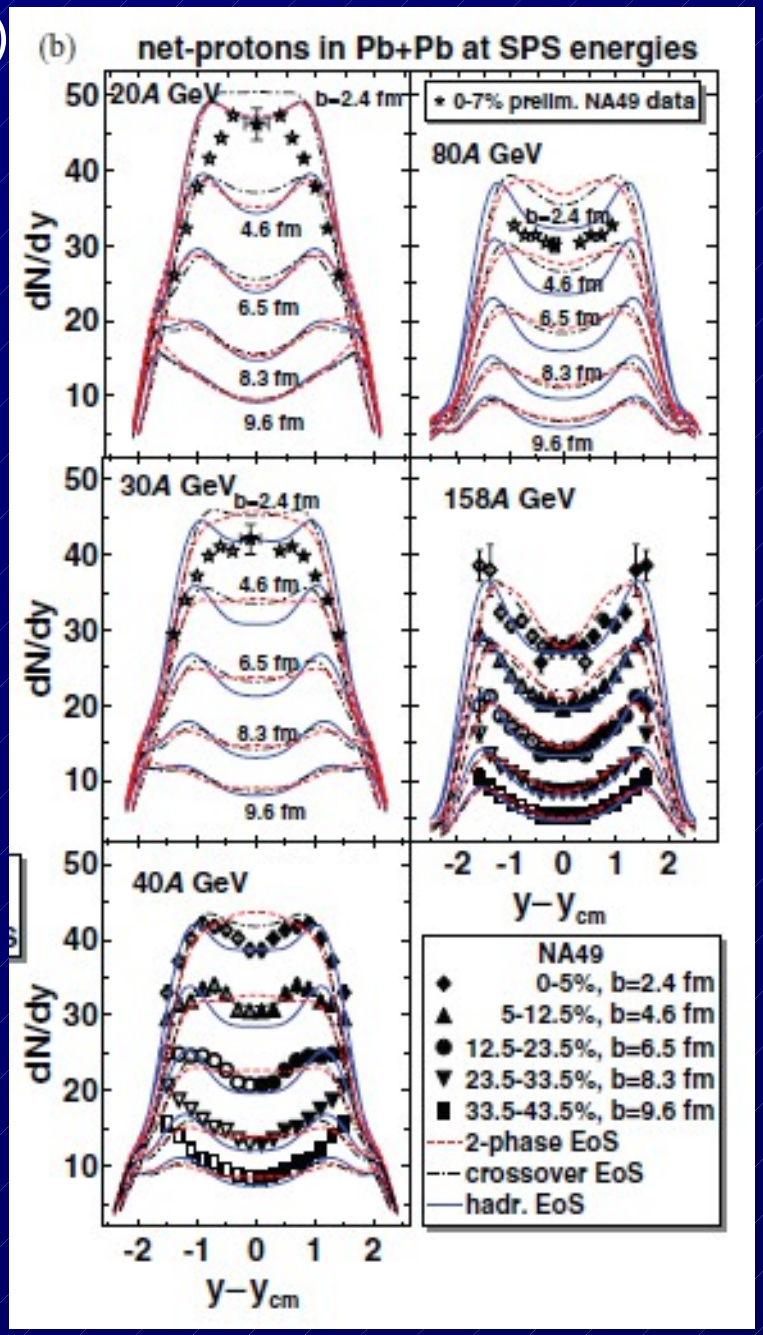

Net proton rapidity distribution – test case for a 1st order PT signal

Event set:
40k AuAu @ √s_NN = 9 GeV [0-5%]
The most reliable region
|eta| < 1.2 ; 0.4 < p_t [GeV/c] < 0.8

Result:
PHSD input → GEANT+MPD
detector reproduces the rapidity distribution !
(previous concerns not confirmed !!)

Signal:

$$C_y = \left(y_{cm}^3 \frac{d^3N}{dy^3}\right)_{y=0} / \left(y_{cm} \frac{dN}{dy}\right)_{y=0}$$

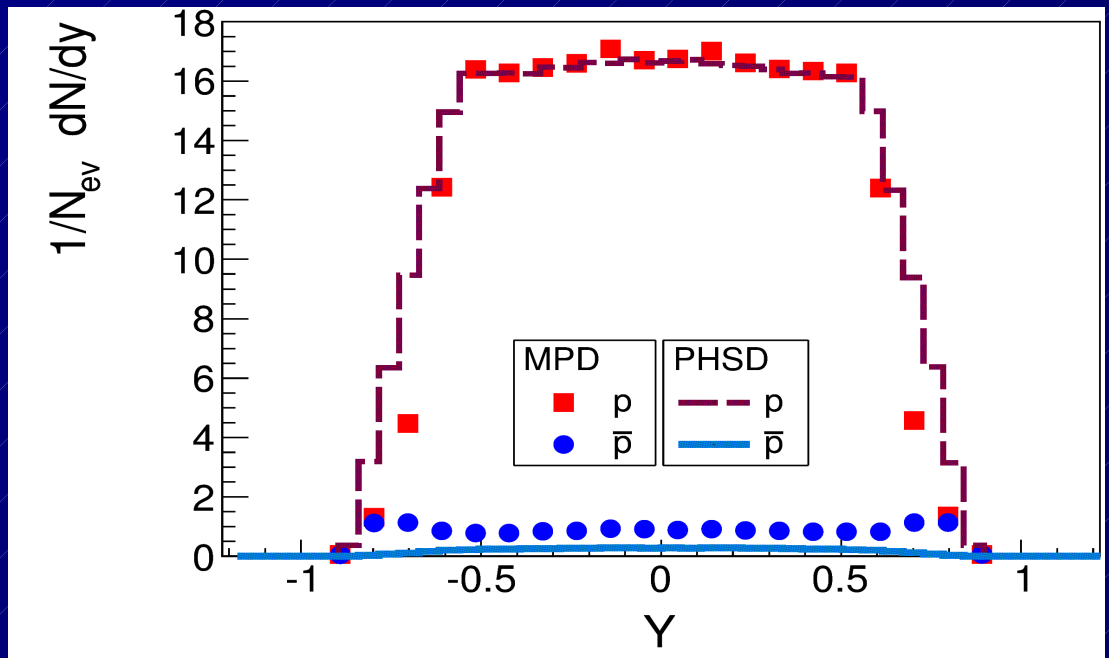

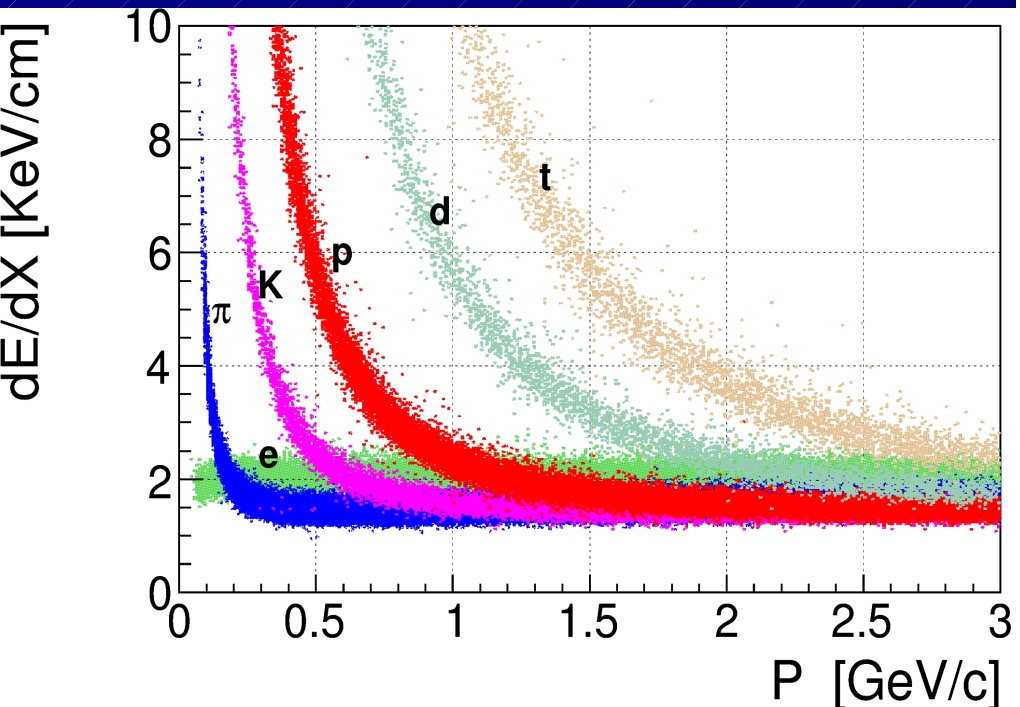

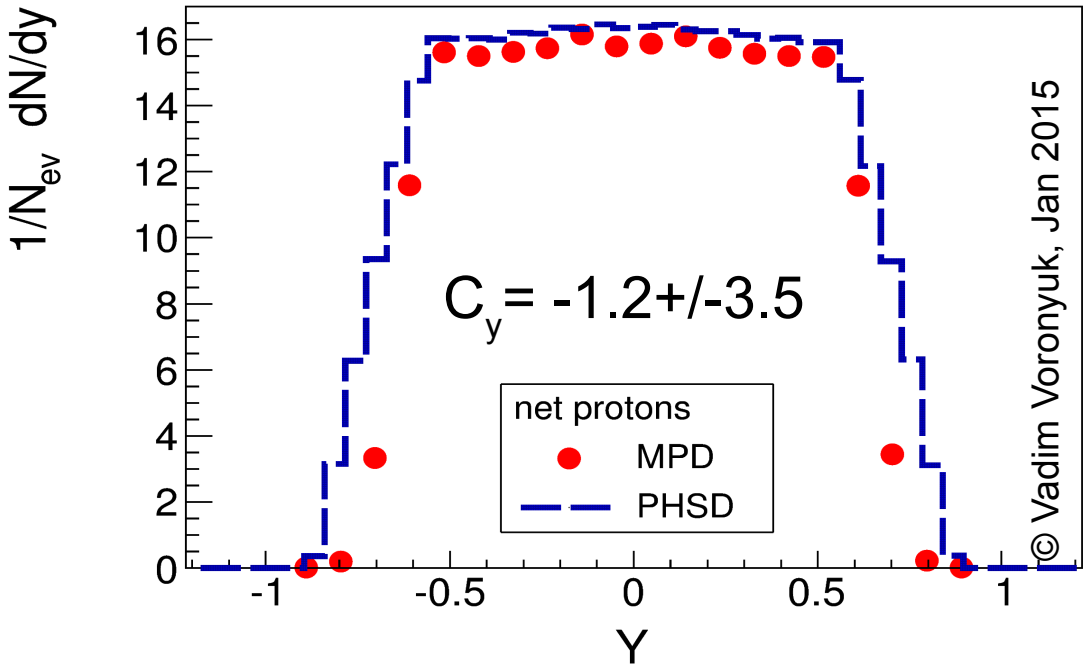

Net proton rapidity distribution – test case for a 1st order PT signal

Investigation of p_T cuts:

Yu. Ivanov & D. Blaschke, arxiv:1504.03992

$$C_y = \left(y_{\rm beam}^3 \frac{d^3N}{dy^3}\right)_{y=0} \Big/ \left(y_{\rm beam}\frac{dN}{dy}\right)_{y=0} = (y_{\rm beam}/w_s)^2\left(\sinh^2 y_s - w_s \cosh y_s\right).$$

i. $0 < p_T < 2$ GeV/c and a very unrestrictive constraint to the rapidity range $|y| < 0.7\, y_{\rm beam}$, where $y_{\rm beam}$ is the beam rapidity in the collider mode, which is practically equivalent to the full acceptance;

ii. $0.4 < p_T < 1$ GeV/c and $|y| < 0.5$, the expected MPD acceptance [17];

iii. $1 < p_T < 2$ GeV/c and $|y| < 0.5$, an acceptance range where low-momentum particles witnessing collective behaviour are largely eliminated;

iv. $0.4 < p_T < 3$ GeV/c and $|y| < 0.5$, the range of the STAR acceptance [18].

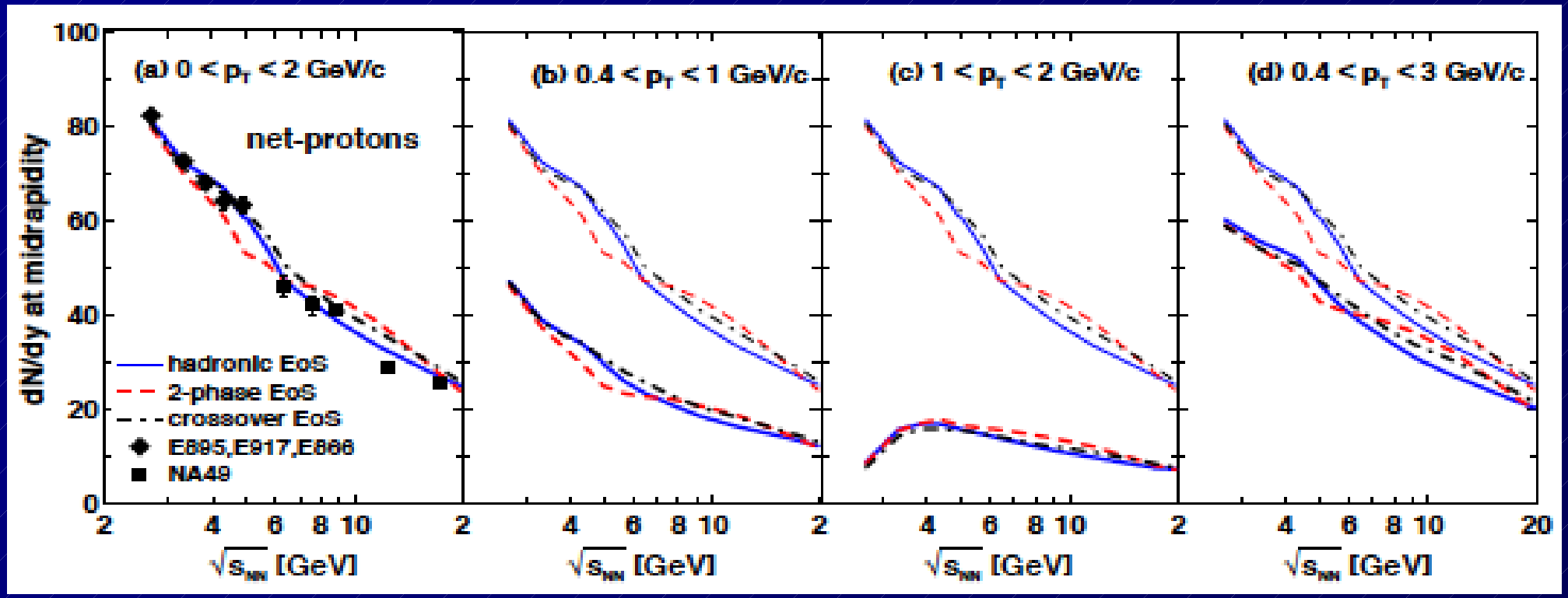

Net proton rapidity distribution – test case for a 1st order PT signal

Investigation of p_T cuts:

Yu. Ivanov & D. B., PRC 92, 024916 (2015)

$$C_y = \left(y_{\rm beam}^3 \frac{d^3N}{dy^3}\right)_{y=0} \Big/ \left(y_{\rm beam}\frac{dN}{dy}\right)_{y=0} = (y_{\rm beam}/w_s)^2\left(\sinh^2 y_s - w_s \cosh y_s\right).$$

- "wiggle" formed in the nonequilibrium compresion stage of the collision, where p_T only in 3FH
- robust against serious p_T cuts
- at high p_T (1 - 2 GeV/c) in convex region
- at low p_T (0.2 - 1 GeV/c) in concave region
- required accuracy in C_y determination: $\Delta C_y < 2$

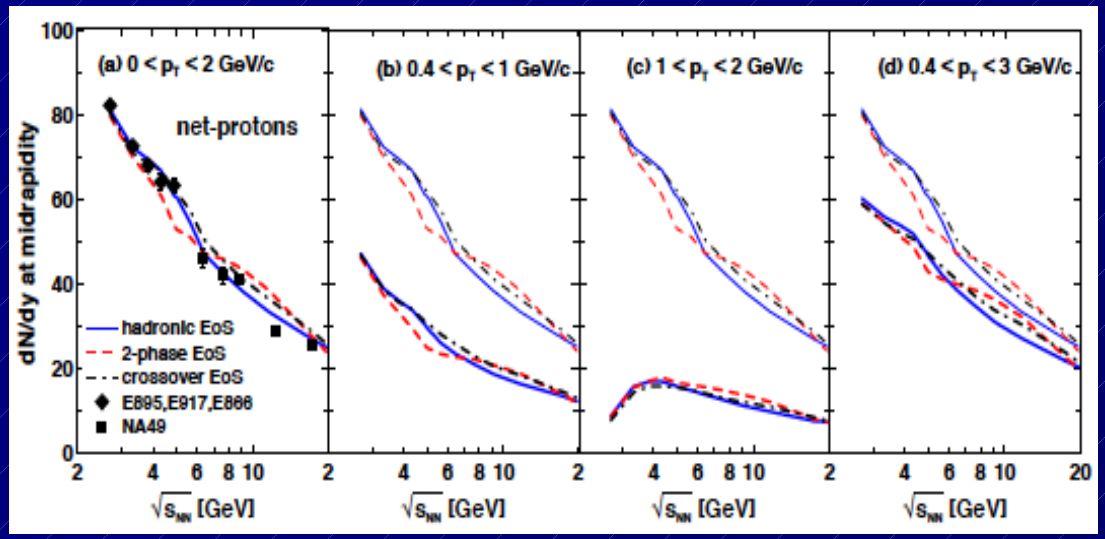

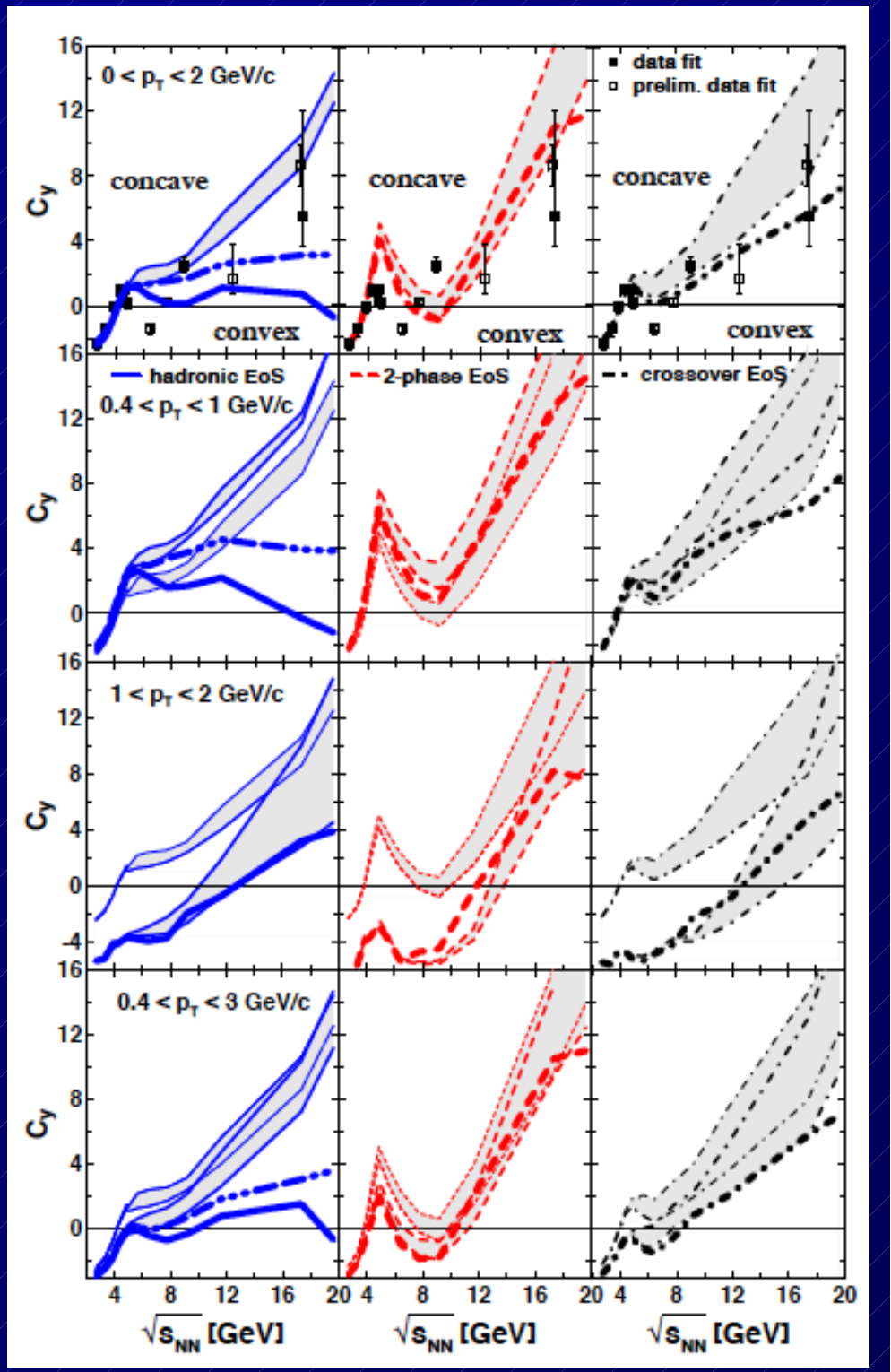

Comparison 2-phase EoS

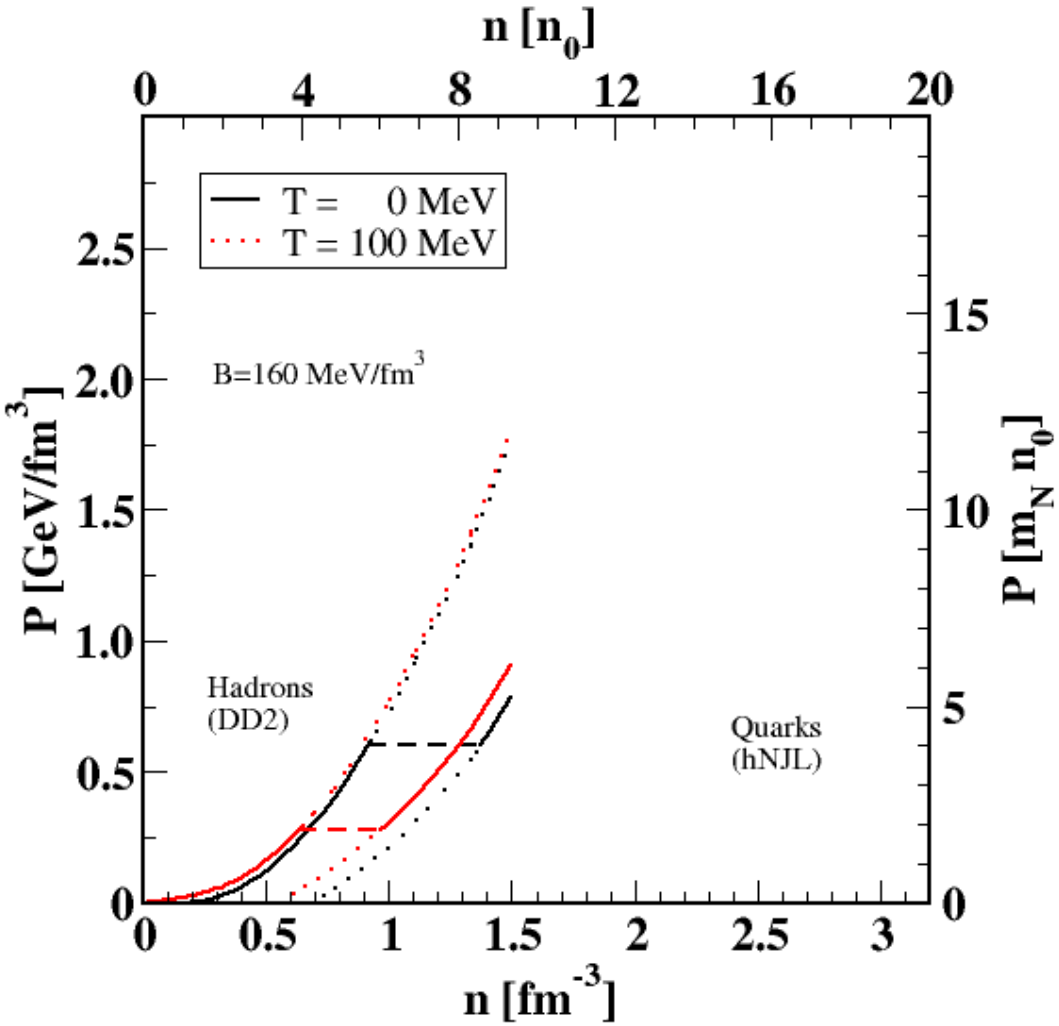

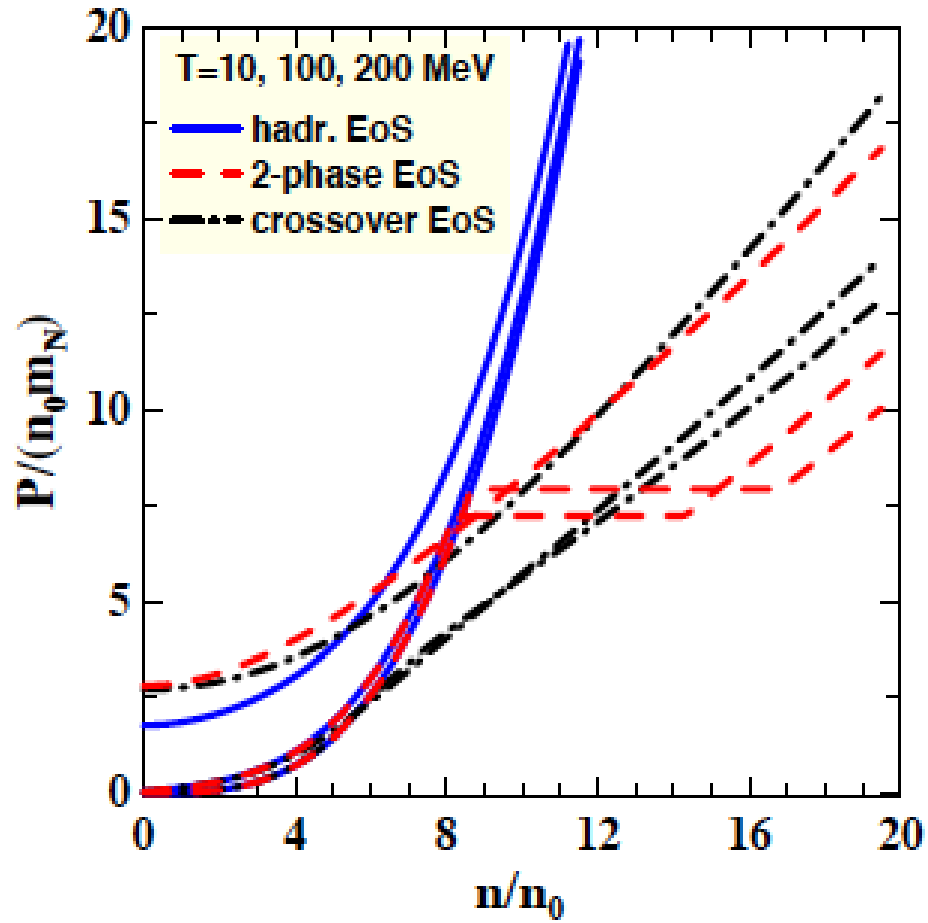

N.-U. Bastian, D. Blaschke (S. Benic, S. Typel), In progress (2015)

A. Khvorostukhin et al. EPJC 48 (2006) 531
Yu. Ivanov, D. Blaschke, arxiv:1504.03992

How to probe the line of CEP's in Astrophysics?

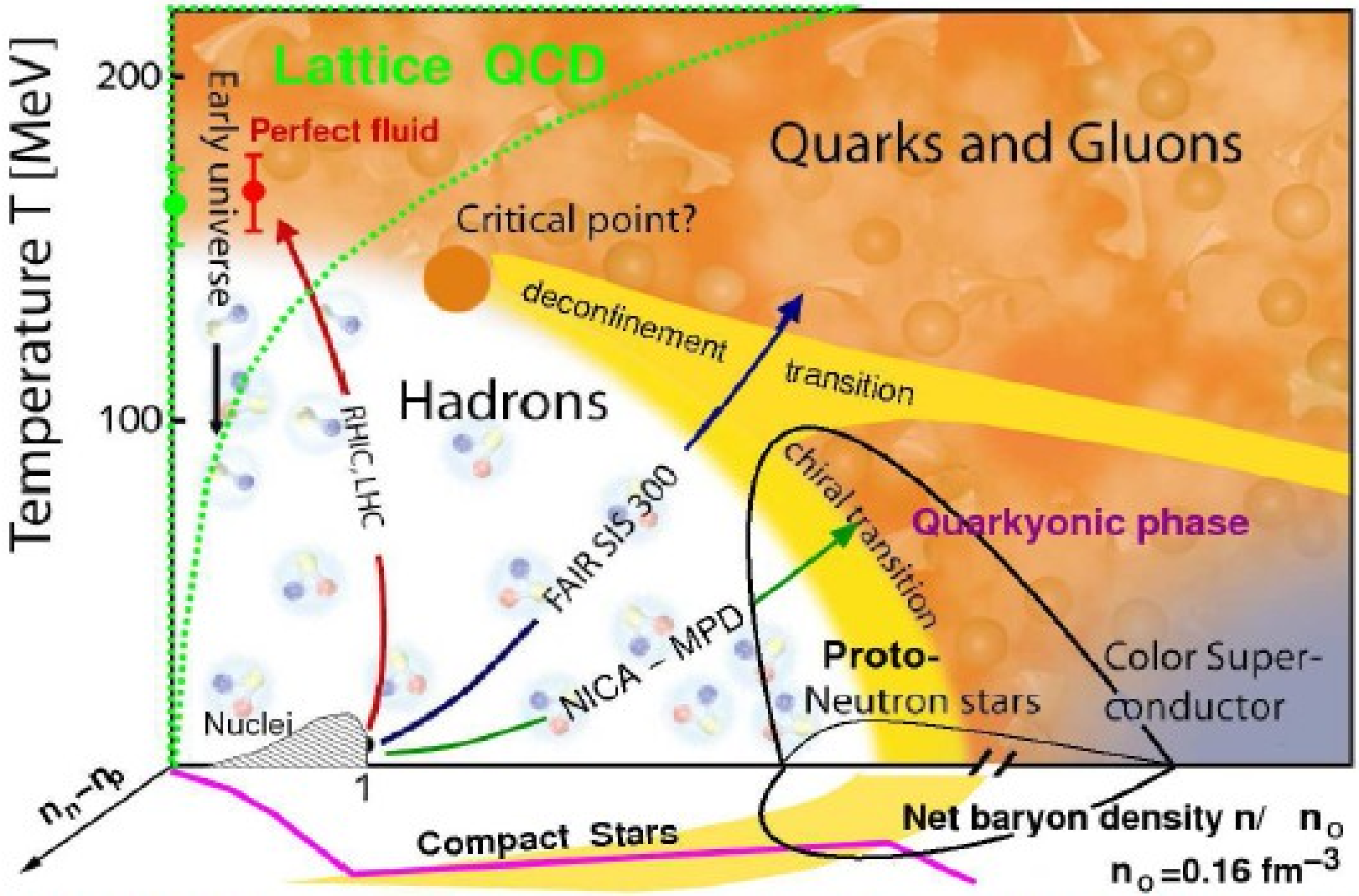

NICA White Paper, http://theor.jinr.ru/twiki-cgi/view/NICA/WebHome

How to probe the line of CEP's in Astrophysics?

→ by sweeping ("flyby") the critical line in SN collapse and BH formation

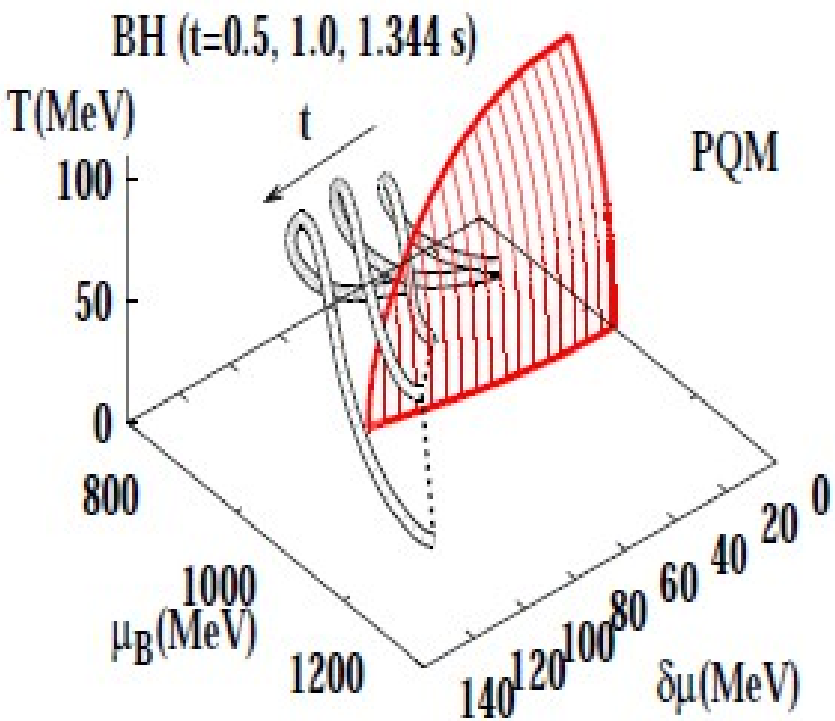

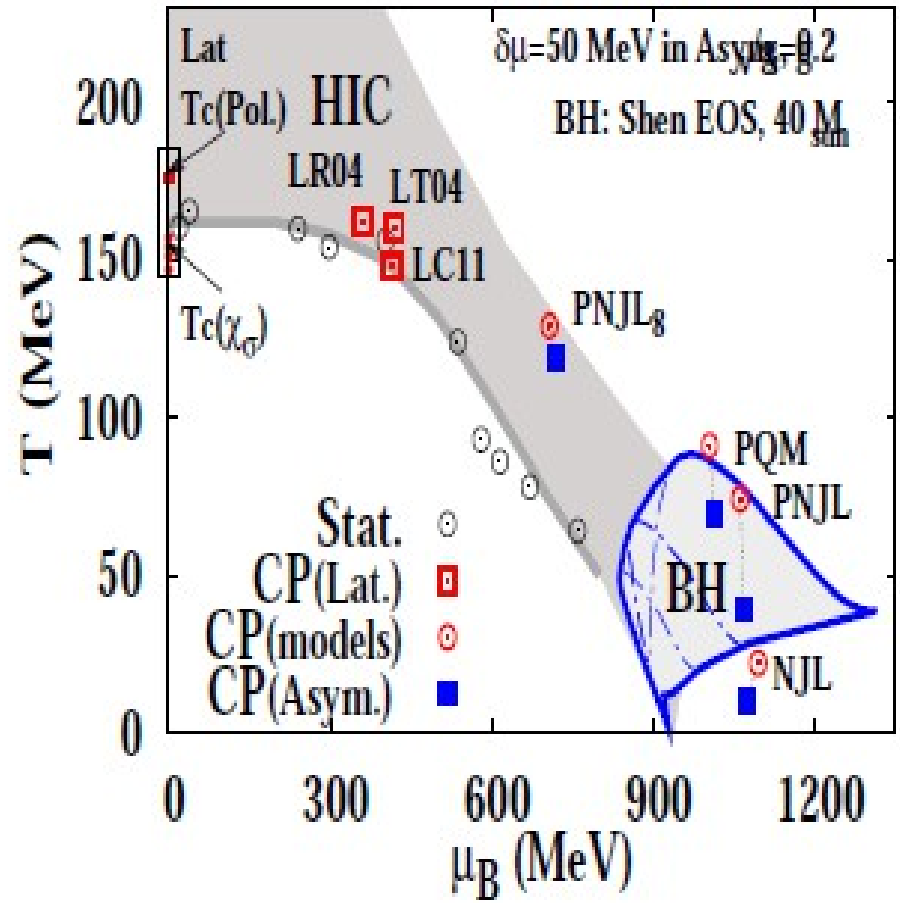

A. Ohnishi, H. Ueda, T. Nakano, M. Ruggieri, K. Sumiyoshi, Phys. Lett. B **704**, (2011) 284.

Perspectives for new Instruments?

THE FUTURE: SKA - SQUARE KILOMETER ARRAY

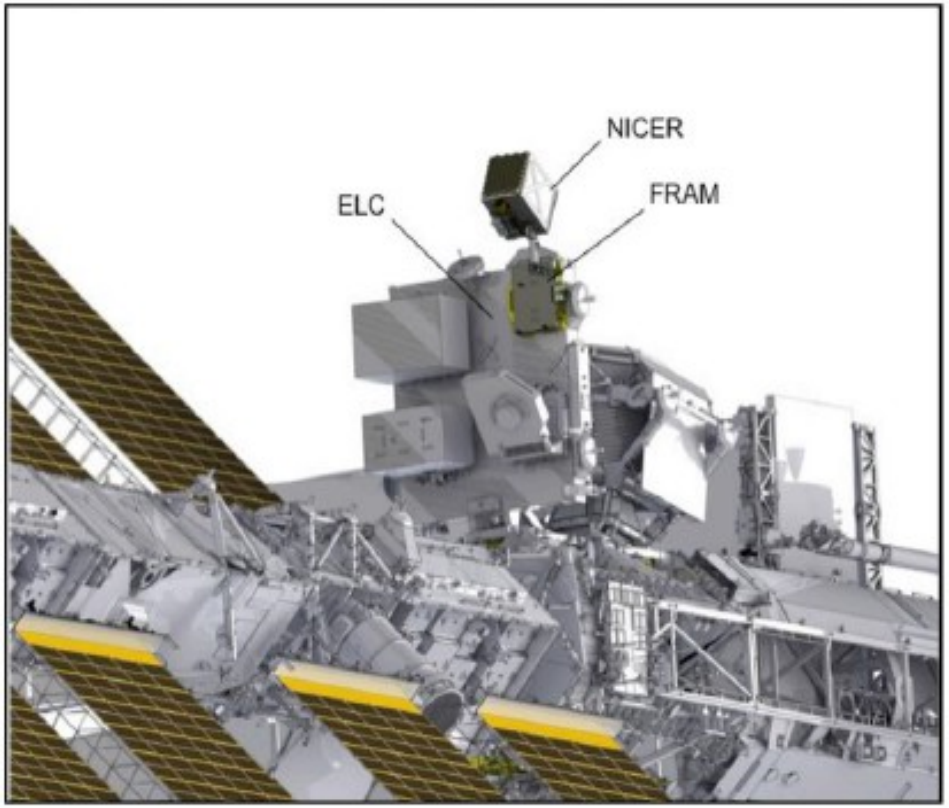

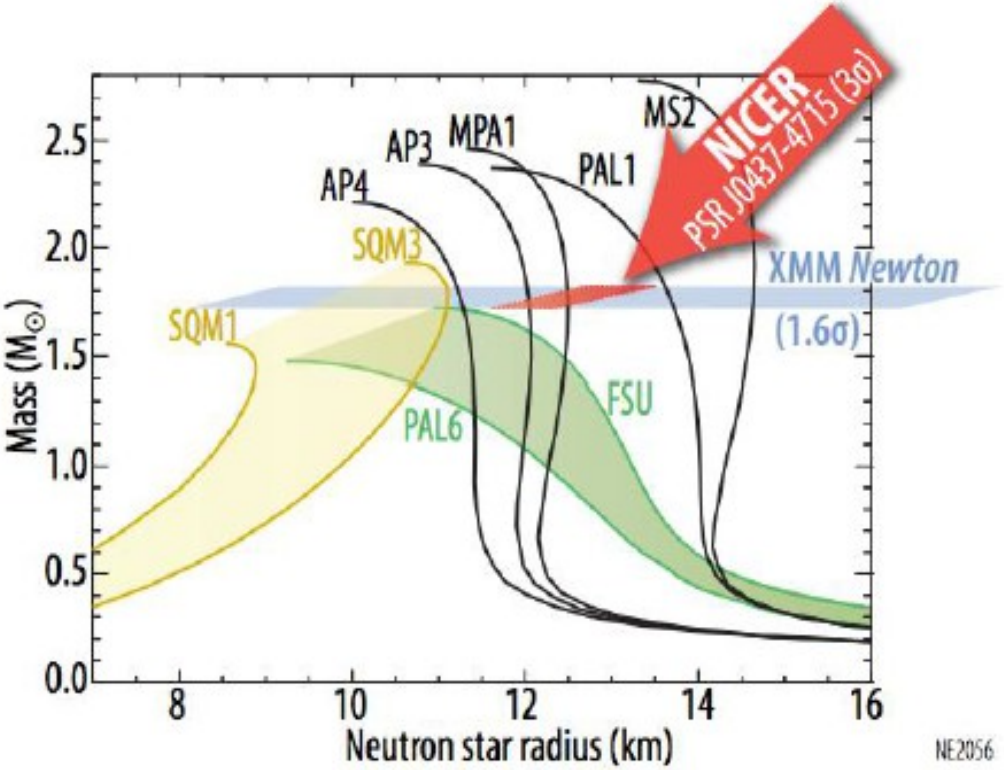

NICER 2017

Gendreau, K. C., Arzoumanian, Z., & Okajima, T. 2012, Proc. SPIE, 8443, 844313


NICER
Neutron star Interior Composition ExploreR

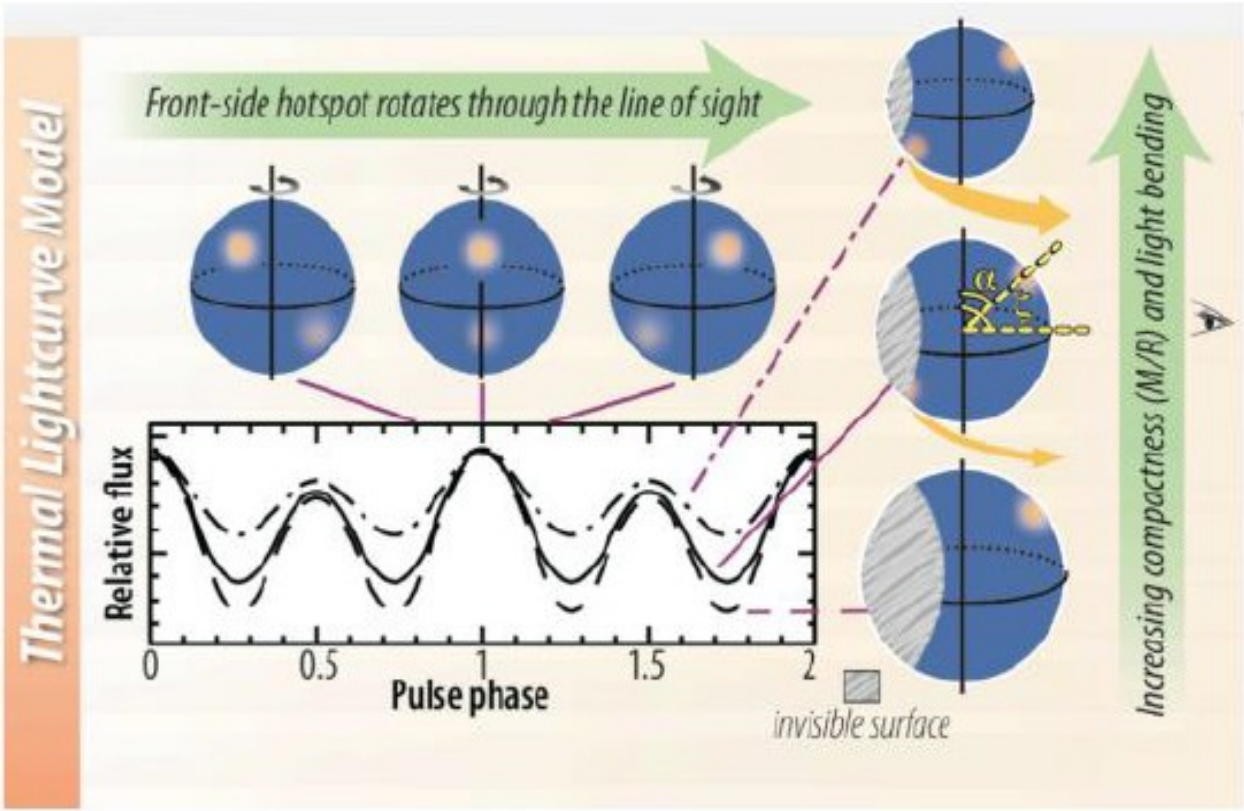
Thermal Lightcurve Model
Front-side hotspot rotates through the line of sight
Relative flux
0
0.5
1
1.5
2
Pulse phase
invisible surface
Increasing compactness (M/R) and light bending

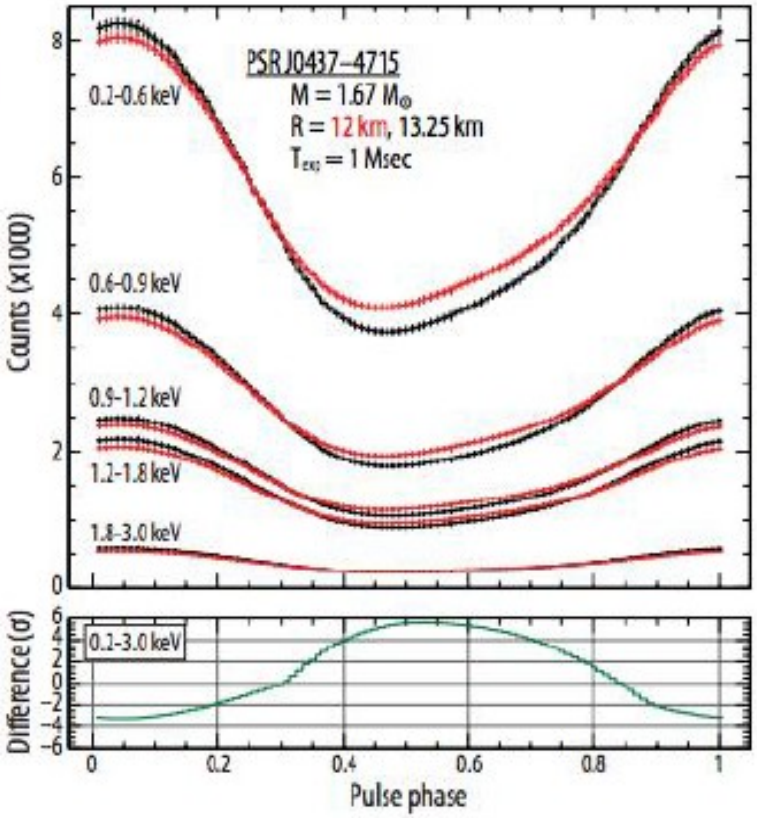
PSR J0437–4715
M = 1.67 M⊙
R = 12 km, 13.25 km
T_exp = 1 Msec
0.2-0.6 keV
0.6-0.9 keV
0.9-1.2 keV
1.2-1.8 keV
1.8-3.0 keV
Counts (x1000)
0.2-3.0 keV
Difference (σ)
Pulse phase

Hot Spots

Conclusion:

Critical endpoint search in the QCD phase diagram with Heavy-Ion Collisions goes well together with Compact Star Astrophysics

Rescue slides ….

A QCD-based hybrid EoS - nonlocal PNJL model

DB, Alvarez Castillo, Benic, Contrera, Lastowiecki, arxiv:1302.6275 (2012)

$$\mathscr{L} = \bar{q}(i\not{D} - m_0)q + \mathscr{L}_{\rm int} + \mathscr{U}(\Phi) \ ,$$

$$\mathscr{L}_{\rm int} = -\frac{G_S}{2}\Big[j_S(x)j_S(x) + j_P(x)j_P(x) - j_p(x)j_p(x)\Big] - \frac{G_V}{2} j_V(x)j_V(x),$$

$$j_a(x) = \int d^4z\, g(z)\, \bar{q}\Big(x+\frac{z}{2}\Big)\, \Gamma_a\, q\Big(x-\frac{z}{2}\Big) \ , \quad a = S,P,V \ , \qquad (\Gamma_S, \Gamma_P, \Gamma_V) = (\mathbf{1}, i\gamma_5\vec{\tau}, \gamma_0)$$

$$j_p(x) = \int d^4z\, f(z)\, \bar{q}\Big(x+\frac{z}{2}\Big)\, \frac{i\overleftrightarrow{\not{\partial}}}{2\,\kappa_p}\, q\Big(x-\frac{z}{2}\Big) \ , \qquad u(x')\overleftrightarrow{\partial}\, v(x) = u(x')\partial_x v(x) - \partial_{x'} u(x')\, v(x)$$

$$\mathscr{U}(\Phi, T, \mu) = (a_0 T^4 + a_1\mu^4 + a_2 T^2\mu^2)\Phi^2 + a_3 T_0^4 \ln(1 - 6\Phi^2 + 8\Phi^3 - 3\Phi^4) \ ,$$

$$\boxed{\Omega^{\rm MFA} = -4T\sum_{n,c}\int \frac{d^3\vec{p}}{(2\pi)^3} \ln\left[\frac{(\tilde{p}^c_{n,\vec{p}})^2 + M^2(p^c_{n,\vec{p}})}{Z^2(p^c_{n,\vec{p}})}\right] + \frac{\sigma_1^2 + \kappa_p^2\,\sigma_2^2}{2\,G_S} - \frac{\omega^2}{2G_V} + \mathscr{U}(\Phi, T) \ ,}$$

$$M(p) = Z(p)\,[m + \sigma_1\, g(p)] \ , \quad Z(p) = [1 - \sigma_2\, f(p)]^{-1} \ . \qquad \tilde{\mu} = \mu - \omega\, g(p)\, Z(p) \ .$$

A QCD-based hybrid EoS

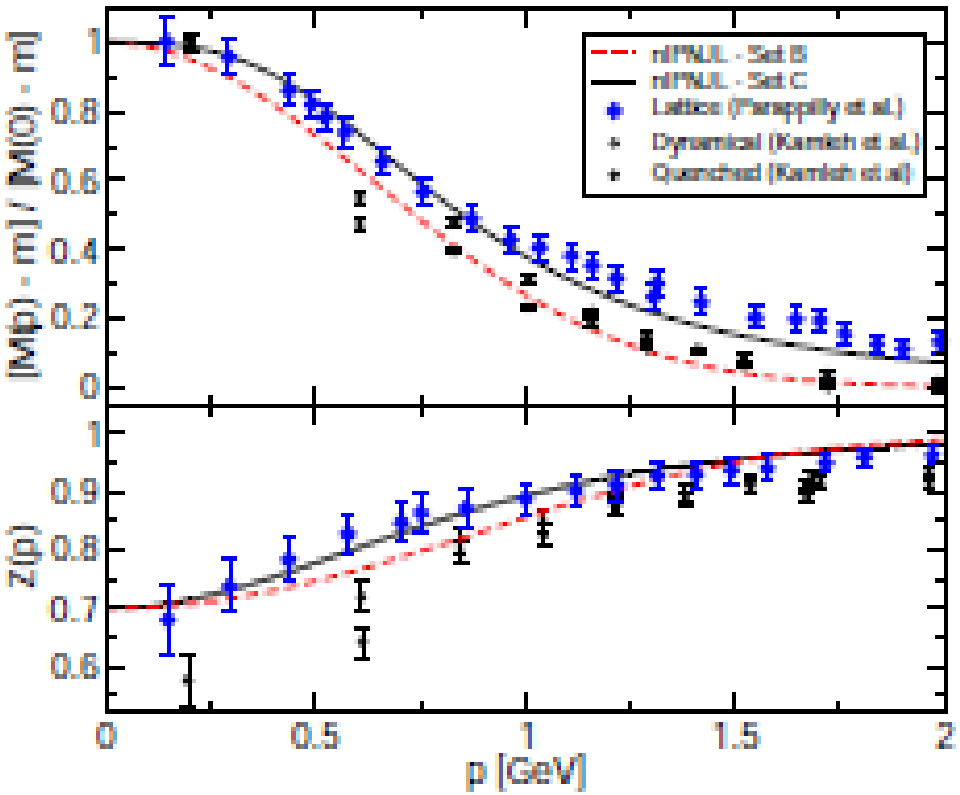

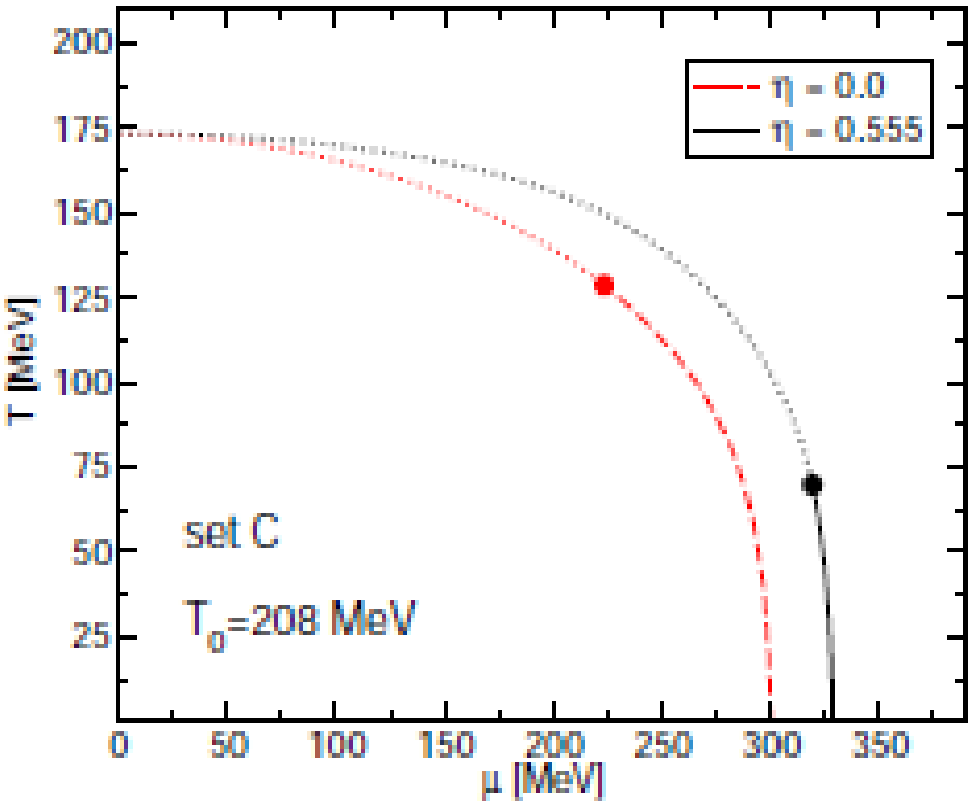

- **Formfactors of the nonlocal chiral quark model fixed by comparison with M(p) and Z(p) from lattice QCD calculations of the quark propagator [Parapilly et al. PRD 73 (2006)**
- **Vector coupling strength adjusted to describe the slope of the pseudocritical temperature In accordance with lattice QCD [Kaczmarek et al., PRD 83 (2011) 014504]**
- **CEP does not vanish !! Controversial discussion, see Hell et al., arxiv:1212.4017 (2012)**

A QCD-based hybrid EoS

Maxwell construction of hybrid EoS

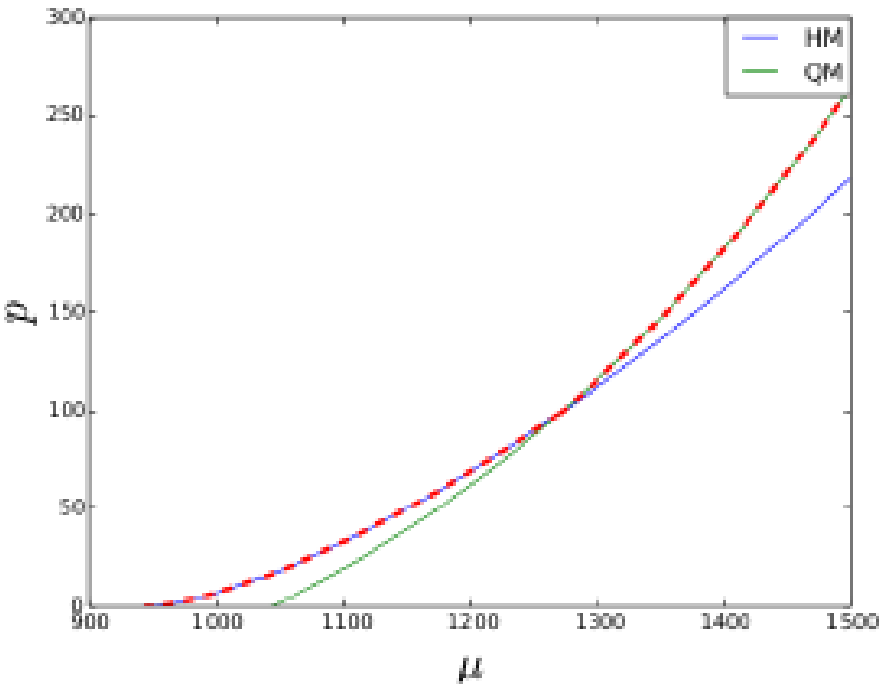

(A) $p(\mu)$ functions.

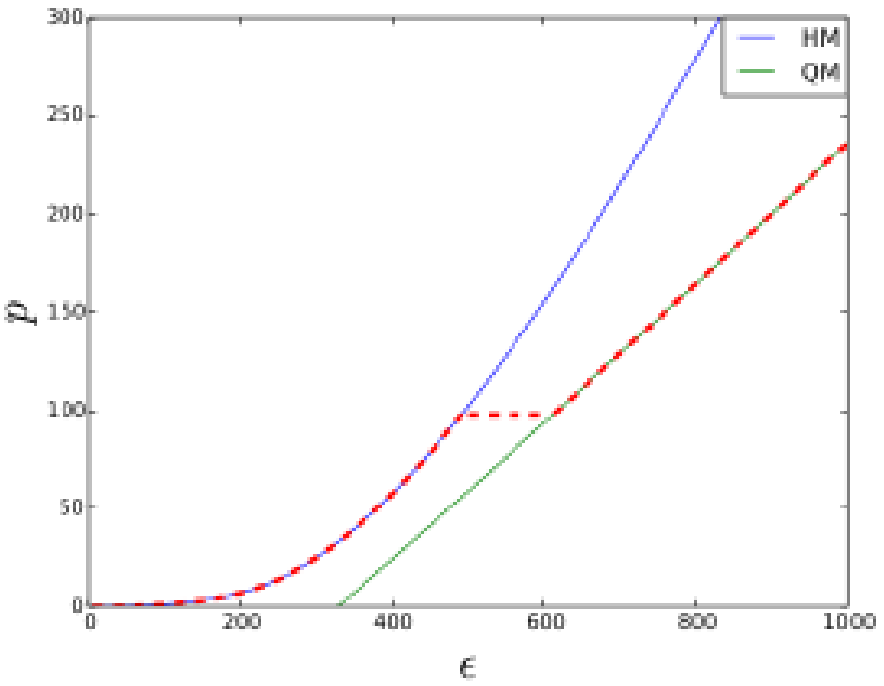

(B) $p(\epsilon)$ functions.

A QCD-based hybrid EoS

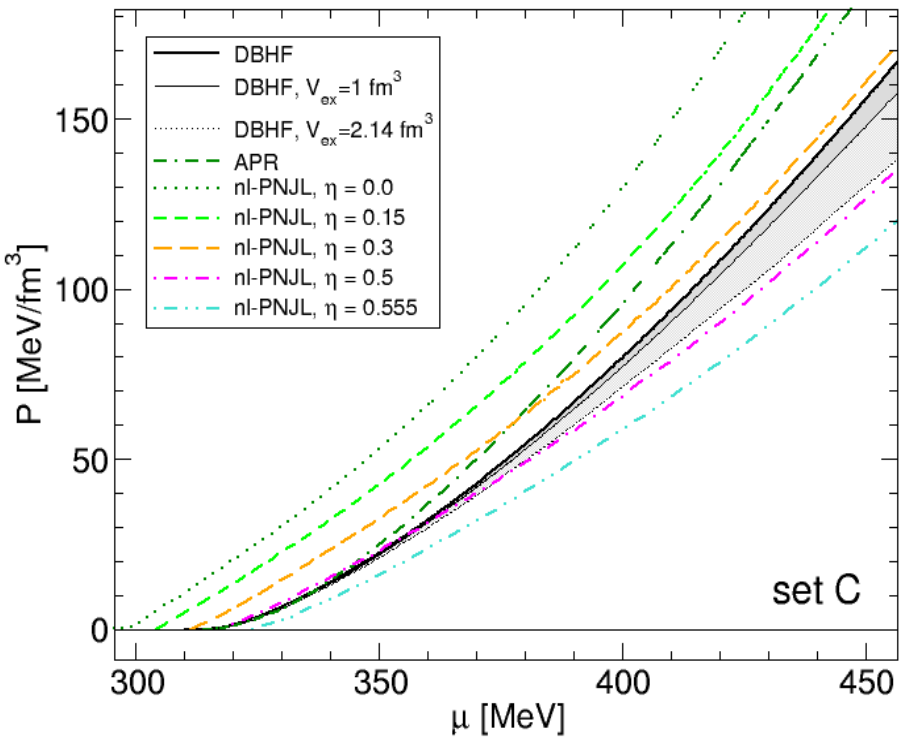

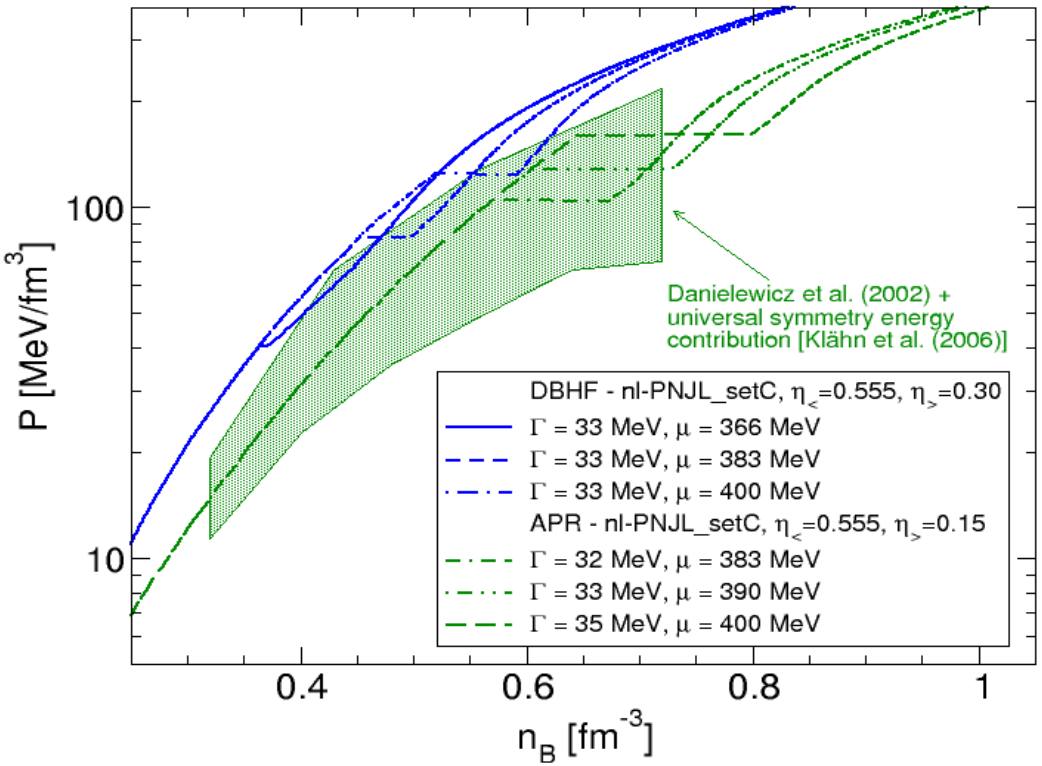

- for strong vector coupling nuclear matter is stable at low densities
- for small vector coupling quark matter is stable at high densities
- for intermediate couplings → masquerade problem [Alford et al. ApJ 629 (2005) 969]

Here:

(A) Maxwell construction

$$P_Q(\mu_c) = P_H(\mu_c)$$

H = DBHF, APR; Q = nl-PNJL

(B) mu-dependent vector coupling:

$$P_Q(\mu) = P(0,\mu;\eta_<)\, f_<(\mu) + P(0,\mu;\eta_>)\, f_>(\mu)\,,$$

$$f_{<}^{>}(\mu) = \frac{1}{2}\left[1 \mp \tanh\left(\frac{\mu-\bar{\mu}}{\Gamma}\right)\right]\,.$$

Result 1: hybrid stars fulfill Demorest and RXJ1856

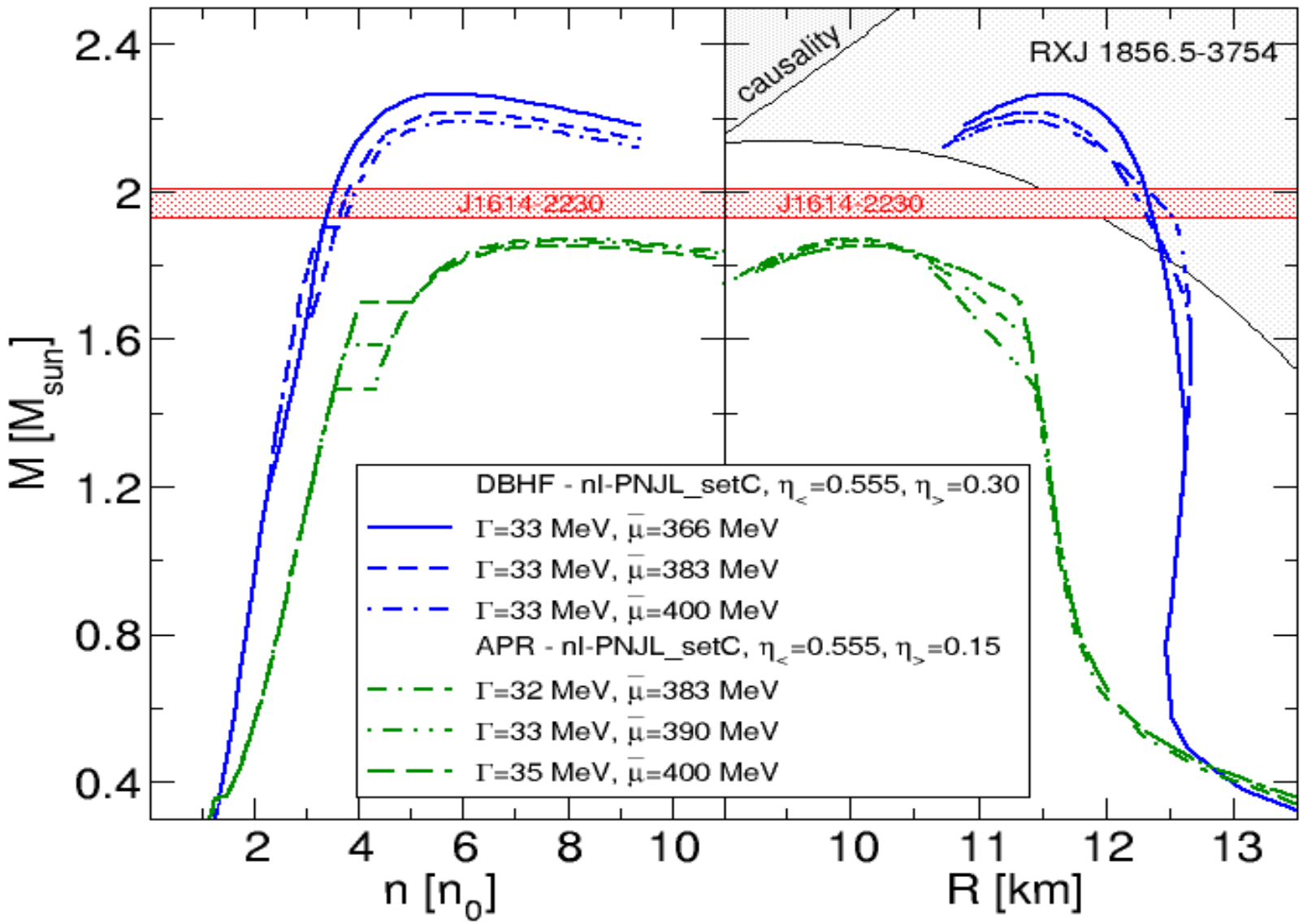

DB, Alvarez Castillo, Benic, Contrera, Lastowiecki, arxiv:1302.6275 (2012)

Result:
High mass twins are possible !

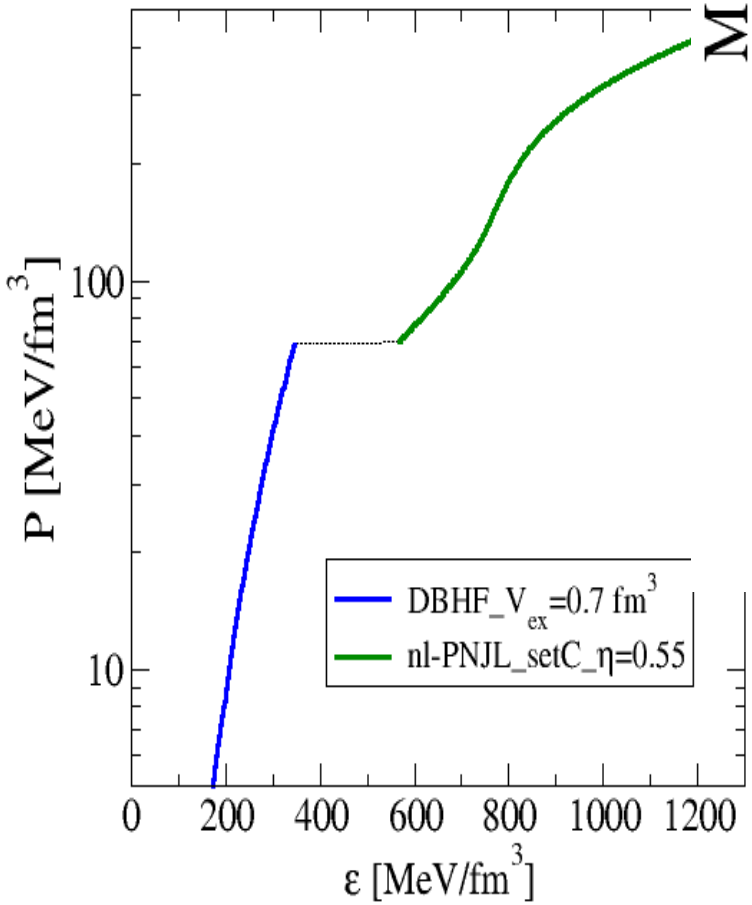

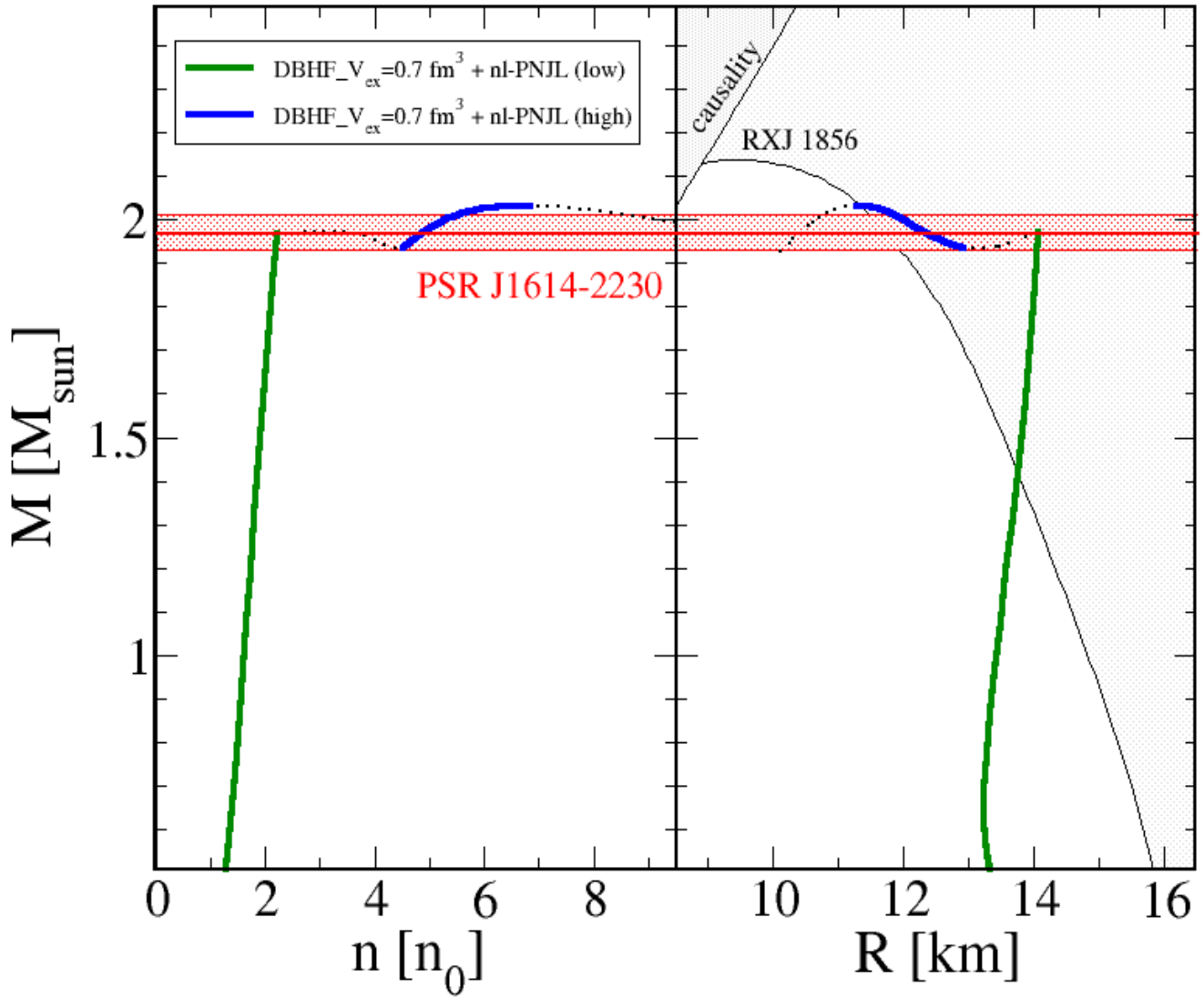

SUMMARY:

- excluded volume (quark Pauli blocking) in DBHF
- high-density quark matter slightly stiffer eta_v=0.25
- the scaled energy density jump (0.65) fulfills the twin condition of the schematic model by Alford et al. (2013)

→ **Find the disconnected star branches !!**

Result:
High mass twins: more examples !

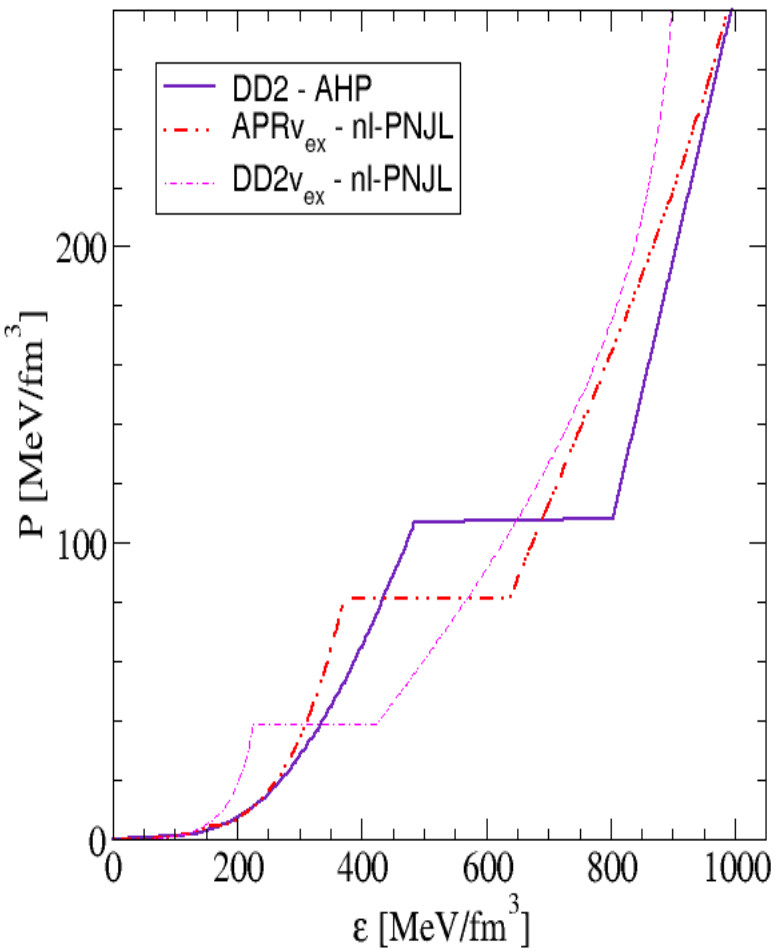

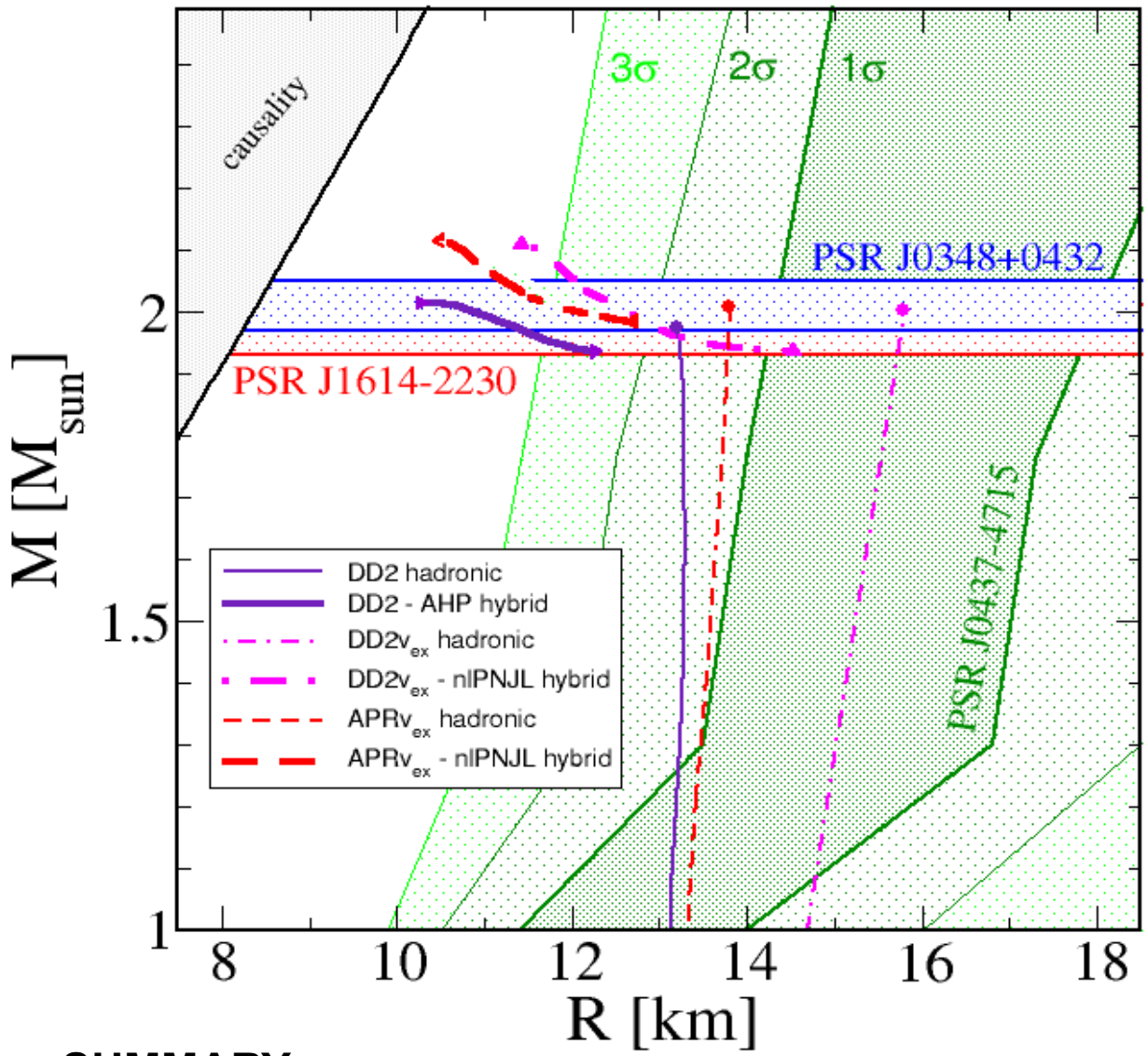

SUMMARY:

- excluded volume (quark Pauli blocking) important
- high-density quark matter slightly stiffer eta_v=0.25
- the scaled energy density jump (0.65) fulfills the twin condition of the schematic model by Alford et al. (2013)

→ **Astronomers: Find disconnected star branches !!**

DB, Alvarez, Benic, arxiv: tomorrow

Main Problem:
Measure Compact Star Radii!

Gravitational binding: double pulsar J0737-3039

Double Pulsar System J0737-3039

Pulsar A $P^{(A)}$ = 22.7 ms, $M^{(A)} \approx 1.338 M_\odot$

Pulsar B $P^{(B)}$ = 2.77 s, $M^{(B)} = 1.249 \pm 0.001 M_\odot$ (record!)

Progenitor ONeMg white dwarf, driven hydrodyn. unstable by e^- captures on Mg & Ne; no mass-loss during collapse

Observational constraint for $M(M_N)$ from PSR J0737-3039:

- observed NSs gravitational mass (remnant star) $M^{(B)} = 1.248 - 1.250 M_\odot$
- critical baryon mass for ONeMg white dwarf $M_N^{(B)} = 1.366 - 1.375 M_\odot$

Theory: $M(M_N)$ characteristic for remnants EoS

$M = 4\pi \int_0^R \mathrm{d}r r^2 \varepsilon(r)$;

$M_N = u N_B = 4\pi u \int_0^R \mathrm{d}r \frac{r^2 n(r)}{\sqrt{1-2GM(r)/r}}$

(conversion of baryon number to mass by $u = 931.5$ MeV)

P. Podsiadlowski et al., Mon. Not. Roy. Astron. Soc. **361**, 1243 (2005)

EoS constraint: double pulsar J0737-3039

Double core scenario:

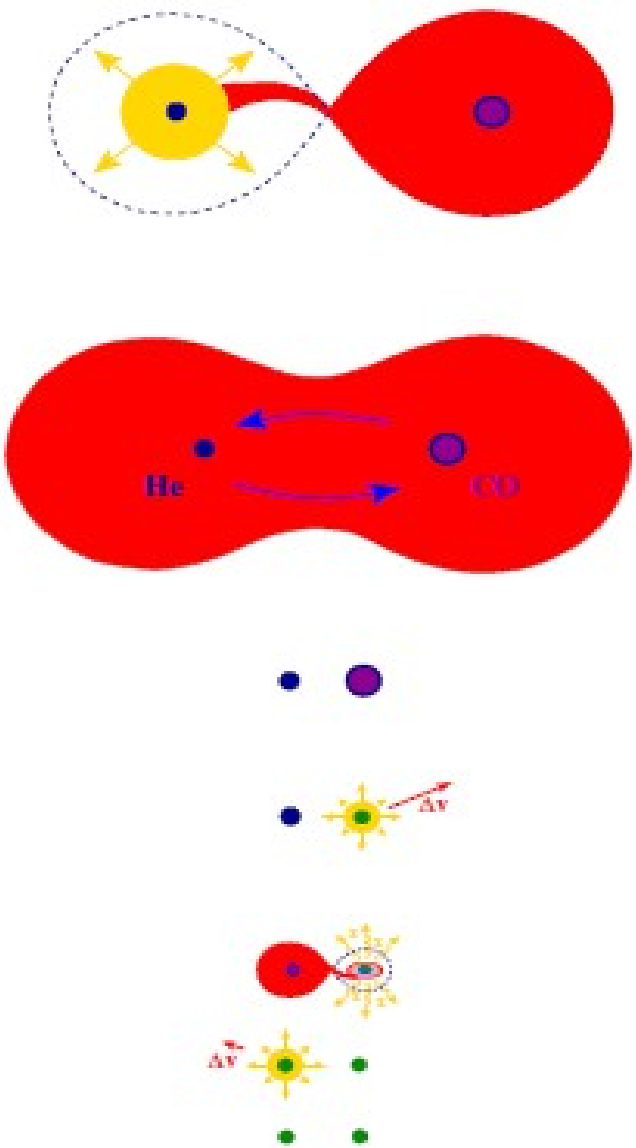

Dewi et al., MNRAS (2006)

Baryon mass vs. gravitational mass - constraint or consistency check?

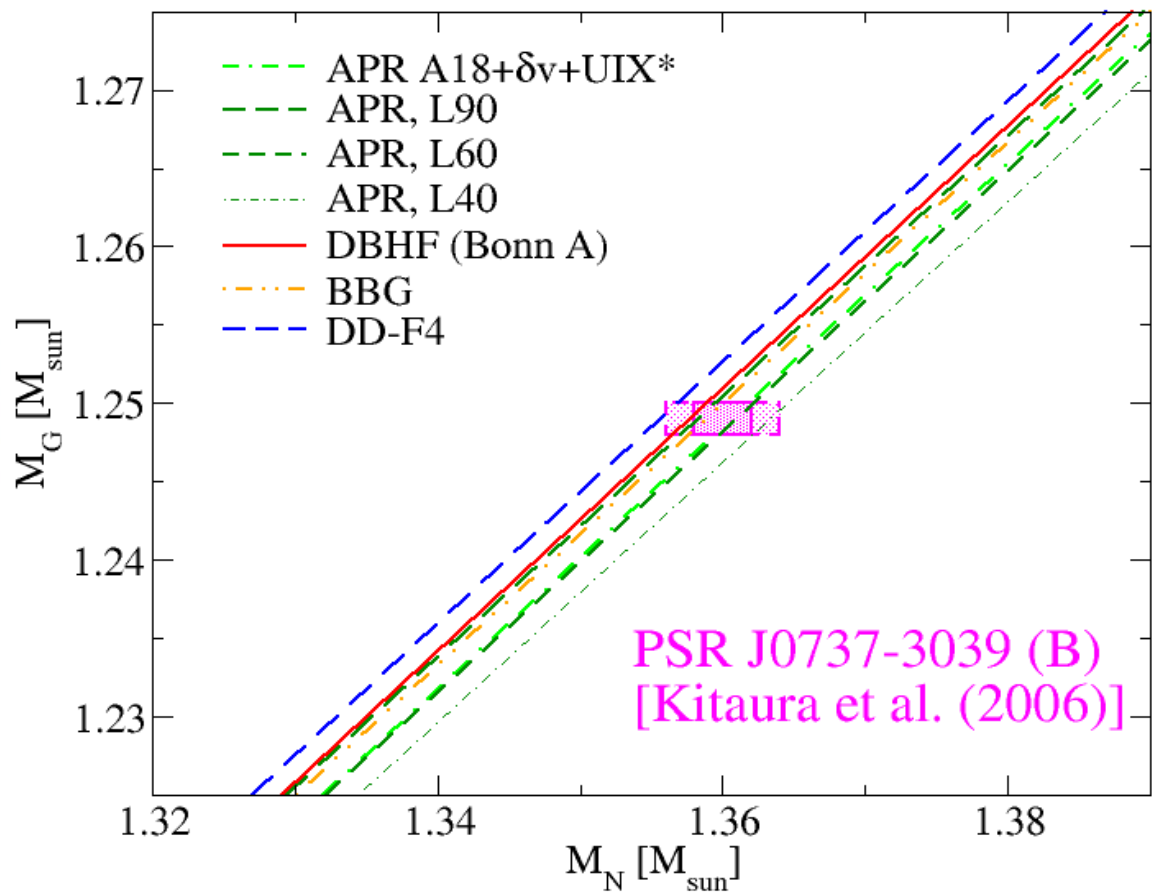

Podsiadlowski et al., MNRAS 361 (2005) 1243
Kitaura, Janka, Hillebrandt, A& A (2006); [astro-ph/0512065]

D.B., T. Klähn, F. Weber, CBM Physics Book (2008)

Double pulsar: mass & radius ?!

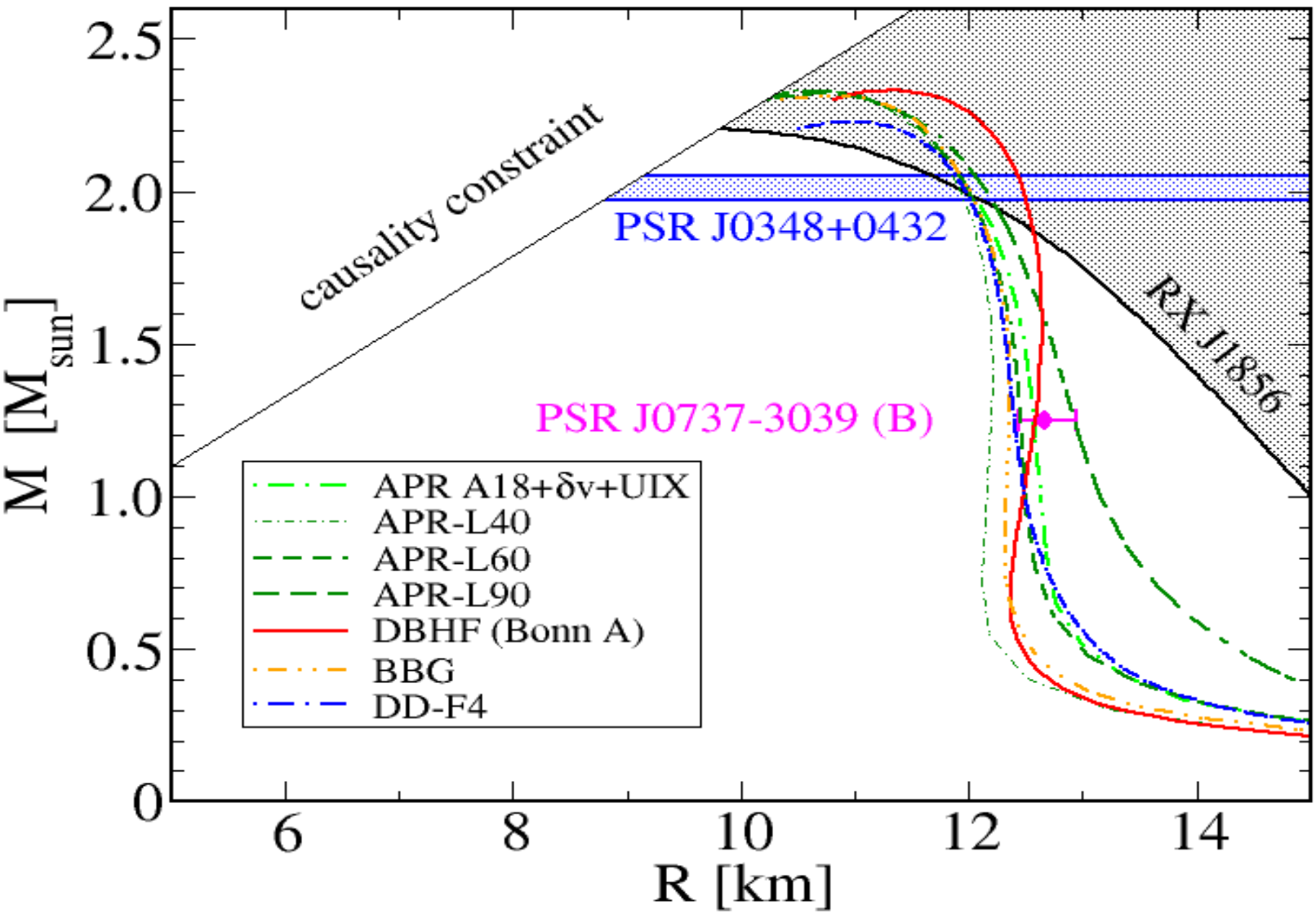

Disjunct M-R constraints for Bayesian analysis !

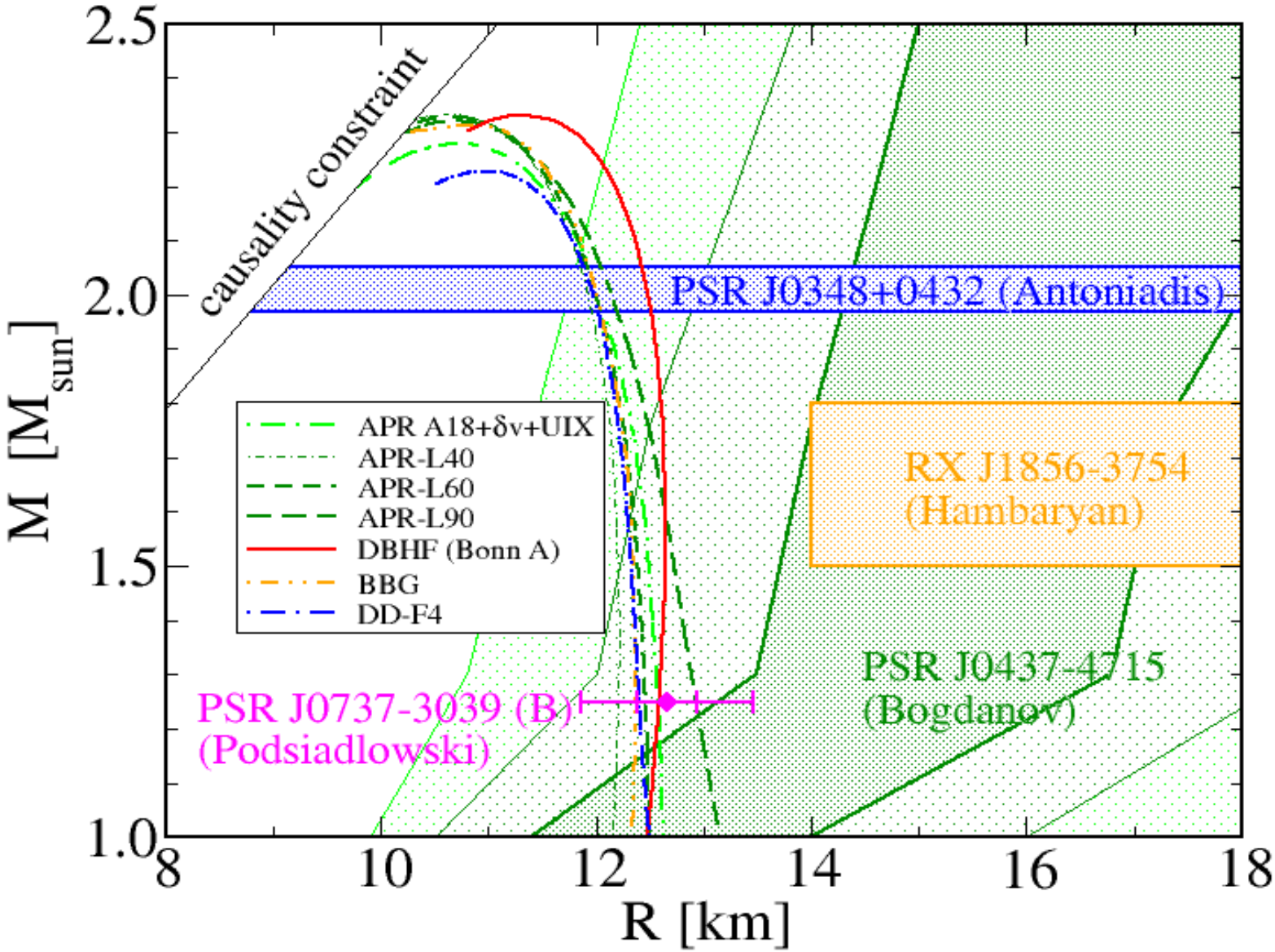

Alvarez, Ayriyan, Blaschke, Grigorian, J. Phys. Conf. Ser. (2014)